UNCERTAINTIES IN TROPICAL RAIN PARAMETERS AND CLIMATE CHANGE

Ph.D. Thesis

By

CHANDRANI CHATTERJEE

DEPARTMENT OF ASTRONOMY, ASTROPHYSICS AND SPACE ENGINEERING

INDIAN INSTITUTE OF TECHNOLOGY INDORE

JULY, 2022

UNCERTAINTIES IN TROPICAL RAIN PARAMETERS AND CLIMATE CHANGE

A THESIS

Submitted in partial fulfillment of the requirements for the award of the degree

of

DOCTOR OF PHILOSOPHY

by

CHANDRANI CHATTERJEE

Roll No. 1901121003

DEPARTMENT OF ASTRONOMY, ASTROPHYSICS AND SPACE ENGINEERING

INDIAN INSTITUTE OF TECHNOLOGY INDORE

JULY, 2022

INDIAN INSTITUTE OF TECHNOLOGY INDORE

CANDIDATE'S DECLARATION

I hereby certify that the work which is being presented in the thesis entitled "**Uncertainties in tropical rain parameters and climate change"** in the partial fulfillment of the requirements for the award of the degree of **DOCTOR OF PHILOSOPHY** and submitted in the **DEPARTMENT OF ASTRONOMY, ASTROPHYSICS AND SPACE ENGINEERING, Indian Institute of Technology Indore**, is an authentic record of my own work carried out during the time period from June, 2019 to June, 2022 under the supervision of Dr. Saurabh Das, Assistant Professor, the **DEPARTMENT OF ASTRONOMY, ASTROPHYSICS AND SPACE ENGINEERING, Indian Institute of Technology Indore.**

The matter presented in this thesis has not been submitted by me for the award of any other degree of this or any other institute.

Chandrani Chatterjee
1/7/22

Signature of the student with date

(CHANDRANI CHATTERJEE)

This is to certify that the above statement made by the candidate is correct to the best of my/our knowledge.

S. Das
4/7/2022

Signature of Thesis Supervisor with date

(DR. SAURABH DAS)

CHANDRANI CHATTERJEE has successfully given his/her Ph.D. Oral Examination held on **June 09, 2022.**

S. Das
4/7/2022

Signature of Thesis Supervisor with date

(DR. SAURABH DAS)

Acknowledgements

Firstly, I would like to express my sincere gratitude to my supervisor, Dr. Saurabh Das for his kind guidance.

I express my heartfelt thanks to Prof. Federico Porcu, University of Bologna for his kind guidance in some very important portion of my thesis. I would like to thank the members of my PSPC (PG Students Progress Committee), Dr. Somnath Dey, Dr. Rajkumar Hajra and Dr. Amit Shukla for their continuous encouragement and guidance. My sincere thanks also goes to the faculties and my fellow lab-mates at Indian Statistical Institute, Kolkata where I began my research and at Indian Institute of Technology, Indore where I completed my doctoral journey, for their constant encouragement and support during the process.

Last but not the least; I would like to thank my family for the continuous support.

Dedicated

to

My Grandmother

***(Late) Smt. Kamala Bandyopadhyay*,**

The biggest support, I ever had

Abstract

Successful assessment of climate change induced uncertainties in precipitation cycle is extremely crucial, especially in an agriculturally dependent economy like India. However, given the enormous inhomogeneity of rainfall process over different parts of the country, proper identification of different rain climatologies is crucial. Remote sensing measurements of rain fall can provide a large spatial coverage, however, limited to last few decades. Moreover, rain microphysical behavior under different rain conditions can vary largely which, in turn can affect the accuracy of radar rain meteorology as the accuracy of radar retrieved rainfall relies on relations dependent on rain microphysical structure. This thesis has first attempted to identify homogeneous monsoon rain regions over India based on multiple rain features including rain types, frequency and recent rain extremes by assimilating satellite and ground data using machine learning techniques. The precipitation cycle over the seven of nine different rain climatologies identified, showed different susceptibility to climate change in recent past. Five of the regions showed statistically significant decreasing trend of monsoon rain whereas; two of them had clearly increasing trend of precipitation. A machine learning based regression model has been developed further to predict lightning density over Indian region based on simple atmospheric feature and cloud microphysical structure. The model has showed an R^2 score of 0.81 during monsoon and 0.71 during pre-monsoon. This thesis also investigated two less explored uncertainties associated with rain microphysics which can modulate the precipitation structure significantly and thereby cause notable errors in radar based QPE. The current work reports notable differences in rain and cloud microphysics during lightning. The relations linking radar retrieved parameters with rain estimates were observed to vary largely under lighting condition. The current work also has carried out a thorough comparative analysis of drop velocity-diameter relation between a tropical and a mid-latitude location and presented the evidences of non-terminal velocities in natural rain of these regions. The results point towards the need of correction in radar retrieved rain data using ground based measurements. Besides, it also indicates notable variation of non-terminal drops in two different rain types and climate regimes.

Research publications

Journals

Papers that are included in this thesis

1) Chatterjee, C., Das, S., On the association between lightning and precipitation microphysics; *Journal of Atmospheric and Solar-Terrestrial Physics*, 2020,207, doi:10.1016/j.jastp.2020.105350.

2) Chatterjee, C., Das, S. Recent changes in Indian monsoon in light of regionalization based on various rain features. *Theoretical and Applied Climatology*, 2021, 146, 1007-1018, https://doi.org/10.1007/s00704-021-03781-z.

3) Chatterjee, C.; Porcù, F.; Das, S.; Bracci, A. An Investigation on Super- and Sub-Terminal Drops in Two Different Rain Categories and Climate Regimes. *Remote Sens.*, **2022**, *14*, 2515. https://doi.org/10.3390/rs14112515.

4) Chatterjee, C., Mandal, J., Das, S., Machine learning approaches for seasonal prediction of lightning activities over India, *International Journal of Climatology* (under review).

Others

5) Das, S., Chatterjee, C., Rain characterization based on maritime and continental origin at a tropical location, *Journal of Atmospheric and Solar-Terrestrial Physics* (2018), doi:10.1016/j.jastp.2018.02.011.10.1016/j.jastp.2018.02.011.

6) Chatterjee, C., Das, S., Characteristic Differences between Two Contrasting Tropical Squalls. *Earth system and science* (under review).

Conferences

1) C. Chatterjee, S. Datta and S. Das, Characteristic Differences between Thunderstorm and Non-Thunderstorm Rain, National Space Science Symposium, 2019.
2) S. Datta, C. Chatterjee and S. Das, Monitoring of Thunderstorm Using Indian Navigation Satellite Constellation NavIC, National Space Science Symposium, 2019.
3) S. Das, C. Chatterjee, S. Chakraborty, A Machine Learning Approach To Re-Classification Of Climate Zones Based On Multiple Rain Features Over India, IGRASS 2019.
4) C. Chatterjee, S. Datta and S. Das, Prediction of Atmospheric Water Vapour from Indian Navigation Data Using Deep Learning Techniques, National Space Science Symposium, 2022.
5) S. Das, C. Chatterjee, N. Singh, Microphysical Evolution of a non-conventional Tropical Squall in Conjunction with NavIC signal, National Space Science Symposium, 2022.
6) C. Chatterjee, S. Das, Change in extreme rainfall over Indian subcontinent, URSI AT-AP-RASC 2022.

Awards

- ❑ Young scientist award: International Union of Radio Sciences combined Atlantic / Asia-Pacific Radio Science Conference (URSI AT-AP-RASC 2022), Gran Canaria, Spain, Europe, 29 May - 3 June 2022.
- ❑ Best thesis award: IEEE International India, Geoscience and Remote Sensing Symposium 2021, virtual conference, 6-10 December, 2021.

Table of contents

List of figures ……….…………………………………………………xii

List of tables……………………………….……………………….xvii

Acronyms …………………………………..…………………..xviii

1 Introduction

1.1 Rain in India……………………………………………………...…..1

1.2 Climate change and Indian rain ……………………………………...2

1.3. Rain measurements techniques and uncertainties…………,,,……..…3

1.4 Organization of the thesis……………………………………………...6

2 Past studies and problem statements

2.1 Introduction…………………………………………..…………...9

2.2 Past studies on rain regionalization…………………………………….9

2.3 Past studies on lightning prediction and rain microphysical alteration due to lightning………………………………………………………..………10

2.4 Past studies on rain drop velocity………………………………………12

2.5 Problem statements …………………………………………………...13

2.6 Thesis contribution…………………………………………………..14

3 Regionalization of Indian rain

3.1. Introduction…………………………………………………………..16

3.2 Data and Method ……………………………………………...….17

3.3 Results……………………………………………………….……18

3.3.1 Clustering analysis………………………………...………………..20

3.3.2 Homogeneous rain zones……………………………………..……24

3.3.3. Study of recent rain trend over newly formed rain zones…………..…24

3.4. Conclusion ……………………………………………….………..30

4 A Machine learning technique for prediction of lightning over Indian subcontinent

4.1 Introduction…………………………………………………………...32

4.2 Data and Methodology……………………………………………..…35

4.2.1.Data…………………………………………..………………....35

4.2.2 Identification of lightning climatologies……………………………..36

4.2.3 Regression models for estimation of lightning activities……………..37

4.2.4 Feature ranking to understand the atmospheric influence on lightning activities…………………………………………………………………...38

4.3. Results……………………………………………………………….. 39

4.3.1 Atmospheric variables and their degree of influence on lightning activities over different climatologies during monsoon and pre-monsoon season…………………………………………………………………48

4.4 Conclusion……………………………………………………………..53

5 Impact of lightning on precipitation microphysics

5.1 Introduction…………………………………………………………..54

5.2 Data and Methodology……………………………………………….55

5.2.1. Instruments…………………………………………………….....55

5.2.2. Data and Methodology of Analysis ……………………………….58

5.3 Results and discussion………………………………………………..68

5.3.1. Case Studies……………………………………………….……..68

5.3.1.1 Lightning event on June 1, 2018…………………………….….68

5.3.1.2. Non-lightning event on Nov. 16, 2017……………………………71

5.3.2 Long term statistics………………………………………………71

5.3.2.1 Rain microphysics…………………………………………………74

5. 3.2.2 Cloud Properties……………………………………………….....74

5. 3.2.3. Rain integral parameters………………………………………….77

5.4. Conclusion………………………………………………………………..79

6. Evidences of super- and sub-terminal drops in different rain categories, and climate regimes

6.1. Introduction……………………………………………………………80

6.2. Materials and Methods…………………………………………………82

6.2.1 Location and Experimental Setup ……………………………………82

6.2.2. Methodology………………………………………………………84

6.3 Results…………………………………………………………..…87

6.3.1 Comparative rain microphysical structure and non-terminal drop occurrences…………………………………………………………87

6.3.2 Investigation of physical processes involved in presence of non-terminal raindrops……………………………………………………95

6.3.3 Identification of causes behind non-terminal drops in individual events…………………………………………….………98

6.4 Conclusion………………………………………………….…..105

7. Major outcomes and discussion

7.1 Introduction…………………………………………………………107

7.2. Regionalization of Indian rain……………………………………..107

7.3 A Machine learning approach for prediction of lightning over Indian subcontinent………………………………………………………………..109

7.4 Lightning influences on Precipitation Microphysics………………….110

7.5 Evidences of super- and sub-terminal drops in different rain categories and climate regimes……………………………………………………………..112

8. Conclusion and future scope

8.1 Conclusion…………………………………………………………..114

8.2 Future scope……………………..…………………..…………………116

Appendices

Appendix- A……………………………………………………….117

Appendix –B………………………………………………………120

Appendix- C……………………………………………………..122

References…………………………………………………………128

List of figures

. 3.1 Spatial variability of rain features over Indian subcontinent: (a) Mean monthly convective rain intensity (mm/h) (b) Mean monthly stratiform rain intensity(mm/h) (c) Mean monthly rain frequency and (d) Average rainfall (mm/day) during summer monsoon and (e) Rainy days/year and (f) heavy rainfall days (> 40 mm rainfall) /year……………….……………….………19

3.2 Performance analysis of clustering using Silhouette plot….....................21

3.3 The distribution of clustered data points for the studied features (in normalized unit): (a) Mean monthly convective rain intensity (b) Mean monthly stratiform rain intensity (c) Mean monthly rain frequency and (d) Average rainfall during summer monsoon and (e) Rainy days/year and (f) heavy rainfall days (> 40 mm rainfall) /year ………………….…………22

3.4 The inter-relationships between rain features in different clusters…………………………………………………………………23

3.5 Proposed regionalization……………………………………………..24

3.6 Variation of mean monthly monsoon rain over the years in newly proposed homogeneous Regions……………………………………………29

4.1 Distribution of (a) atmospheric temperature (K) at a height of 2 meter above the ground (a) before and (b) after the interpolation………………………………………………………………....37

4.2 Distribution of Lightning density (Flash/km^2/day) (a) before and (b) after the interpolation……………………………………………………………….37

4.3 Spatial distribution of average (a) atmospheric temperature (K), (b) CAPE (J/Kg), (c) specific humidity (at 300 hpa) [Kg/Kg] and (d) number of lightning flash (Flash/km2/day) over the Indian subcontinent during the year 2003-2014……………………………………………………………………….…40

4.4. Clusters over Indian subcontinent based on lightning activities……………………..40

4.5 Elbow plot for the clustering process …………………………………41

4.6 Distribution of various atmospheric features in different clusters…………………………………………………………………...…42

4.7 The comparison between actual and predicted annual lightning density (Flash/km^2/day) in the seven clusters estimated by Random forest model…………………………………………………………………………45

4.8 Time series (for consecutive months in 2012-2013) for the actual and predicted values of lightning strikes in the seven clusters by Random forest model……………………………………………………………………..46

4.9 Spatial distribution of annual lightning density (Flash/km^2/day) over Indian region (a) estimated and (b) LIS retrieved actual value…………………………………………………………………………47

4.10 Spatial distribution of monsoon lightning density (Flash/km^2/day) over Indian region (a) estimated and (b) LIS retrieved actual value…………………………………………………………………………48

4.11 Spatial distribution of pre-monsoon lightning density (Flash/km^2/day) over Indian region (a) estimated and (b) LIS retrieved actual value …………………………………………………………………………….49

4.12 Rank of features for the seven clusters. Absolute value of Pearson coefficient used for ranking. The white filled dot represents negative correlation…………………………………………………………………...…52

5.1: Study location (https://www.google.com/maps/place/Kolkata)..56

5.2: (a) cloud effective radius and (b) cloud top temperature on June 1, 1, 2018 …………………………………………………………………...69

5.3: (a) Rain DSD, rain rate and lightning flashes d) Maximum reflectivity obtained from Doppler weather radar volume scan on June 1, 2018………..70

5.4: (a) Rain DSD, rain rate and lightning flashes (b) Maximum reflectivity obtained from Doppler weather radar volume scan on Nov 16, 2017………72

5.5 (a) cloud effective radius and (b) cloud top temperature on Nov 16, 2017……………………………………………………………………….73

5.6: Average number concentration for rain categories without and with lightning for rain rate (a) 1 -5 mm/h, (b) 5-10 mm/h, (c) 10-40 mm/h, and (d) 40-200 mm/h ……………………………………………………………….75

5.7: Mass weighted volume diameter for two types of rain…………………76

5.8: Probability density function of cloud properties: (a) Cloud effective radius (b) Cloud top temperature……………………………………………77

5.9: Z-R relation obtained for two rain events with and without lightning…78

5.10: Specific path attenuation for rain with lightning (WL) and without lightning (WNL) at 13.6 GHz and 35.5 GHz………………………………..78

6.1**:** Location of the two study areas………………………………………...83

6.2: Rain drop size distribution in Kolkata and Bologna for (a) whole dataset, (b) convective rain, (c) stratiform rain……………………………………………88

6.3: Spread of velocity-diameter spectra for the whole dataset in (a) Kolkata and (b) Bologna; for convective rain in (c) Kolkata and (d) Bologna and for stratiform rain in (e) Kolkata and (f) Bologna. The colors represent the number of drops on the $\log_{10}$ scale. The green line is the GK line, and the red line is the mean of the V-D relationship observed for the dataset with the standard deviation shown as error bars……………………………………..90

6.4: Fraction of (a) super- and (b) sub-terminal drops in the natural rain of Kolkata and Bologna. The fraction of sub- and super-terminal drops represents the ratio between these drops and the total number of drops…....92

6.5: Fraction of super-terminal drops for (a) convective and (b) stratiform rain in Kolkata and Bologna. The fraction of super-terminal drops represents the ratio of these drops and the total number of drops…………………………..93

6.6: Fraction of sub-terminal drops for (a) convective and (b) stratiform rain in Kolkata and Bologna. The fraction of sub-terminal drops represents the ratio of these drops and the total number of drops…………………………..94

6.7: Distribution of HS values in natural rain of Bologna and Kolkata…….95

6.8: Distribution of wind speed during the rain events……………………...96

6.9: Fraction of super- terminal drops in the rain events in (a) Kolkata and (b) Bologna. The color bar represents the fraction of drops……………………99

6.10: Fraction of sub-terminal drops in the rain events in (a) Kolkata and (b) Bologna. The color bar represents the fraction of drops…………………100

6.11: Distribution of fraction of break-up minutes in events with lower (than average) and higher (than average) percentage of super-terminal drops in (a)

Kolkata and (b) Bologna. The break-up minutes fraction represents the ratio of the number of break-up minutes with the total rain minutes……………102

6.12: Distribution of peak D_m in events with lower (than average) and higher (than average) percentage of sub-terminal drops in (a) Kolkata and (b) Bologna…………………………………………………………………103

6.13: Relation between (a) break-up minutes fraction and fraction of super-terminal drops and (b) peak D_m and fraction of sub-terminal drops in Kolkata and Bologna. The break-up minutes fraction represents the ratio of the number of break-up minutes with the total rain minute……………104

List of tables

3.1 Trend of Monsoon rainfall over the years in proposed rain zones

with Mann Kendall trend analysis results…………………………….…….30

4.1 Hyper-parameters and performance of the regression models……..….43

4.2 Performance of different regression models…………………..……….44

4.3 Actual and predicted mean and variability of lightning density in different clusters ……………………………………………………..…………..…..49

5.1 Details of the events studied…………………………………….……...60

5.2 DSD parameters of the two rain categories……………………..…....67

6.1 Number of DSDs in the C/S classes…………………………………....87

6.2 Number of DSD samples (2 minutes) in different HS classes. Cells in grey represent classes where break-up exists…………………………..……97

6.3 Statistics of non-terminal drops in Bologna and Kolkata…….105

Acronyms

DPR: Dual Precipitation Radar

DSD: Drop size distribution

GPM: Global Precipitation Measurement Mission

GK: Gunn-Kinzer

IGB: Indo-Gangetic Basin

IMD: Indian Meteorological Department

ITCZ: Inter -Tropical Convergence Zone

TRMM: Tropical Rain Measuring Mission

GPM : Global precipitation Mission

ML: Machine Learning

QPE: Quantitative Precipitation Estimation

Chapter 1

Introduction

1.1 Rain in India

Rain is probably the most impactful atmospheric factor controlling the weather as well as the long term climatology of a region. Every climatological zone has a unique rain pattern defining the seasonal and spatial distribution of precipitation. Proper understandings of various rain features are crucial in assessing the rain climate of any given region.However, rain is a complex process regulated by various climatological and topographic features. Any change in climatological factors can influence rainfall over a particular geographic location. Moreover, rain is a very inhomogeneous process which varies widely in different geographic locations.

India largely depends on agriculture for its economy. The major source of agricultural water in India is rainfall, particularly the monsoon rain. Any uncertainty or irregularity introduced in the rain cycle, therefore, affects the country's wellbeing directly. The country has an enormous variety of topographic elements ranging from high mountains, large plateaus to lowlands and depositional plains of mighty rivers. The presence of Himalayas at the northern part plays a role in the intensity and distribution of Indian monsoon [1].Therefore, proper understanding and characterization of Indian monsoon over different parts of the country is crucial. However, the enormous topographic variety offers large inhomogeneity of the rainfall process over different regions across the country.

1.2. Climate change and Indian rain

Recent climatic changes haveimpacted all the climatological variables and their interplay. Increasing global temperature and its consequences on the precipitation cycle are evident all around the globe. The scenario over India is also not much different. The changes are reflected not only in the annual mean temperature but most disturbingly, the frequency of warm and cold extremes have also increased significantly over last four decades [2]. According to Clausius-Clapeyron, atmospheric water holding capacity increases by 7% for each 1°C increase in temperature [3].However, the increase is not uniform everywhere in atmosphere.The resulting water cycle intensification is responsible for development of disastrous storms. Several reports from all over the world have shown that the places (mainly coastal places) which are already hotspots of tropical storms, cyclone are getting prone to even more such intense rainfall and destructive events. On the other hand, the areas which were already dry and distant from coast, are being prone to draughts.(https://public.wmo.int/en/media/news/climate-changeincreased-extreme-rainfall-southeast-africa-storms). IPCC mentioned in their report in 2021 that water cycle is likely to intensify over some region whereas, some other regions will be subjected to increased draught.(https://www.ipcc.ch/2021/08/09/ar6-wg1-20210809-pr/). In [4], authors has reported notable decrease in monsoon rainfall over different parts of India whereas, significant changes have been observed in the time cycle of monsoon [5]. The one day extreme rainfall has increased significantlyover majority of coastal places[6].

Another very important component of this increasing extremity is lightning.The lightning activity during a thunderstorm indicates the degree of atmospheric convection. The convection in atmosphere is a result of the atmospheric instability majorly due to the boundary layer heating. Interestingly, these regions of instability have a well-organized pattern over the world, strongly correlated with the global climate which is driven by the differential heating of the earth’s surface by the sun. Therefore, any change in the climate is likely to alter the regions of convection, their intensity, and therefore, the lightning patterns around the globe[7]. A significant rise in the frequency, intensity and geographical spread of lightning strikes has been observed over India in recent past. Climate Resilient Observing Systems Promotion Council (CROPC) reported a 34% jump in lightning strikes (http://www.cropc.org) resulting in significant fatalities.However, proper characterization and projection of the rainfall and lightning process need understanding of different rainand lightning climatologies prevailing over different parts of this country given the topographic and climatic variety offered by the country.

1.3. Rain measurementtechniques and uncertainties

The first known reference about a rain measurement was mention in Arthasastra by Kautilya in the fourth century BC [8] in India. The first standardized rain gauge was invented in Korea in 1441. In India, even though measurement based on rain gauges started much early with several stations established over the country, all these came under one umbrella after the establishment of Indian Meteorological Department in 1875.However, techniques like stain method or flour-pellet method were manual. The automatic rain measurement techniques which started much later, are broadly of two classes i.e. in-situ and remote sensing based measurement techniques. Tipping bucket rain gauges happened to be the simplest form of in-situ rain measuring techniques which provides the rainfall amount. Disdrometers can measure the rain drop size depending upon the equivalent mechanical/electrical energy or magnetic induction generated by a falling drop in to the measuring plate or using Doppler principle. The recent advancement of rain measuring techniques allowed the use of laser in the measurements. The laser based precipitation meter sends a pulse from the transmitter towards the receiver terminal and measures both the rain drop diameter and velocity with the help of measured voltage drop and delay. The rain measurements have come along a very long way from a limited accuracy static measurement to a very precise measurements of very tiny to very large drops with very low to very high velocities e.g. OTT PARSIVEL2 is able to record hydrometeors within a diameter range of 0.062mm-24.5mm and a velocity range of 0.05m/s-20.8 m/s.However, point based measurements of rainfall cannot provide the spatial variation of the rainfall process which is crucial in rain analysis.

Remote sensing based rainfall measurements can majorly be achieved using either radars or radiometers. Microwave radiometers have gained high interest in recent past for its high temporal and sounding accuracy featuring successful prediction of convection.However, satellite radiometric measurements are prone to errors over land surfaces. The radars, on the other hand, measures the reflectivity (and/or Doppler velocity) of rain and cloud particles in appropriate frequency ranges. In India, IMD operates 29Doppler radar stations spread across the country operating at S, X or C band frequencies (https://mausam.imd.gov.in). Satellite based radar measurements, for e.g. TRMM and GPM, can complement upto some extent the data gaps in ground based radars and rain gauges. Precipitation radars on-board earth observing satellites usually operates at Ku, Ka or higher frequency bands for global precipitation monitoring. Precipitation Radar (PR) operating at 13.6 GHz onboard Tropical Rainfall Measuring Mission (TRMM) facilitated detailed rain measurements over tropics during the period of 1997-2015[9].The currently operating successor, Global Precipitation Measuring Mission (GPM) is capable of providing detailed microphysical structure of the precipitation system using a Dual-frequency precipitation radar (DPR) operating at 13.6 and 35.5 GHz[10].

The analysis and prediction of rainfall over such a vast country of varied and insurmountable topography can only be achieved with radar measurements speciallyby the satellite-borne ones. Quantitative Precipitation Estimation (QPE) in radar remote sensing is one of the major research focuses in meteorology and climatology, and can facilitate improved modeling of hydrogeological disasters. However, radar-based QPE is challenging due to various uncertainties associated with it. As radar measures only the radar reflectivity or Doppler velocity of falling rain drops, the accuracy of the rainfall estimation depends on the relations between the measured parameters and rainfall estimates. The rain integral parameters like rain rate and radar reflectivity depend strongly on the rain microphysics [11]. The rain microphysics, on the other hand, largely depends on weather conditions and precipitation forming processes. The fundamentals behind precipitation measurement science lie in measuring statistical distribution of different sized rain drops i.e. Drop size distribution (DSD), their spatio-temporal evolution and drop growth/break up mechanism.

The nature of DSD and its relationships with the radar retrieved parameters varies significantly for different rain origin and types and under different rain conditions. Therefore, successful retrieval and analysis of the DSD under varied scenarios facilitate for the estimation of EM response to atmospheric states [12], which makes it crucial for radar meteorology and DSD can serve as the pathway for rectifications of radar data. The relationships between DSD and the radar retrieved parameters show significant spatio-temporal alterations due to several reasons including topography, origin and climatic conditions[13]. This is significantly prominent between tropical and temperate locations [14-15] e.g. varied populations of large drops have been reported from different parts of the world, with the highest concentration in tropical rain [16]. Seasonal impacts seemed to be extremely crucial in the radar reflectivity and rainfall relationships [17]. The power law relationship connecting reflectivity and rainfall has been long argued to vary notably for different rain types [18]. Also, it has been observed to differ strongly with rain intensity [20]. The wind circulation also influences the rain microphysics significantly. The rain originating from maritime wind offers more numbers of tiny rain drops in the rain spectra than that in rain resulting from the continental winds [20]. The radar reflectivity and rainfall relationship shows visibly different nature under the two said precipitation process. The vertical evolution in natural rainfall is also very crucial which introduces errors in both ground-based and satellite-borne radar estimations [21]. The said inaccuracies are majorly due to the growth mechanism of raindrops, which are mostly caused by coalescence, melting, evaporation, and breakup in atmosphere. The rain rate estimation along the vertical profile can thus be influenced notably due to this variation of DSD. Many researchers have carried out detailed analysis on the same [23-25].

The successful retrieval of rain microphysics is also crucial in studying the recently increasing rain extremes as well. The severe thunderstorm events associated with very heavy precipitations and flash floods are nowadays notably increasing over the coastal parts of India. The variation of rain microphysics, however can serve as a pathway for predicting the severity of a mesoscale system and locating its trajectory. Authors in [26],studied the characteristics of the DSD in seven Tropical Cyclones during the year 2004–06.The study reported more tiny (diameter < 1 mm) and midsize drops (from 1 to 3 mm) and a few large drops (>3 mm) while the maximum diameter rarely reached 4 mm. DSD characteristics of 13 typhoons were studied using 2D video disdrometer in northern Taiwan which revealed the DSDs to be neither the typical maritime nor the continental types of convective systems[27].This characteristic were attributed as the influence of terrain. Typhoon Morakot (2009) showed significantly different DSD characteristics between the outer rainband and the eyewall[28]. In [29], authors proposed an improved methodology to estimate the relation linking rain microphysical parameters with the rain reflectivity under a squall line event in Brazil.

Therefore, it is quite evident that various uncertainties play there parts in measurements of rainfall parameters which influences the accuracy of radar based QPE. Among all these factors, this thesis aims to focus on two less explored areas i.e. uncertainties due to lightning and the notion of terminal velocity in natural rain.

1.4 Organization of the thesis

This thesis identifies different monsoon rain climatologies over India based on multiple rain features and recent rain extremesby assimilating the satellite and raingauge data for the first time. It proposes a novel lightning prediction approach using satellite measurements and characterizes rain microphysical parameters for two significant error sources in radar rain measurements.

Chapter 2 presents the previous literatures and the problem statements attempted in this thesis.

Chapter 3 provides a description of the rain regionalization performed using machine learning over Indian subcontinent based on multiple rain parameters including the rain extremity features by assimilating satellite and ground rain measurements. It identifies the different rain climatologies existing over different parts of the country and investigates the monsoon rain trends over those regions over last four decades in order to identify the climate change susceptible regions over India.

Chapter 4 presents a machine learning approach, developed to predict lightning density over different parts of the country in view of the recently increasing thunderstorm fatalities due to climatic changes.

Chapter 5presents the investigation on rain microphysics during lightning. It shows the characteristic differences of cloud system and ground rain during lightning and non-lightning conditions from a tropical location.The differences in microphysical as well as the integral parameters of rain were studied based on the experimental measurements at Kolkata, a tropical location in India.

Chapter 6 presents the analysis of rain drop fall velocity and diameter relation in natural rain occurring over tropical and mid-latitude locations. This chapter presents the evidences of non-terminal velocity drops in natural rain and quantifies the super- (exceeding terminal velocity) and sub- (below terminal velocity) terminal drops in natural rain of the two places, Kolkata (tropical) and Bologna (mid-latitude).The roles of multiple physical processes behind the phenomenon are also investigated in this chapter.

Chapter 7discusses the important outcomes of this thesis.

Chapter 8 presents the conclusions drawn from this thesis work and shows the future scope of this study in view of Indian rain and its susceptibility to climate change.

Chapter 2

Past studies and problem statements

2.1 Introduction

Appropriate methodology for identification of homogenous rain regions is of utmost importance to understand the rainfall process over a large geographic area of interest. The increasing extremities and irregularities of the precipitation cycle makes it even more crucial. This is especially true for a country like India. However, the successful rainfall analysis over a large country is impossible with point measurements. Remote sensing data, on the other hand, can facilitate an accurate modeling of rainfall over India. However, achieving accurate radar based QPE is challenging under various rain conditions due to their varied microphysical structure. This chapter summarized the previous studies on these threetopics, i.e. rain regionalization, prediction of lightning activities and rain microphysics, particularly from Indian perspective.

2.2 Past studies on rain regionalization

Different approaches were attempted by variousresearchers to address the rainfall inhomogeneity by subdividing the country into homogeneous rainfall regions. Some of the approaches were based on conventional methods while machine learning was used for a few of them. Indian Institute of Tropical Meteorology (IITM)proposedthe rain regions to be six,based on thresholding of century-long rain intensity measurements. In [30], authors used correlation analysis and identified 26 homogeneous monsoon rain regions based on seasonal and annual rain data procured from 1025 rain measuring stations across the country. The rain zoneswere reported to be homogeneous in rain frequency, rain type, and temporal scale. However,better coherence was observed during excess rainfall years.Author in [31], proposed five rainfall zones based on the probability of century-long daily rain measurements. The effect of the recent warming on the rain zones were attempted in this study as well. The homogeneous regions obtained were reported to be notably different during the two time epochs of study i.e. 1901-1975 and 1976-2004. The regions looked more scattereddduring the subsequent one.

In [32],authors attempted shared nearest neighbor clustering technique based on summer monsoon rain.Five consistent regions were identified by the authors here by examining the points with high, medium and low connectivity strengths.Authors in [33], reported different homogeneous rain zones over India using the RCDA cluster ensemble algorithm, based on 53 years of rain data during 1951-2003. Till date all the studies attempted monsoon rain regionalization over India based on a single rain feature i.e. rain intensity.However, rain climatologyneeds consideration of many more rain features like rain types, frequency and recent rain extremity.

2.3 Past studies on lightning prediction and rain microphysical alteration due to lightning

Recent water cycle intensification has resulted in frequent formations of severe mesoscale convective systems which can affect human lives with two major components i.e. heavy rainfall and lightning. India witnessesnotable lightning activities due to the ITCZ (Inter-Tropical Convergence Zone) line passing through the central part of the country [34].Recent climatic changes have increased the lightning severity significantly over the country (http://www.cropc.org). The successful prediction of lightning activities over different parts of the country therefore,hasbecome even more crucial these days.Many researchers have ventured into theforecasting and parameterization of the lightning activities over Indian region [35-36]. The maximum surface air temperature were reported to have a positive link with flash density [34].Similar correlation of lightning strikes was reported with CAPE over the north-eastern India and IGB (Indo-Gangetic basin) region [37]. The specific humidity both at lower tropospheric and boundary layer heights seemed to correspond positively with convection and lightning activity over IGBand central and eastern part of Indian subcontinent [37].The lightning activity over north-eastern and north-western arc of the Himalayashas been reported to be well-correlated with the specific humidity of the upper troposphere[37]. A successfullightning parameterization schemes were attempted using WRF model to simulate lightning activities over Maharashtra, India[38].The spatial lightning pattern were predicted by authors in [39]as a function of cloud top height and vertically integrated ice water path. Cloud top height defined by reflectivity threshold were utilized to predict the lightning density over Mahrashtra in another study [40] which successfullyforecasted it during sixteen events. However, the studies mostly focused on prediction of lightning activities over a small geographic area of interest.

The lightning has been reported to be strongly associated with cloud microphysical parameters [41-42]. The nature of association, however, is complex. Other environmental conditions and initial perturbation also seemed to have significant impact on this [43].In [43], authors reported negative association between cloud top temperature and lightning activities. The relationship between columnar ice content in a cloud and lightning flash rate found to be proportional. The vertical distribution of ice particles showed direct correspondence with lightning flashes [45].However, the interdependence varies during different phases of mesoscale system development [46].

Microphysics of ground rain is another very important aspect of a precipitation system. The rain drop size distribution (DSD) has been reported to vary significantly with the number of lightning flashes [47]. Severe convective thunderstorm systems are usually associated with very rapid change in rain DSD. Such events typically contain updraft with large rain drops or groupel[48]. The cloud to ground lightning, in specific seemed to have a negative association with the rain spatial distribution [49].The rain amount resulting from a convective mesoscale system reportedly has a significant correlation with the polarity of lightning strike [50]. Higher volume of rain water was found to be closely linked with occurrences of positive cloud-ground lightning flashes. The shape parameter reportedly gets modified largely by the cloud-to-ground lightning density. The association between rain amount and number of lightning strikes was reported by various researchers from different part of the world [51-52]. Therefore, the difference of precipitation microphysics during rain with and without lightning can be crucial in rain structure and thereby in radar remote sensing of rain.

2.4 Past studies on rain drop velocity

Another very important source of error that can corrupt the radar measurement of rainfall is the consideration of standard velocity diameter relationship in natural rainfall. Most of therain measuring instruments likeJW disdrometers [53] or vertical pointing Doppler radars [54] use the terminal velocity concept to convert the measured velocity to rain drop diameter. The initial form of this was based on laboratory experiments[55].The air density was considered as that in the sea level in Gunn-Kinzer (GK hereafter) relationship. Authors in [56-57], proposed some correctional empirical factors in the equation to take care of the altitude. Changes in the flow field produced in rotational flow region of a rain drop can cause the change in drag force applied to another drop falling just above it.The dimension of this region depends on drop fall velocity and wind turbulence [58].

However, the modified equations were also not able to accommodate the presence of drops outside the terminal velocities.Presence of such drops were reported by various researchers from different part of the world [59-61]. The unstable large drops in natural rain break into smaller dropsto attain stability (hydrodynamical breakup) or this can happen after collisions with smaller drops (collisional breakup) [62-63]. Break-up results in large number of smaller drops. Interestingly, the small drops keep falling with the previous high speed due to inertia. These drops are known assuper-terminal raindrops. Similarly, collisional coalescence of two small drops result into large slow travelling drops called sub-terminal drops. However, the existence of high speed small drops were long argued to be a result of measurement errors but the advancement of highly precise rain measuring instruments like laser precipitation monitor and 2DVD disdrometers, and reports from all around the globe have strengthen the idea[65-66]. In [66], authors have witnessed substantial percentage of super-terminal drops in natural rain during six separate rain events studied using a network of disdrometers[59]. Notable sub-terminal drops were reported by couple of authors especially in drops larger than 3 mm diameter [67, 60]. The high speed small drops have been found to decrease with increasing rain intensity [68]. The fraction of non-terminal drops also showed great dependence on rain types. Such studies are, however, extremely limited and mostly case-based and majorly belong to the temperate locations.

2.5 Problem statements

This thesis focuses on two major areas. Firstly, the thesis aims to explore the process of regionalization of rain and lightning to study the recent rain pattern and predict lightning activities over the entire Indian region.Secondly, the thesis aims to investigate the uncertainties in rainfall parameters for an improved radar based QPE.Following are the major issues this thesis aims to address:

- ❑ This work aims toidentify the different monsoon rain climatologies existing over India based on multiple rain features with careful consideration of rain types and recent rain extremes for the first time. It also plans to look into the susceptibility of monsoon rain over these resulting regions to climate change.
- ❑ The thesis aims to develop a ML(Machine Learning) based lightning prediction model to predict lightning density over different parts of the country based on basic atmospheric features and consideration of different lightning regions in context of the rising thunderstorm fatalities in recent past.

- The thesis focuses on characterizing the differences ofprecipitation microphysics between rain with and without lightning
- This thesisalso aims to have a comparative investigation on the evidences of non-terminal drops in natural rain between a tropical and a mid-latitude location and to quantify the super- and sub- terminal drop percentage in natural rain spectra in specific. Investigating the probable physical processes behind the phenomenon happens to be another important goal of this work.

2.6 Thesis contribution

- The novelty of this work lies in regionalizing Indian subcontinent in homogeneous monsoon rain zones for the first time based on six rain features i.e. convective and strartiform rain intensity, rain frequency, monsoon rainfall amount, number of rainy days/year and number of
- heavy rainfall days (> 40 mm rainfall) /year using k-medoids clustering algorithm. The study reports significantly varied inter-relationships between different rain fetaures in different clusters which confirms the presence of distinct rain climatologies over different parts of the country. The work also reports statistically significant distinct monsoon rain trends in seven of the nine reported rain zones, showing varied susceptibility of Indian rain to climate change.
- The study has subdivided Indian subcontinent based on lightning and associated atmospheric features and proposed a single machine learning based regression model to predict lightning density over the entire Indian region using this clustering information and basic satellite retrieved parameters.

- This work has reported significant characteristic differences between rain under lightning and non-lightning conditions for the first time from a location situated almost on the top of Inter Tropical Convergence Line. Noteworthy distinction has been evidenced in both rain and cloud microphysics under the two said rain conditions. Rain integral parameters also indicated notable variation during lightning.

- This work carried out a rigorous investigation on a large dataset and presented the comparative evidences of non-terminal drops in natural rain of tropics and mid-latitude. The study quantified the sub- (below 70 % of terminal velocity) and super-terminal (exceeding 130 % of terminal velocity) drops in natural rain of Kolkata and Bologna. The study also reports significant contribution of break-up and coalescence in natural rain of the two places.

Chapter 3

Regionalization of Indian rain

The chapter is based on the article "Chatterjee, C., Das, S. Recent changes in Indian monsoon in light of regionalization based on various rain features. *Theoretical and Applied Climatology,* 2021, 146, 1007-1018, https://doi.org/10.1007/s00704-021-03781-z"

3.1. Introduction

Precipitation is an inhomogeneous process both in space and time. It is influenced by several weather parameters and topography. Identification of homogenous rain region is, therefore, important to study and quantify the climate change signature. Till date all the monsoon rain regionalization over India were solely based on a single rain feature i.e. the rain amount. The reason behind the same lies in the fact that the long term rain measurements were accomplished with ground based rain gauges over the country which can facilitate in achieving rain intensity values but measurements based on rain types cannot be procured with such instruments. However, the identification of rain climatologies also depends on rain frequency, types and recent rise in rain extremity. Besides, the dense arrangements of rain gauges and radars are rare over the country to attain a reasonably good spatial resolutions.The only way to address these issues is to utilize satellite data. This study assimilated satellite measurements with ground based data. Tropical Rain Measuring Mission data serves for both spatial variation of rain over large geographic area of interest and multiple rain features including information on two broad classes of rain i.e. convective and strartiform rain. Even though the temporal span of satellite data is limited but this approach can definitely give an indication of the recent rain climatologies over the country.

The current study attempts to regionalize Indian subcontinent in homogeneous rainfall zones based on six different rain features including information on rain types and recent rain extremities. The recent trends of monsoon rain were also investigated over the identified climatologies.

3.2. Data and Method

Six different rain features i.e. convective rain intensity (mm/h), stratiform rain intensity (mm/h), rain frequency and average rainfall amount (mm/day) of monsoon period (JJAS) and number of rainy days/ year and heavy rainfall days (> 40 mm rainfall) /year have been used in this study for the regionalization purpose. The first three feature were retrieved from 3A25 data product of TRMM (Tropical Rain Measuring Mission) satellite whereas, the rest of the three were obtained from CPC (Climate Prediction Center) Global Unified Precipitation data provided by the NOAA/OAR/ESRL PSL, Boulder, Colorado, USA (*https://psl.noaa.gov/* in).The rain features were averaged over the time period of 2003-2014. So, basically a single grid contained six different values as features here. The values are then normalized in order to combat for the computational disproportion. Machine learning provides an inherent advantage ofhandling multiple features simultaneously.K-medoids[69] clustering was performed on the grids over Indian subcontinent to sub divide the country based on the similarities of these six parameters.

K-medoids is a very simple clustering algorithm relying on the idea of minimizing distance of each sample point from the selected *K* number of Medoids.Use of medoids in place of average adds on to the robustness of the method and makes it more efficient against outliers. Here, in the current study the algorithm creates the by cutting down the 6-D distance between the medoidsand data points in eachof the cluster. Visualizing the 6-D relationships are not practical. Therefore, the inter-relationship between multiple sets of two features in the resulting clusters have been studied.The number of clusters has been decided based on experimental results using Silhouette values.

The monsoon rain trend of last forty years have been studied based on GPCP monthly rain data accessed from NOAA over the proposed monsoon zones. The use of the said dataset has provided a long data span of forty years and on the other hand, facilitated the testing of trend with an independent dataset.The trend analysis has been carried out using Mann-Kendal (MK) method (mentioned in detail in Appendix-A) because of its excellent capability in handling outliers, crucial in studying natural climate variables.

3.3. Results

There is prominent inhomogeneity of the rainfall process over different parts of India. The spatial variation of different rain feature (convective rain intensity, stratiform rain intensity, rain frequency and average rainfall amount of monsoon period (JJAS), number of rainy days/year and heavy rainfall days (> 40 mm rainfall) /year /year) in the country were studied to understand the variation of the features in different parts of the country (Fig. 3.1(a-f)).The use of satellite data imposes a constraint of limited data period (12 years) for some of the said features which may not facilitate for trend analysis but it can, for sure help to identify the climatology of a region. The monsoon rain average is temporal average (2003-2014) of mean daily total rain during monsoon. TRMM rain rates (C/S) are mean monthly surface rain rate (successfully classified as C/S). Monthly rain frequency is fraction of pixels having rain among total observed pixels.

The convective rain intensity (Fig. 3.1(a)) is seemed to be largest in the northern part of the subcontinent which decreases in the southward direction. Strartiform rain intensity also showed more or less similar variation pattern (Fig. 3.1(b)) except the width of the similar intensity zones. The extreme northern and southern part of the country has the highest frequency of rainfall (Fig. 3.1(c)).

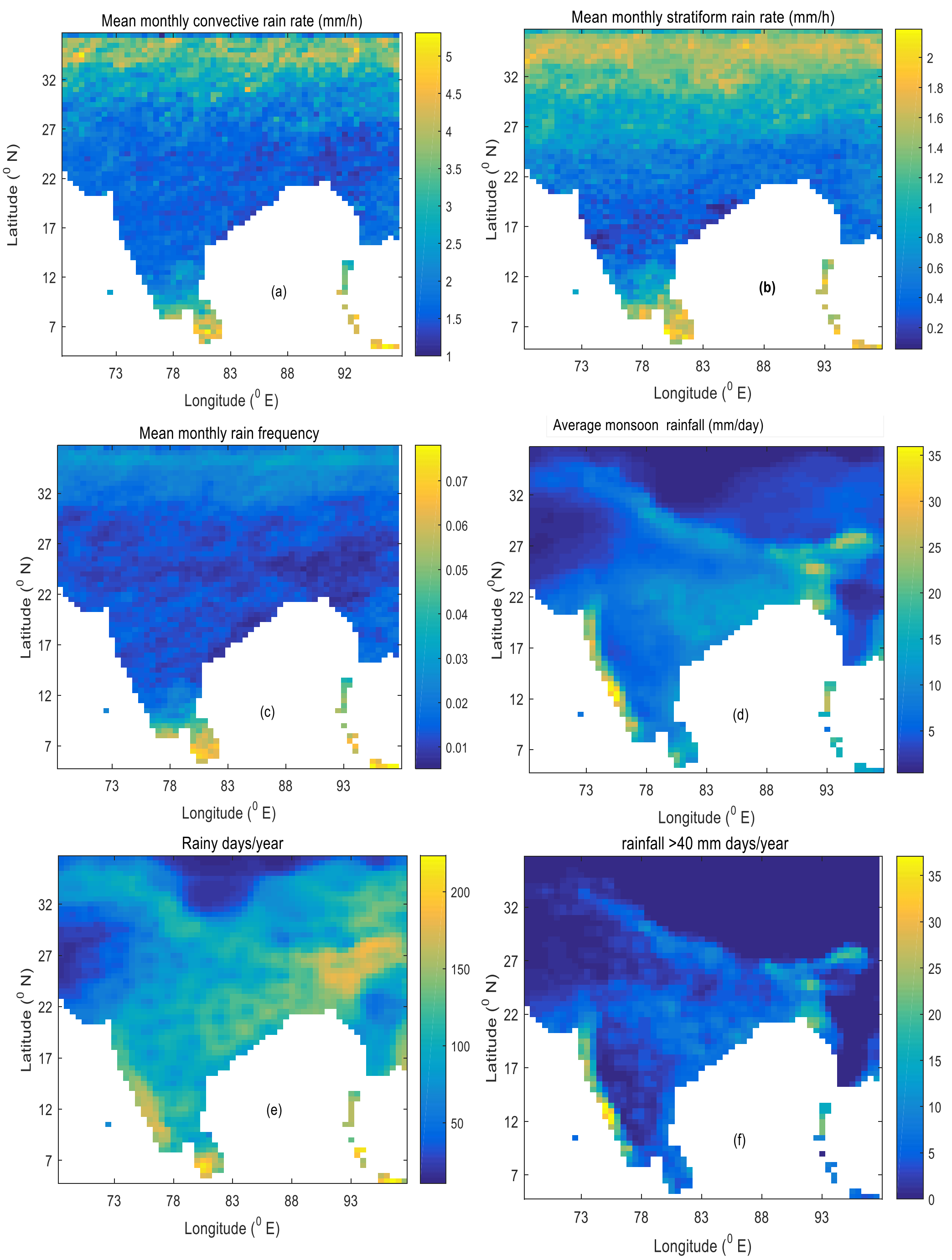

Fig. 3.1 Spatial variability of rain features over Indian subcontinent: (a) Mean monthly convective rain intensity (mm/h) (b) Mean monthly stratiform rain intensity(mm/h) (c) Mean monthly rain frequency and (d) Average rainfall (mm/day) during summer monsoon and (e) Rainy days/year and (f) heavy rainfall days (> 40 mm rainfall) /year

IGB seemed to receive maximum amount of rainfall in the country (Fig. 3.1(d)). North –Eastern part of India gets the maximum number of rainy day/year (Fig. 3.1(e)). The coastal parts of India also gets a good number of rainy days. The number maximizes in the western coast of India when extreme rain fall days are considered which is pretty high over the Indo-gangetic plains as well (Fig. 3.1(f)). It is evident that the different rain features, behave differently over different parts of the subcontinent.It is, therefore, extremely crucial to have a proper regionalization of rain climatologies existing in the country to have a clear idea about the effect of climate change.

3.3.1 Clustering analysis

The K-medoids clustering based on six different rain features has resulted in nine distinct rain zones over the subcontinent which was checked for the consistency using Silhouette plot (Fig. 3.2). A silhouette plot is a representation of how well the objects are clustered. Silhouette value can range between -1 to +1, and a positive silhouette value indicates that the object is well-matched to its assigned clustered, whereas, a negative value represents a poorly matched object. The Silhouette Coefficient is calculated by two factors, namely the mean intra-cluster distance *'a'* and the mean nearest-cluster distance (distance between a sample and the nearest cluster other than its own cluster) 'b' for each sample. The Silhouette Coefficient for a sample is given by

$$S(i) = (b - a)/max(b, a) \qquad (1)$$

The mean silhouette value for all points in a specific cluster provides how tightly that cluster points are grouped. Therefore it gives a measure of how well the data is clustered if we take a mean over entire dataset. So, if too many or too few clusters are chosen then the silhouette figure will show narrower columns for some clusters in comparison to others. Here, Fig. 3.2 indicates a positive Silhouette value for 2289 sample points among 2420 points, which confirms consistency of the clusters.

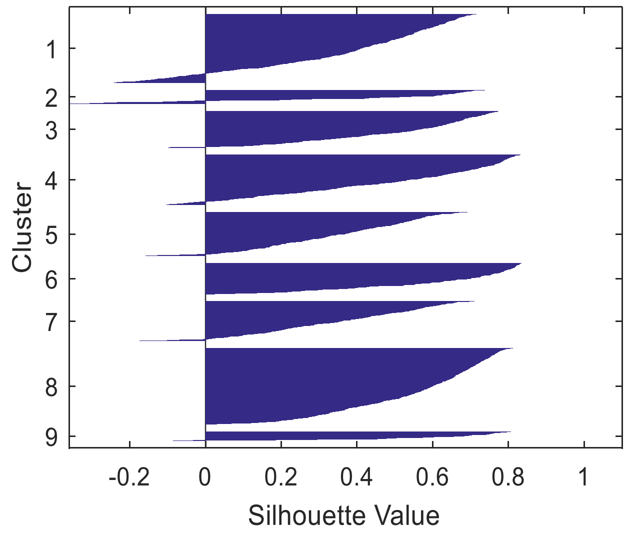

Fig. 3.2 Performance analysis of clustering using Silhouette plot

In order to understand the separability among the nine clusters, the distribution of each of the rain features are then studied for different clusters. Fig. 3.3(a-f) shows the fitted histograms for all the rain features. It is evident that the rain features are clearly separable in various clusters. As an example, the convective rain intensity (Fig. 3.3(a)) has the steepest peak towards a lower range in cluster 8 whereas it has a much wider spread in cluster 6. In cluster 4 and cluster 3, it has clear dominance of low and high values respectively. Similarly, the distribution of stratiform rain intensity (Fig. 3.3 (b)) has a clear gradual right shift starting from cluster 8 while moving towards cluster 4,5,7,6 and 3.

Next, the association among different rain features are investigated. The results indicate that the association between different features also varies in different parts of the subcontinent. Fig. 3.4(a-i) shows some of the inter-relations between features in different clusters. For example, if we focus on the relationship between convective rain intensity and rainy days /year (Fig. 3.4(a)), then we can see that convective rain intensity does not vary much with rainy days/year in cluster 6 whereas, it has almost a linear relationship in cluster 9. On the other hand, rain frequency and rainy days/year (Fig. 3.4(c)) has a negative correlation in cluster 8 but it has a positive correspondence in cluster 3. Stratiform and convective rain intensity seemed to have a strong linear dependence on each in cluster 7 but it is merely relatable in cluster 1(Fig. 3.4(d)). These clear variation in inter-relationships between the features, in the different clusters, indicate the presence of different rain climatology over different regions of the subcontinent.

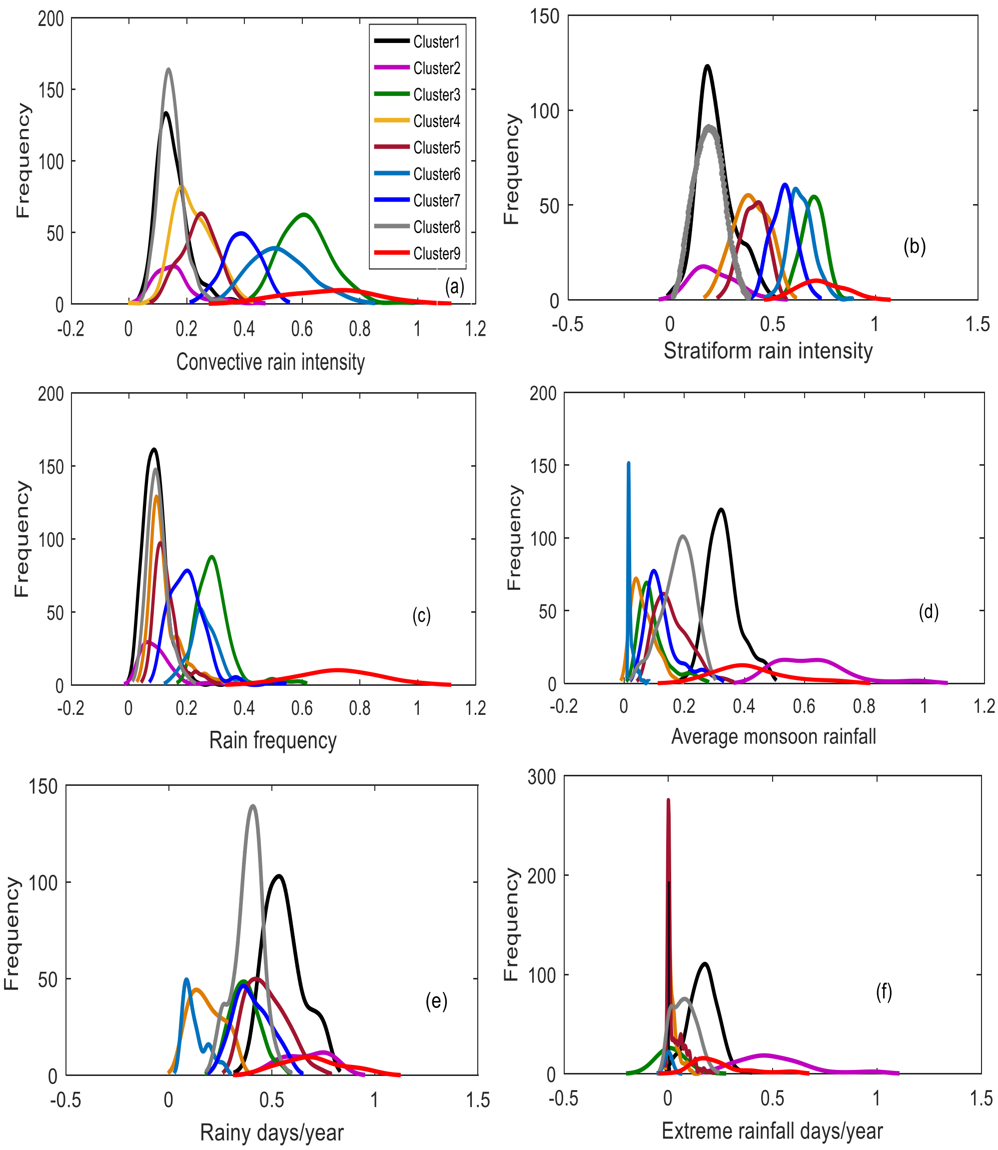

Fig. 3.3 The distribution of clustered data points for the studied features (in normalized unit): (a) Mean monthly convective rain intensity (b) Mean monthly stratiform rain intensity (c) Mean monthly rain frequency and (d) Average rainfall during summer monsoon and (e) Rainy days/year and (f) heavy rainfall days (> 40 mm rainfall) /year

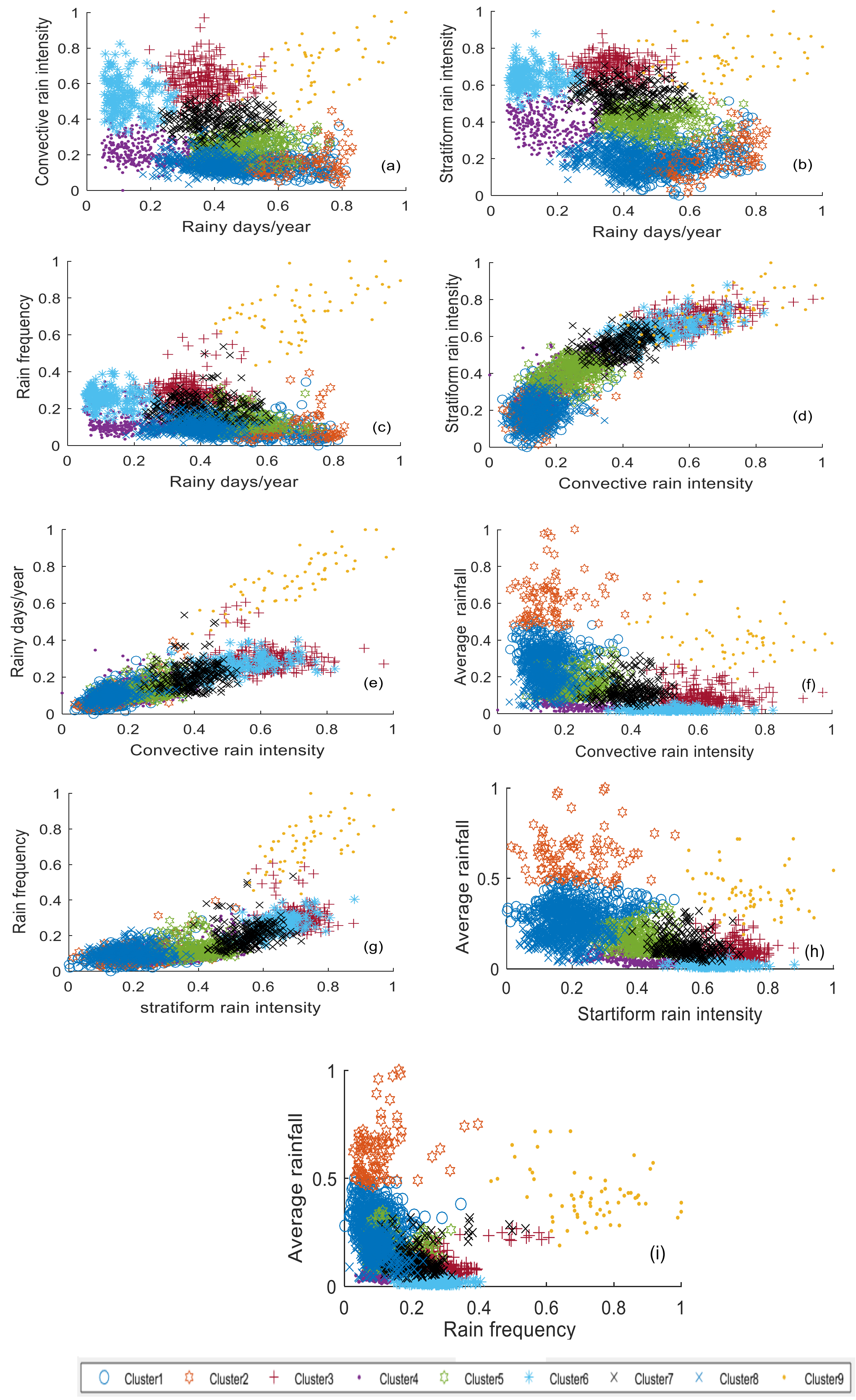

Fig. 3.4 The inter-relationships between rain features in different clusters

3.3.2 Homogeneous rain zones

The proposed regionalization has clustered India in nine distinct homogeneous monsoon zones, and the locations of the regions are shown in Fig. 3.5. The different colours indicate different clusters and numbered as C1, C2, etc. for the sake of readability. The data points of a single cluster are found to occupy more or less the same neighbourhood. However, it is also to be noted that some of the clusters, such as C5 and C3, appears at two disjoint regions. This simply indicates similar rain climatology at two different locations and are treated as part of the same homogenous region for further analysis.

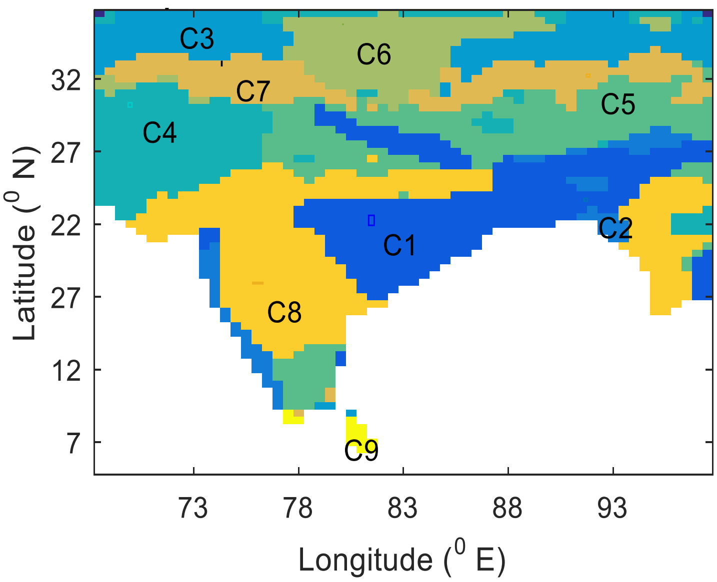

Fig.3.5 Proposed regionalization

3.3.3. Study of recent rain trend over newly formed rain zones

The homogenous regions are formed using the satellite and rain gauge data of 12 years. However, to understand the consistency of the proposed regionalization, monsoon rain trend is studied for each of these said zones. Since satellite data are of limited temporal coverage, the *GPCP monthly precipitation data* of 40 years (1979-2018) has been used for this purpose. Each of these proposed zones are studied separately to investigate if there is any noticeable trend in monsoon rain over the time and whether it is consistent with the previous studies (Fig. 3.6(a-i)).

1) Region C1

This rain zone is primarily spread across the eastern coast of India i.e. along the Bay of Bengal. The trend of monsoon rain here is shown in Fig. 3.6(i). A decreasing rate of 0.370 mm/year is observed in average monsoon rain intensity. The result of Mann Kendall trend analysis presented in Table I also confirmed this signature. The H and p value observed are 1 and 0.012 respectively. This indicates the presence of a monotonic trend. The nature of this trend is confirmed as a downward one with the negative value of Mann Kendall statistics Z_{MK} (-2.645). The state-wise trend reported by [70] also supports this nature of rainfall trend.

2) Region C2

This monsoon zone mainly covers western coast of India, coastal part of Myanmar and a small portion of Indian state Assam. The monsoon rain intensity of this zone during last forty years is shown in Fig. 3.6(b). Mean monsoon rain intensity shows a steep fall over time at a rate of 0.056 mm/year. This trend is further validated with Mann-Kendall trend analysis test (Table I). The trend test rejects (H=1) the null hypothesis of no trend with a p value of 0.046. The result implies a monotonic trend in the data. This region has showed a Mann Kendall statistics Z_{MK} value of -1.990. Z_{MK} reveals an important downward trend in rainfall during last forty years over this particular rain zone. The trend observed here finds good agreement with previously reported 100 years rain trend over western coastal part of India [71].

3) Region C3

This rain zone mostly covers two major parts in Himalayan belt, separately. In one part it includes a portion of Afghanistan and some portion of upper Jammu and Kashmir State of India. In other part, a portion of China shows similar rain climatology. No strong rain trend (Table I) in precipitation is observed in these regions (Fig. 3.6c)).

4) Region C4

This region is located in north-west portion of India and mainly covers the Great Indian Desert along with a small portion of Pakistan. Fig. 3.6(d) shows the monsoon rain intensity over this region during last forty years. The intensity plot points out an increasing trend of average monsoon rain intensity with a rate of 0.020 mm/year. Mann-Kendall trend analysis test (Table I) is performed in order to verify the trend. The H value of test is 1 i.e. the trend test rejects the null hypothesis of no monotonic trend. The p value is obtained as 0.039. This indicates the presence of a monotonic trend. The high positive value (2.060) of Mann Kendall statistics, Z_{MK} indicates a significant increasing trend of rainfall. Climate change seemed to increase mean monsoon precipitation in the Indian desert. Similar results are also obtained by [71] which showed a significant increase in rain amount in this region during the last century using sub divisional rain data prepared by Indian Institute of Tropical Meteorology.

5) Region C5

This homogenous monsoon zone consists a part of the Indo-Gangetic plains (IGP), some portion of north eastern India, small portion of south India and a small portion of Southern China. The mean monsoon rain intensity shows a decreasing rate of 0.023 mm/year as shown in Fig. 3.6(e). Mann-Kendall trend analysis test (shown in Table I) is performed on the data to confirm the trend. The H value of test is 1 and the p value of the test is 0.031. This indicates successful rejection of no monotonic trend assumption. The Mann Kendall statistics Z_{MK} shown a significant negative value (-2.150) which concludes in favour of a falling rainfall trend in this region over time. Authors in[72], has shown similar rain trend over southern China.

The precipitation characteristics of IGP has been studied exhaustively by many researchers and the present study is consistent with the earlier reports.Rain over theIGB has been reported to have a strong a dependence on El-Nino and therefore possess several periodicities[73]. However, many of the studies are able to detect the weakening trend of the precipitation irrespective of these short term trends. The weakening of monsoon rain in IGB is also reported previously by [73].

2) Region C6

The eastern part of Jammu and Kashmir and a small part of western China come under this rain cluster. The region showed weak increasing trend of rainfall, however, the trend observed here is not significant (Fig. 3.6(f) and Table 3.1).

7) Region C7

This rain zone covers the small part of Pakistan, Indian states Punjab, Himachal Pradesh and Uttarakhand (partially) and some part of China. The average monsoon rain intensity over this region (Fig. 3.6(g)) shows an increase rate of 0.017 mm/year. The result of the Mann-Kendall trend test shown in Table I suggests that the null hypothesis of no trend is rejected with a p value of 0.043. Z_{MK} value of 2.015 reflects a rising trend of rainfall in this region over the years. Similar trend is observed over Punjab by [74].In [75], authors has also performed a seasonal rainfall trend analysis and reported increase in monsoon rainfall over Himachal Pradesh.

8) Region C8

This region mostly covers a major portion of central India. The monsoon rain intensity over this region during last forty years is shown in Fig. 3.6(h). The time series of mean monsoon rain intensity clearly indicates a decreasing rate of 0.037 mm/year over the region and this trend is validated by Mann-Kendall trend analysis test (Table I).Authors of [76] also reported decreasing monsoon rain trend over central Indian regions since 1960.The trend test rejects the null hypothesis of no trend with a *p*-value of 0.017 which is much lower than α (0.05). Hence the test suggests the presence of a monotonic trend over the observation period. The Mann Kendall statistics Z_{MK} is obtained as -2.395. This significant negative value of Z_{MK} supports a downward trend of rainfall over this region during last forty years. Authors of [71] have also reported similar trend of rainfall over central Indian landmasses using gridded rainfall data from IITM.

9) Region C9

The C9 rain cluster comprises of the southern-most tip of the country along with the neighbouring island nation, Srilanka. This small region has shown a very significant decreasing trend (Fig. 3.6(i)) in monsoon rain intensity with a decreasing rate of 0.033 mm/year which is confirmed by the Mann-Kendall analysis (Table I). The value of p (0.030) clearly depicts the successful rejection of no trend hypothesis. The Mann-Kendall coefficient is obtained as -2.106. This negative value proves the presence of a falling rain trend. The result finds good agreement with the result obtained by [77] which has also reported similar decreasing rainfall trends for 13 rain gauge stations in Srilanka.

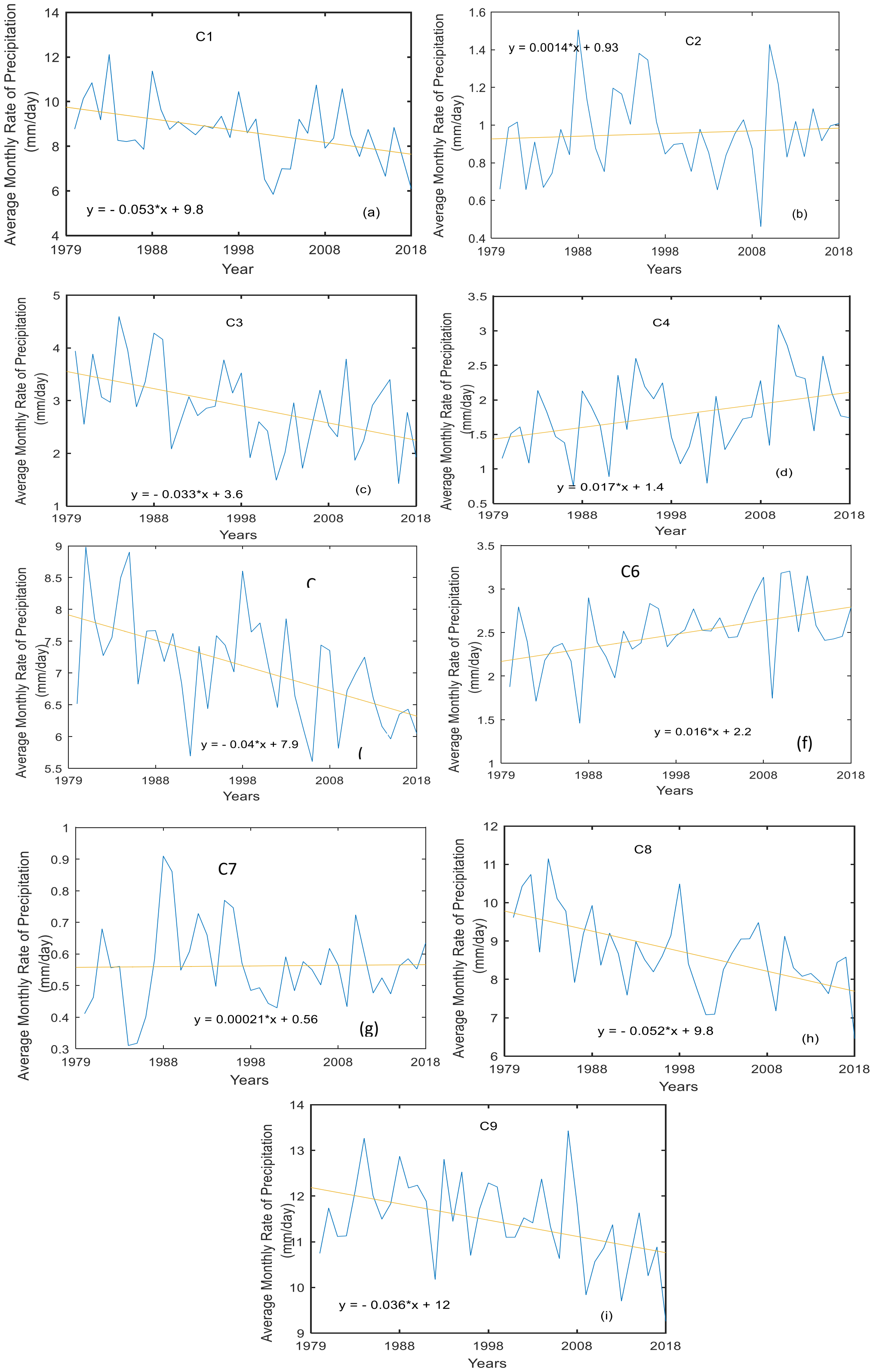

Fig.3. 6 Variation of mean monthly monsoon rain over the years in newly proposed homogeneous regions

Table 3.1: Trend of Monsoon rainfall over the years in proposed rain zones with Mann Kendall trend analysis results

Homogeneous Monsoon zone	**Result of Mann-Kendall trend analysis**			**Conclusion drawn from the test on the trend of Monsoon rain over last 40 years**
	H	***P***	***Z***	
	H	P	Z	
C1	1	0.012	-2.645	decreasing
C2	1	0.046	-1.990	decreasing
C3	0	0.380	0.870	No trend
C4	1	0.039	2.060	increasing
C5	1	0.031	-2.150	decreasing
C6	0	0.450	0.750	no trend
C7	1	0.043	2.015	increasing
C8	1	0.017	-2.395	decreasing
C9	1	0.030	-2.106	decreasing

3.4. Conclusion

The present study proposed a novel rain regionalization approach based on six rain features including information on different rain types and recent rain extremity, obtained byassimilation of satellite data and ground based rainfall measurements. Nine distinct rain climatologies were identified by the clustering process. The regions showed significantly varied inter-relationships between rain features which confirm the presence of different rain climatologies over different parts of the country.

The study reportsstatistically significant decreasing monsoon rain trend over five newly identified homogenous region out of nine. Two rain zones have shown strong increasing trends of monsoon rain. The rain trends observed over newly formed monsoon zones indicate that majority of Indian regions are vulnerable to recent climatic changes. Even though this study focuses on Indian subcontinent, the use of satellite data for the regionalization makes this approach suitable for global rain climatologies. It should be noted that the homogenous region will change if there is a substantial change in climate. The use of averaged value for a longer period may minimize the year-to-year variability, but long term change will change the homogenous regions. As the newly defined homogenous regions are having distinct rain features, the causal relation between monsoon rain and other meteorological parameters can be explored separately for these locations. The results can help in better quantification of climate change effect on these regions and will be attempted in future.

Chapter 4

A Machine learning approach for prediction of lightning over Indian subcontinent

This chapter is based on the article "Chatterjee, C., Mandal, J., Das, S., Machine learning approaches for seasonal prediction of lightning activities over India, *International Journal of Climatology* (under review)"

4.1 Introduction

Another major concern for India, in recent climate change scenario is the increasing lightning fatalities. Lightning can play a direct role in severe impoverishment of human lives and resources. Aviation, wired transmissions of powers can also be interrupted with high surges of cloud-ground lightning. The widely accepted theorybehind the development of the thunderstorm charge dipole is separation of oppositely charged particles.Larger cloud particles due to gravity while the smaller particles are transported in the updraught. When these particles carry negative and positive charges respectively, normal charge dipole is likely to form. Several factors have been proposed to play a role here. [78]observed the electric effect associated with drop break-up near waterfalls. The larger droplets turned positively charged while the tiny ones were negative. This phenomenon can better be presumed from the negative electric charge on the surface of water that is carried away on the smaller fragment droplets. However, break up of droplets is an extremely rare event when clouds system is considered as surface tension forces holds drops together even when severe turbulence is present. Collision between drops may be a factor responsible for drop break up within a cloud system. Even though our knowledge of the many processes involved in the triggering of hydrometeors are today recognized as the dominant source of convective storm electrification. Two categories of processesi.e.noninductive and the inductive mechanisms—are commonly considered to explain electric charge separation within the clouds. The noninductive mechanism is responsible for charge transfer during the elastic collisions between particles [79, 80]. The initial electrification of the storm is thought to be caused by this process and it is also a major contributor to its subsequent intensification or maintenance.On the contrary, the inductive mechanism needs an already existing strong electric field to polarize hydrometeors [81]. Therefore, it can initiate only after the sufficient elecreification of the storm by non-inductive mechanism [82]. The charge separation leads to the typical trioplecharge distribution with positive charges in the upper part of the storm (cloud ice and snow), negative charges in between (graupel) and a thinner positively charged layer from cloud base. Lightning discharges take place when the electric field that builds up from charge separation crosses a threshold value.A convective system strengthens with enhancement in moist static energy(MSE) which occurs mainly due to upward transfer of surface heat fluxes and subsequent warming of the upper troposphere [83]. The gradient of equivalent potential temperature θe is significant near the outflow boundary in the thunderstorms, where dense lightning flashes are observed. As the storm propagates, θe decreases correspondingly and over 80% of lightning flashes occur over regions with θe deficits [84]. When the θe deficits are significant enough, the lightning frequency rises and reaches its maximum value 20-30 minutes later. MSE is capable of capturing overall structures of θe, some important features will still be distorted, specifically the low-MSE pool outside the eyewall. Lightning activity in a convection is closely connected with lifting of condensed water to the mixed phase region and upper troposphere.Strong updrafts that mostly exceed 15m, with a few exceeding 30m, are reported to be linked with all deep convection cases both over land or ocean. land-based and sea-breeze convection usually observed to have higher reflectivities and wider convective cores in comparison with oceanic and tropical cyclone convection [85].

The prediction of short scale weather events like lightning, rainfall etc. have been attempted all over the globe since last few decades. The strong association between charge separation in the cloud and collisions of hydometeors has facilitated for numerical parameterization of lightning activities based on hydrometeor properties [79]. Numerical weather prediction models to predict lightning activities provided a breakthrough in timely assessment of it. Authors in [40]proposed a formulation for estimating both total and cloud-to-ground lightning flash rates over land and ocean based on the convective cloud-top heights. A more elaborated parameterization was proposed by [86] based on cloud-top height and convective mass flux diagnosed by the ECHAM4 global circulation model. Magnitude of Convective Available Potential Energy (CAPE) helps in the updraft and vertical distribution of hydrometeors helps in the charge generation process in a thundercloud [87].Authors of [88] parameterized the lightning trend over the United States based on precipitation and convective available potential energy. Lightning has been linked with different cloud and atmospheric fetaures which happen to be crucial in forecasting the same. Aerosol content in a cloud system has been reported to have a vital role in lightning severity [89, 82]. A simple parameterization of lightning activities were proposed by [90] depending only on the content of hydrometeors. A new parameterization, in the similar line has been proposed to express the lightning densities as a function of short scale variabilities like hydrometeors contents, CAPE, and cloud-base height [48].

Several researchers have attempted the prediction and parameterization of lightning activities over different geographic regions based on both short scale and large scale influencers mostly relying on the conventional methods. The, complex dynamics of thunderstorm process, however, requires a large number for parameters and vast data flow for which machine learning techniques can be an excellent yet simple alternative. The union of atmospheric science and machine learning can facilitate for easier ways in weather forecast. In [91], authors have proposed a hail prediction model over North-eastern Italy based on neural network ensemble. The physical and statistical insight about the regression models to predict the extreme rainfall events gained high attention in recent times [92]. In a very interesting study, [93] reported feasibility of using simple atmospheric datasets in successful prediction of lightning strikes. A 30 min advance lightning now-cast based on air pressure, air temperature 2 m above ground, relative humidity and wind speed was proposed by the authors.

However, all the previous studies were focused on some specific regions.This is because llightning is an extremely dynamic process both in spatial and temporal scale. This is more relatable in a country like India, having such enormous topographic and climatic variety [89,94]. This study, for the first time has attempted prediction of lightning density over the entire Indian region. However, a single model for prediction of lightning density over such a large and varied topography is impossible without the consideration of different lightning climatologies existing over different regions. Besides, the recent climate change scenario has impacted the global lightning activity already. Understanding theinhomogeneity of the lightning process in different Indian region can also help in projecting its vulnerability in various parts of the country[95].

This study aims to regionalize India in different lighting climatologies using lightning density and associated atmospheric variables. The work proposes a ML based regression model for estimating the annual and seasonal (monsoon and pre-monsoon) lightning activities over the entire Indian region based on the regionalization information and various atmospheric parameters, namely specific humidity at four different pressure levels, Convective Available Potential Energy (CAPE), air temperature (2 meter above the surface), K-index, cloud ice particle size and cloud liquid particle size. The current study also aims to provide a ranking of different atmospheric features based on their influences on the lightning activity over different lightning climatologies.

4.2Data and Methodology

4.2.1 Data

The lightning density and atmospheric variables i.e. specific humidity, Convective Available Potential Energy (CAPE), air temperature above 2 meter from the surface, K-index, cloud ice particle size and cloud liquid particle size have been used in this study. The data period of the variables happened to be January, 2003 –December, 2013.

Lightning data were retrieved from Lightning Imaging Sensor (LIS). This sensor on-board TRMM satellite can provide measurements on both cloud-cloud and cloud-ground lightning during day and night and thereby, facilitate the global lightning monitoring. Lightning flash densitywere obtained from LIS/OTD Monthly Climatology Time Series (LRMTS) dataset with a resolution of $2.5° \times 2.5°$ [96]. Specific humidity at four different pressure levels (300 mbar, 500 mbar, 850 mbar, 1000mbar), CAPE, temperature (2 meter above the surface) and k-index data were obtained from ERA5 monthly data product [97]. Cloud particle size data were collected from MODIS level 3 (Aqua/Terra) monthly dataset at $1° \times 1°$ resolution [98].

It is to be noted that the resolution of the different datasets were different.All ERA5 Reanalysis datasets are of resolution $0.25° \times 0.25°$, LRMTS lightning dataset is $2.5° \times 2.5°$ gridded data, whereas MODIS dataset has $1° \times 1°$ spatial resolution. Therefore, all the variables were mapped to a resolution of $1.5° \times 1.5°$ using linear interpolation method for grid matching purpose. The integrity of original and interpolated data wasverified with the distribution. Fig. 4.1(a-b) and Fig. 4.2(a-b) showed the distribution of one down-sampled and one up-sampled data respectively which confirm the distributions before and after the interpolation are consistent.

4.2.2. Identification of lightning climatologies

Understanding of different lightning regions was attempted at first to have a single accurate prediction model for such a large and varied topography like India. The above mentioned dataset were sub-divided in two portions.i.e. 2003-2011 and 2012-2013.

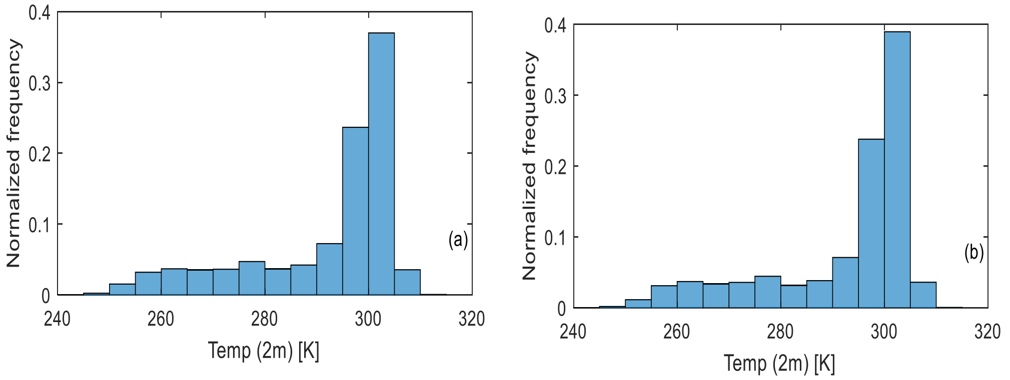

Fig. 4.1 Distribution of (a) atmospheric temperature (K) at a height of 2 meter above the ground (a) before and (b) after the interpolation.

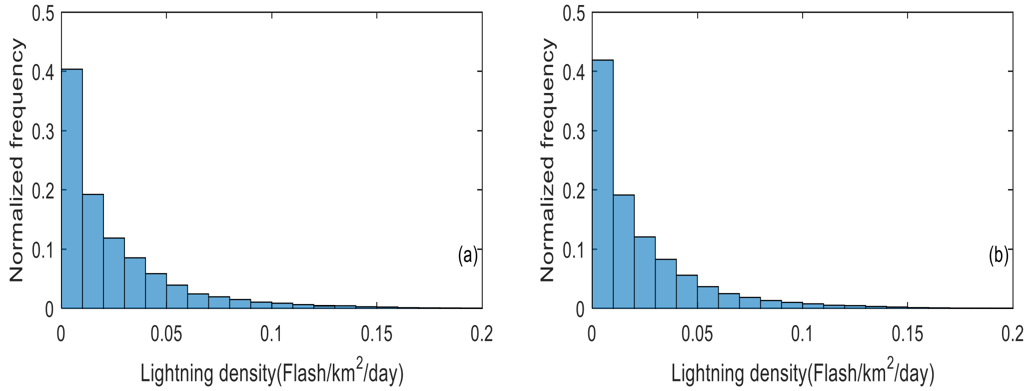

Fig. 4.2 Distribution of Lightning density (Flash/km^2/day) (a) before and (b) after the interpolation

The regionalization process were attempted using the first portion of data while keeping the other portion untouched. K-mean [99] clustering has been used to cluster the Indian region based on lightning density and mentioned atmospheric variables. The simplicity and efficient generalization capability of K-means (mentioned in detail in Appendix-B) was the prime reason behind choosing the algorithm. The computational disproportion were mitigated using normalization of the features. Scikit-learn [100]algorithmwere used here to impute the missing data. This method is based on K-Nearest Neighbors approach.

4.2.3 Regression models for prediction of lightning activities

The prediction of the lightning densitywere attempted using four machine learning based regression models i.e. Ridge regression [101], Lasso regression [102], Decision tree [103] and Random forest [104](details of the models are mentioned in Appendix-B). The dataset on lightning and atmospheric variables were sub-divided in two portions i.e. 2003-2011 and 2012-2013. The prediction model were trained with the first portion of dataset while the second one was used for testing purpose. The train and test sets has47628 and 10584 data points respectively. Here, all the above mentioned atmospheric variables along with the cluster and month information have been used as predictors. Each time the one hot encoding was used on categorical variables (month and cluster), the first column of both encoded categorical variables were dropped to avoid a dummy variable trap. One hot encoding has been done for month and cluster information. The data were normalized to avoid any sort of computational disproportions in case of Ridge and Lasso regression. Data with degree 3 polynomial features have been provided as an input to the models.

R-squared scores for each cluster were computed as a metric to evaluate the performances of the models. The hyper-parameter tuning has been done using 9-fold cross-validation for each of the model. A single year of data were used in each fold. The hyper-parameters providing best mean score has been chosen as best hyper-parameters. The models were trained with best set of hyper-parameters.

4.2.4. Feature ranking to understand the atmospheric influence on lightning activities

Different atmospheric variables have varied association with lightning density. The study has attempted a ranking of the said connection using Pearson correlation separately in the reported clusters.

4.3. Results

Understanding of the spatial pattern of lightning and its influencers in different Indian regions has been attempted firstly.

The hilly areas of Himalayan region showed lower average temperature than that in the Western Ghats. However, these regions are extremely different in from any other region over the Indian subcontinent (Fig. 4.3(a)). The southern and western regions of the country seemed to be hotter than the northern and specially the eastern parts. North-Eastern part of the country showed high CAPE.CAPE values were high over the coastal regions as well whereas; it is a little low over the western part (Fig. 4.3(b)). In [94], authors reported similar spatial distribution of CAPE. The specific humidity increasestowards the south-eastern part fromthe north-western regions (Fig. 4.3(c)). Himalayan region and north eastern India have notably distinct high lightning activities from the rest of the Indian regions (Fig. 4.3(d)) which finds good agreement with previous studies [105]. The western part of the country, on the other hand, shows low lightning activities.The above spatial inhomogeneity indicates the varied pattern of lightning and its influencers over different parts of the country.

The clustering analysis has regionalized Indian subcontinent in seven distinct regions (Fig. 4.4). The neighboring pixels indicated in similar color identify a single cluster. It is evident that all the clusters are very distinctly separable. The clusters are represented as C0-C6 for easy interpretability. The number of clusters and consistency of the clusters has been verified with Elbow method (Fig. 4.5).

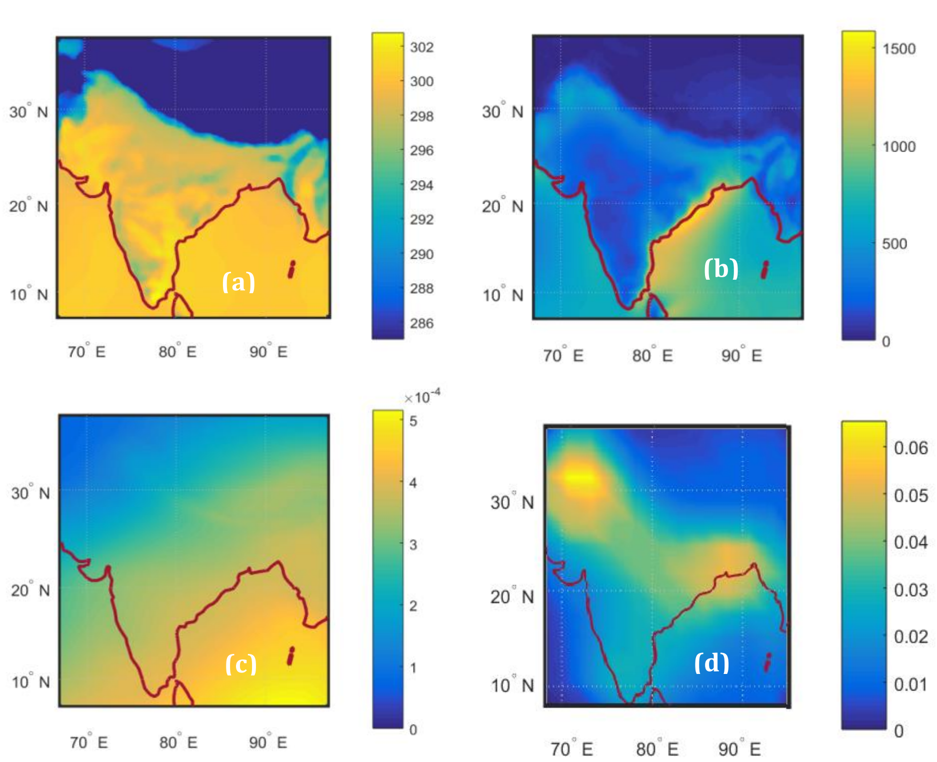

Fig. 4.3 Spatial distribution of average (a) atmospheric temperature (K), (b) CAPE (J/Kg), (c) specific humidity (at 300 hpa) [Kg/Kg] and (d) number of lightning flash (Flash/km2/day) over the Indian subcontinent during the year 2003-2014.

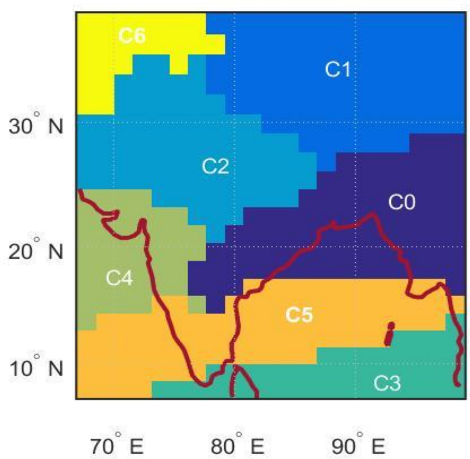

Fig. 4.4. Clusters over Indian subcontinent based on lightning activities

The distributions of the features have been studied next to confirm the separability of the atmospheric variables in different clusters (Fig. 4.6). The distribution of the variables in all the seven clusters showed visible difference which finds good agreement with the separability and consistency of clusters indicated by Elbow method.

For example, distribution of specific humidity at 850 mbar is unimodal for cluster 1 and 6 where cluster 6 showed much larger values. On the other hand, for cluster 2 the distribution is bimodal. Distribution for cluster 3 and 5 is left skewed and unimodal with dominance of larger values in cluster 5.

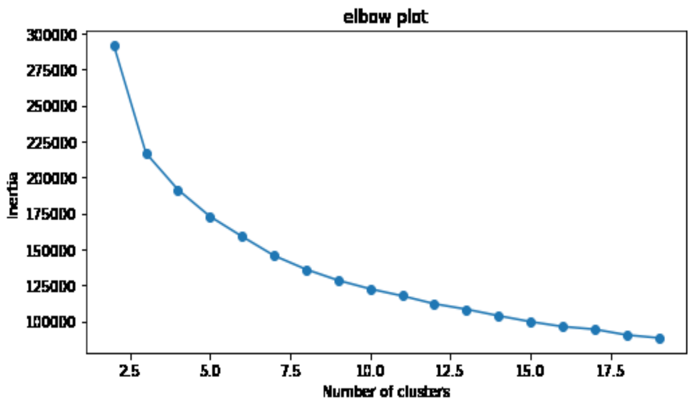

Fig. 4.5 Elbow plot for the clustering process

The prediction of lightning activities has been attempted next using four ML based regression models i.e. Ridge regression , Decision tree and Random forest. Performance of each fold (years) in the 9-fold cross validation has been shown for each algorithm (Table 4.1). Random forest showed the best mean score although in some of the folds Ridge or Lasso regression showed better results. Decision Tree, however, seemed to under-perform in this case. The R-squared scores for individual ML models has been presented for the test set in Table 4.2.

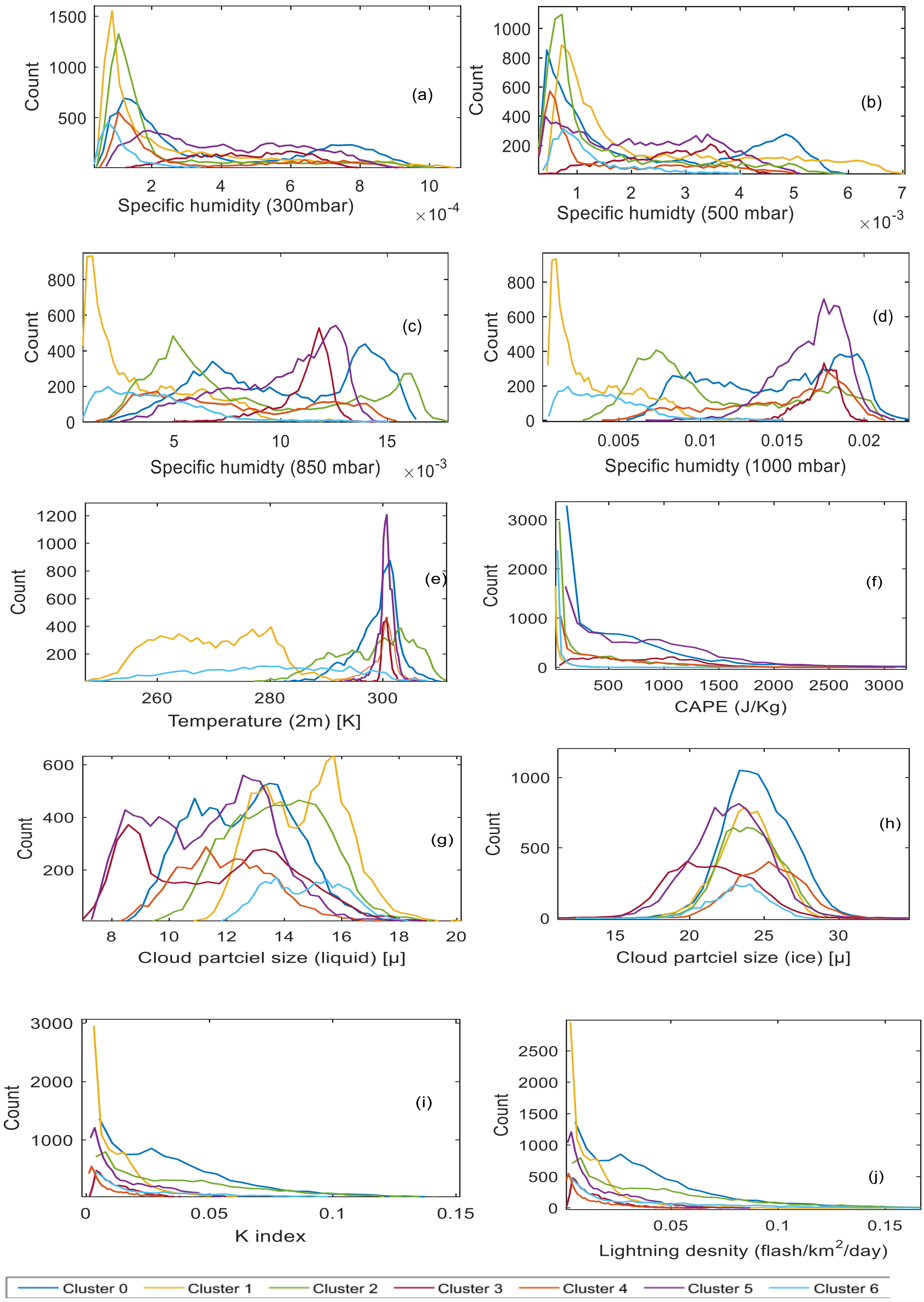

Fig. 4.6 Distribution of various atmospheric features in different cluster

Table 4.1: Hyper-parameters and performance of the regression models

ML Algorithm	Best hyper-parameter	R-squared score of each fold (year)									Mean score	Standard deviation
		2003	**2004**	**2005**	**2006**	**2007**	**2008**	**2009**	**2010**	**2011**		
Ridge	alpha :10	0.85	0.83	0.81	0.85	0.83	0.83	0.80	0.73	0.83	0.82	0.03
Lasso	alpha: 1e-07	0.85	0.82	0.80	0.83	0.82	0.81	0.79	0.74	0.82	0.81	0.03
Decision Tree	max depth: 22 min samples split: 55	0.77	0.70	0.68	0.72	0.74	0.75	0.71	0.68	0.78	0.72	0.03
Random Forest	n estimators: 600 max. depth: 27 min samples split: 5 max. samples: 0.9	0.84	0.84	0.85	0.87	0.84	0.84	0.85	0.73	0.85	0.83	0.04

Random forest regression showed the best R-squared score on the test set i.e. 0.81. Therefore, prediction of lightning density has been carried out using Random forest algorithm which seemed to be the best performing one here,

Table 4.2: Performance of different regression models

Models	R^2 score
Ridge Regression	0.79
Lasso Regression	0.79
Decision Tree	0.71
Random Forest	0.81

The prediction model has been tested with the monthly lightning data during 2012-2013. Fig. 4.7(a-g) presents a comparison between actual and predicted lightning activities in each of the clusters formed. Good matching has been observed in cluster 1, 2, 5 and 6 (Fig. 4.7(b, c, f and g)). Clusters 0 and 4 seemed to show moderate match (Fig. 4.7(a, e)). The prediction accuracy was a little low in cluster 3.

The time series of the comparison between the actual and predicted values are studied further to investigate whether there is any seasonal dependence of the performance (Fig. 4.8(a-g)). The model predicted the lightning activities significantly well in cluster 0 throughout the time range except April –June in the year 2013 (Fig. 4.8(a)). Cluster 1 seemedto under perform during the pre-monsoon months (Fig. 4.8(b)).

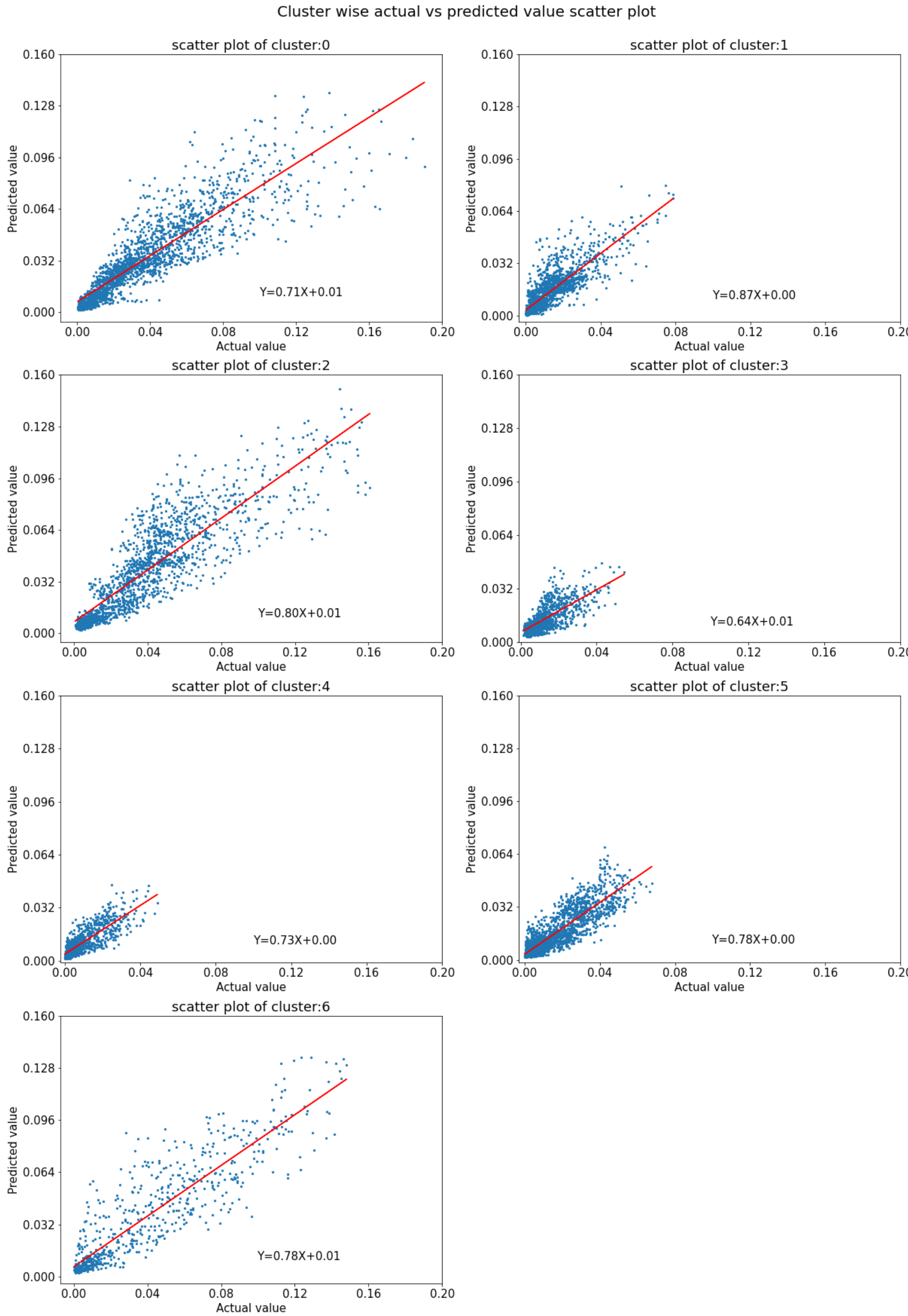

Fig. 4.7 The comparison between actual and predicted annual lightning density (Flash/km^2/day) in the seven clusterspredicted by Random forest model

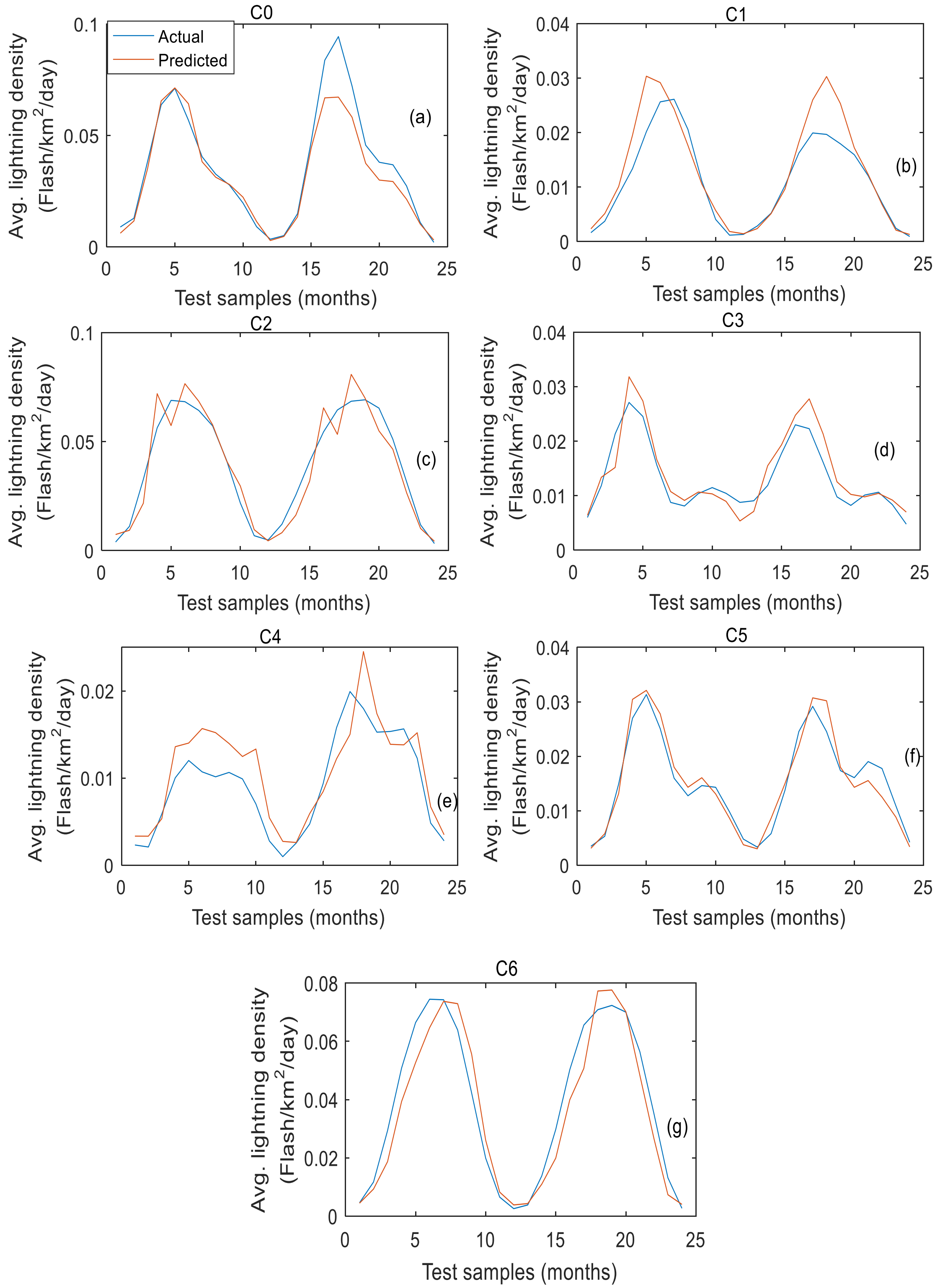

Fig. 4.8 Time series (for consecutive months in 2012-2013) for the actual and predicted values of lightning strikes in the seven clusters by Random forest model

Good match between predicted and actual values have been observed in clusters 2, 3, 5 and 6 (Fig. 4.8(c, d, f)) during all seasons whereas, the model seemed to under-perform during monsoon months in cluster 4 (Fig. 4.8(g)). This seasonal impact on model performance pointed towards the need of studying the model performance separately during the two most lightning prone seasons in India i.e. pre-monsoon and monsoon. The R^2 squared score (average over all the clusters) for the monsoon and pre-monsoon period were found to be 0.81 and 0.71 respectively. The spatial distribution of the predicted and actual lightning values retrieved from LIS for annual and seasonal (pre-monsoon and monsoon) period have been compared to have a look at the performance variability of the model over different Indian regions. Fig. 4.9 (a) showed the predicted annual lightning density. It is evident from the LIS retrieved (Fig. 4.9(b)) values that spatial pattern of the lightning density were well captured by the model. However, there was some underestimation of values in very high lightning zones i.e. in North-eastern and Northern Himalayan part.

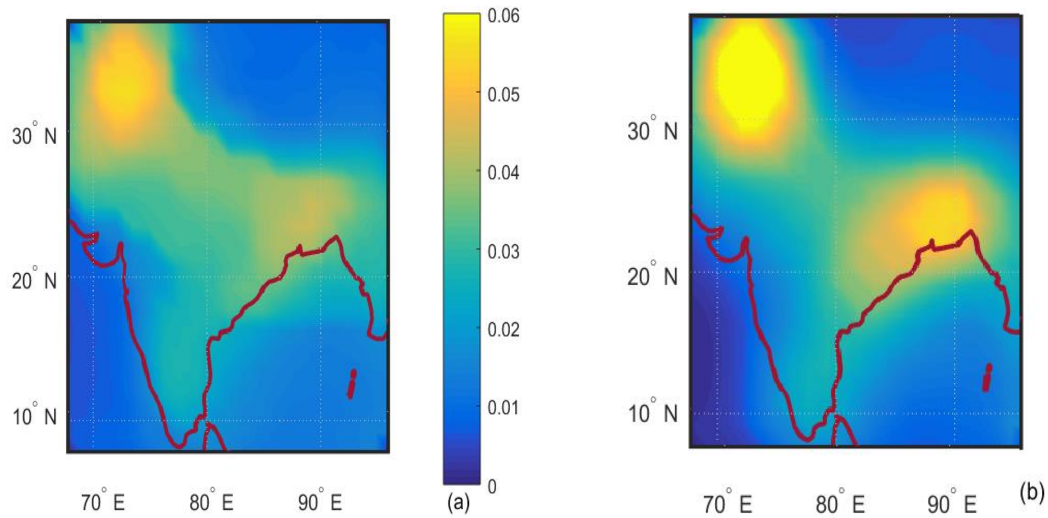

Fig. 4.9 Spatial distribution of annual lightning density (Flash/km^2/day) over Indian region (a) predicted and (b) LIS retrieved actual value

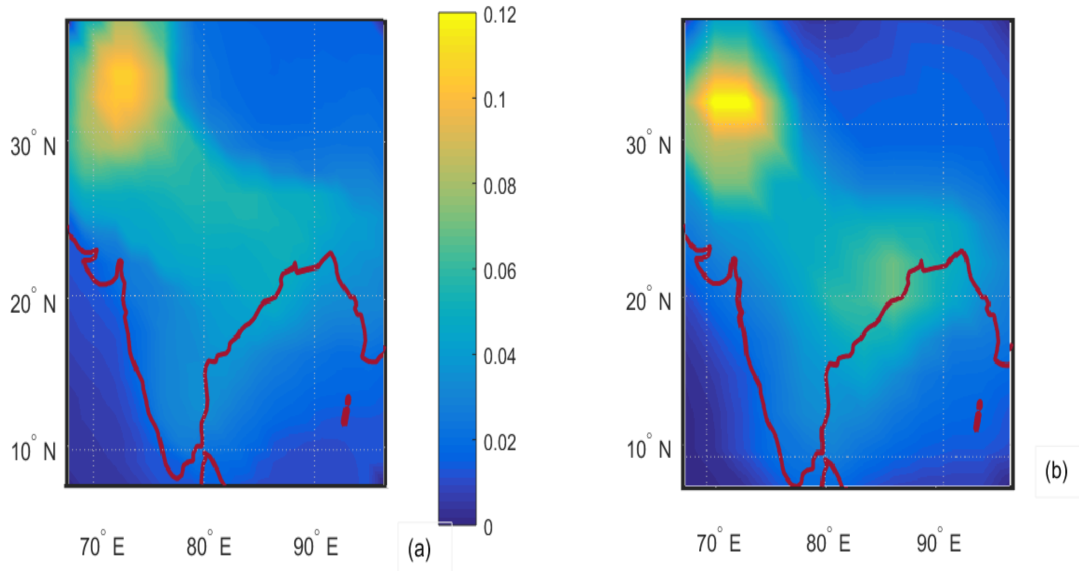

Fig. 4.10 Spatial distribution of monsoon lightning density (Flash/km^2/day) over Indian region (a)predictedand (b) LIS retrieved actual value

The lightning density during monsoon is very high over Northern Himalayan region (Fig. 4.10(a). The model identified the spatial pattern including the very high lightning zone in northern Himalayan. The central portion of this region, however, showed little lower lightning density than in actual data (Fig. 4.10(b)). Pre-monsoon also showed similar performance with little underestimation of values in North-eastern region (Fig. 4.11 (a-b)). However, the spatial pattern of lightning is well estimated.

The mean and variability of actual and predicted lightning density in each of the clusters showed good matching (Table 4.3).

4.3.1 Atmospheric variables and their degree of influence on lightning activities over different climatologies during monsoon and pre-monsoon season:

Several researchers have revealed the dependence of lightning activities on atmospheric variable like CAPE, specific humidity and temperature [106, 37].

But, the degree of dependence has been reported to vary widely in different spatial scales [107].

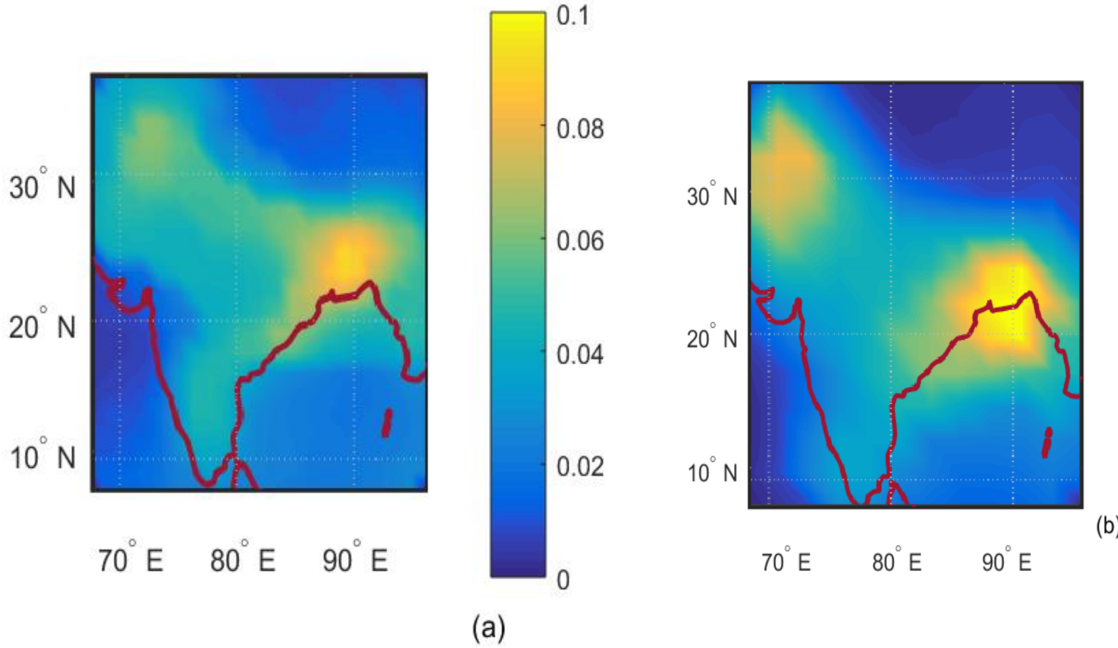

Fig. 4.11 Spatial distribution of pre-monsoon lightning density (Flash/km^2/day) over Indian region (a) predicted and (b) LIS retrieved actual value

Table 4.3: Actual and predicted mean and variability of lightning density in different clusters

	Annual				Monsoon				Pre-monsoon			
	Actual		Predicted		Actual		Predicted		Actual		Predicted	
	Mean	Std.	Mean	Std.	Mean	Std.	Mean	Std.	Mean	Std.	Mean	Std.
C0	0.07	0.02	0.07	0.01	0.09	0.03	0.08	0.01	0.13	0.05	0.12	0.03
C1	0.02	0.01	0.03	0.01	0.04	0.02	0.04	0.01	0.03	0.03	0.04	0.02
C2	0.08	0.03	0.08	0.02	0.12	0.06	0.12	0.04	0.11	0.04	0.14	0.01
C3	0.03	0.01	0.03	0.01	0.02	0.01	0.03	0.01	0.05	0.02	0.05	0.01

C4	0.02	0.01	0.02	0.01	0.03	0.02	0.03	0.01	0.02	0.02	0.02	0.01
C5	0.03	0.02	0.03	0.01	0.04	0.02	0.04	0.02	0.05	0.03	0.05	0.02
C6	0.08	0.04	0.07	0.02	0.13	0.07	0.14	0.05	0.10	0.05	0.07	0.02

Therefore, this study has attempted to rank the above mentioned atmospheric variables based on their influences on lightning activities in different lightning climatologies derived over the country based on Pearson correlation (Fig. 4.12(a-n)). Cluster 0 majorly covers the Eastern coast of India. CAPE and surface temperature were found to have good association with lightning activities in this region during monsoon whereas, specific humidity at 850mbar and cloud ice particle size seemed to govern the process during pre-monsoon (Fig. 4.12(b)). Authors in [108], also reported major role of CAPEin lightning activities during monsoon in this region. Lightning is not controlled alone by CAPE over Indian region during pre-monsoon whereas; it plays a major role in monsoon convection. Several other factors like moisture availability and orography play their parts in dictating the lightning patternduring pre-monsoon [109] which finds good agreement with the results.The Tibetan plateaucomes under cluster 1(Fig. 4.12(c-d)). The region showed good correspondence between specific humidity at 1000 and 850 mbar and lightning strikes during both the seasons.Authors in [110], also reported similar correlation in this area.The mountainous topography of the region play a more vital role in convection forming process than CAPE. The central and north-western region (cluster2) also showed good association of CAPE and cloud particle size with lightning activities during monsoon region (Fig. 4.12(e)). Lightning activities in this region seemed to have strong association with k-index and specific humidity at 300mbar during pre-monsoon (Fig. 4.12(f)). The temperature remains high over these regions in pre-monsoon. Even though the Central and Northern parts of country maintain low CAPE, the lightning activity is interestingly higher than the coastal places with high CAPE. Therefore, the lightning activity during pre-monsoon over major parts of the country is not governed solely by CAPE. Authors in [109], also reported similar findings.The lower portion of Indian Ocean comes under cluster 3. The pre-monsoon lightning activity in this region showed strong correlation with CAPE (Fig. 4.12(h)).The convective activity remain high over Indian Ocean during Nov-Apr. Lightning in tropical storms is very low over Indian ocean when CAPE remains low. Lightning during oceanic storms in high CAPE areas is equally disastrous as the land based storms[109].Cloud particle size and specific humidity at 850 mbar are strongly connected to the monsoon lightning activity in this region (Fig. 4.12(g)). The lightning activity over Arabian sea (cluster 4) seemed to be strongly correlated with the specific humidity at different pressure levels and thermal instability indicated by k-index during both the seasons (Fig.4.12(i-j)). This supports the previous reporting of lightning over this area being majorly controlled by temperature induces effects [110]. A portion of South India and some parts of Arabian sea and Bay of Bengal come under the limits of cluster 5.The moisture content in the South Indian regions was reported to be strongly linked with lightning activities[109].The current results (Fig. 4.12(k-l))finds good agreement with the previous findings during monsoon and pre-monsoon. Cluster 6 majorly covers a portion of Pakistan.Here, the pre-monsoon lightning density seemed to be well-connected with specific humidity at 850mbar and 1000mbar (Fig. 4.12(n)). Effect of CAPE is not that prominent here probably due to convective inhibition during pre-monsoon [111]. On the other hand, both CAPE and humidity seemed to be strongly associated with monsoon lightning activities over this region (Fig. 4.12(m)). It is to be noted here, this section (based on Fig. 4.12) presented the analysis based on absolute values of the Pearson co-efficient to show the degree of correlation.This is entirely to rank the features and not to talk about the nature of association. However, the information on the nature of the correlation has also been indicated in the figures (Fig. 4.12)).

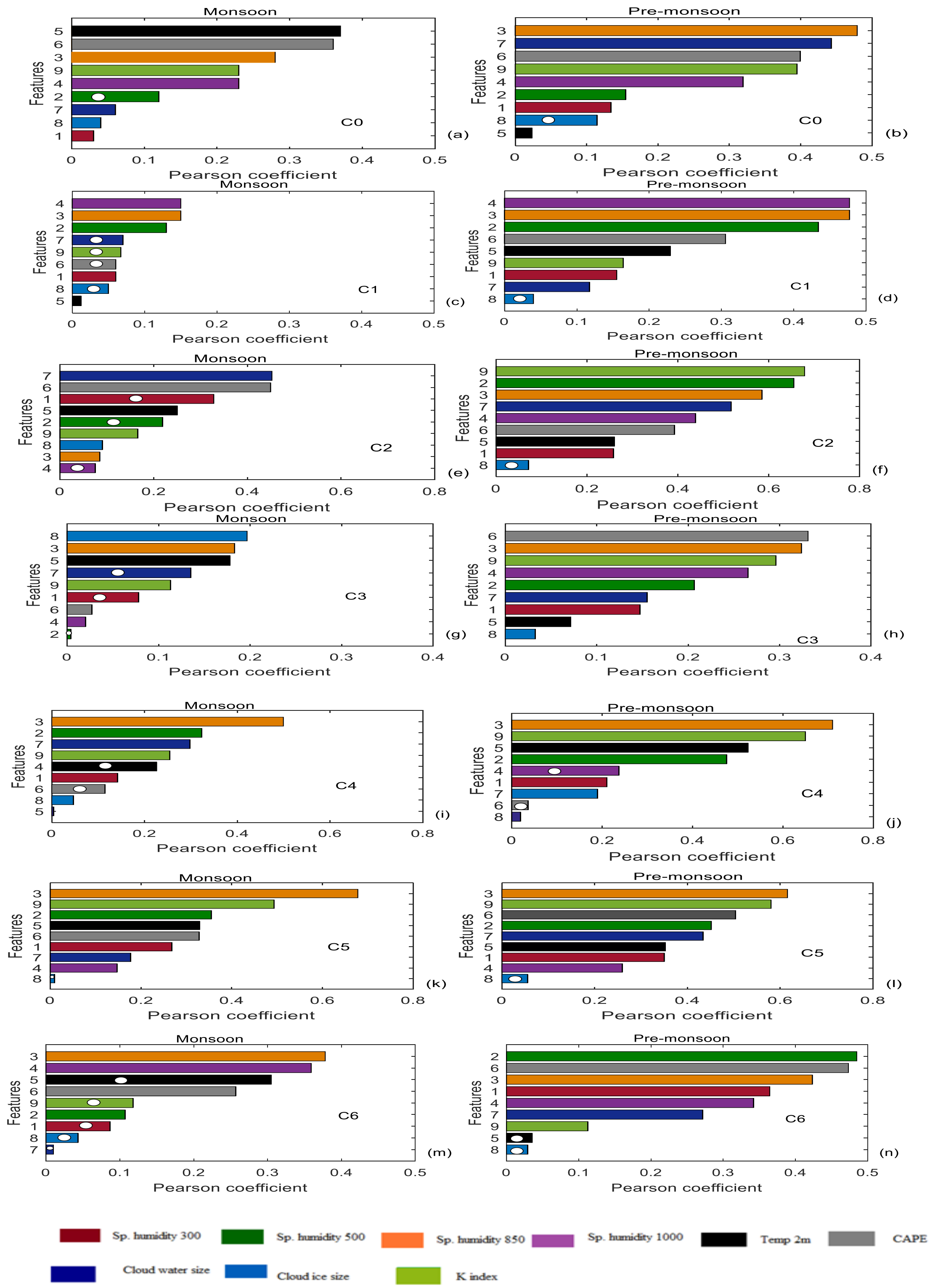

Fig. 4.12: Rank of features for the seven clusters.Absolute value of Pearson coefficient usedfor ranking. The white filled dot represents negative correlation

4.4. Conclusion

Lightning is one of the most severe weather concerns for India. Proper prediction of lightning activities are extremely crucial especially in recent scenario of increasing climate extremities.The study has regionalized Indian subcontinent in seven clusters based on lightning density and associated weather variables.Results showed notably varied degree of correlation between the atmospheric features and lightning over the different regions.Prediction of monthly lightning density was attempted using four ML based regression model among which Random forest performed the best. The R^2 score during monsoon and pre-monsoon were found to be 0.81 and 0.71 respectively. The ranking of atmospheric variables catalyzing lightning activities over different parts of the country reported by this study point out the varied process of lightning over different portion of the country. The said associations were found to vary significantly in different seasons as well. Even though the current work has focused on Indian region, use of satellite data makes this approach suitable for any region around the globe. The simplistic lightning prediction approach presented here, based on easily retrievable atmospheric variables can be useful for modeling and prediction of lightning activities over a large geographic region.

Chapter 5

Impact of lightning on precipitation microphysics

This chapter is based on the article "Chatterjee, C., Das, S., On the association between lightning and precipitation microphysics,*Journal of Atmospheric and Solar-Terrestrial Physics*, 2020,207, doi:10.1016/j.jastp.2020.105350"

5.1 Introduction

India is a large country with varied topographic features. Successful study of rainfall and its modulation under climatic changes as reported in Chapter 3 over such a vast geographic area of interest needs accurate radar measurements. However, radar measurements suffer from several uncertainties under different rain conditions. Since a radar detects the power backscattered by falling raindrops (i.e., reflectivity), the accuracy of the rainfall estimation depends, among others, on the relation between the measured reflectivity and rainfall rate, which is strongly related to the rain microphysical structure, that disdrometric measurements can infer. The said relations can vary significant for different seasons [17], topography[21], updraft velocities, wind circulation[20], lightning condition etc. An improvedradar based QPE is therefore, challenging. India witnesses large number of thunderstorm events with significant lightning strikes and very heavy rainfall. Such events have increased notably over recent pastdue to the climate change scenario. It is extremely crucial to investigate the modulation of precipitation microphysics during lightning. Any change in precipitation structure can greatly affect the standard relationships used in radar meteorology to estimate rainfall integral parameters resulting noteworthy degradation in QPE. Understanding the association between lightning and precipitation microphysics, is therefore, crucial. Besides, lightning is an excellent indicator of the convection in large scale mesoscale systems responsible for such events. Therefore, development of such systems can be monitored with lightning activities to achieve a successful prediction of the severities.However, understanding of the connection between lightning and microphysical structure of the precipitation system happens to be poor.

In this work, for the first time, behaviorofthe precipitation system during lightning has been reported from a location (Kolkata (22.57^0 N, 88.36^0 E), India) almost on the top of ITCZ line. The work investigates alternations in both cloud and ground rain microphysics due to lightning. The modulation of standard relationships linking radar retrieved parameters and rain estimation were also investigated under lightning condition.

5.2Data and Methodology

5.2.1 Instruments

The DSD measurement has been procured by a laser based optical disdrometer (OTT PARSIVEL2) installed at Indian Statistical Institute, Kolkata. Kolkata is situated in the lower Ganges delta of eastern India on the bank of Hooghly River (Fig. 5.1). Kolkata is a tropical location in the ITCZ region. Kolkata gets most of its rain during June- Sept due to the south eastern monsoon wind. The average annual rain is about 1600mm. Kolkata reportedly gets 70 thunderstorm days/year on an average.

The disdrometer used, is a particle size and velocity measuring device which is capable of measuring rain drops within a diameter range of 0.062mm-24.5mm and a velocity range of 0.05m/s-20.8 m/s binned in 32 x 32 diameter and velocity classes. It generates a horizontal laser beam from the transmitter to receiver. Raindrops, depending upon their size, reduce the voltage at the receiver by blocking the beam. The magnitude of this voltage reduction gives the rain drop size whereas, the time span of this voltage reduction provides the particle speed. The two main limitations of PARSIVEL disdrometer are complementary to each other. Firstly, the sampling area is limited and secondly, there is a possibility of getting multiple rain drops at a time in the sampling area. In practice, the chances of multiple drops at a time is reduced by achieving a smaller sampling area of ~54 cm^2. However, there still remains a small possibility of getting multiple drops simultaneously. This results in impractically large drop measurements. So, the drops with diameter >5 mm are discarded. The integration time of the measurements is fixed as 60s to reduce the statistical uncertainty. PARSIVEL disdrometer provides a limited accuracy in detecting drops smaller than 1 mm, however, the PARSIVEL 2 gives a significantly improved accuracy over the previous version of PARSIVEL 1[112].

The lightning information is primarily collected from a ground network WWLLN, and used along with the LIS observation. WWLLN is a global lightning network managed by University of Washington with 70 stations

Fig. 5.1: Study location (https://www.google.com/maps/place/Kolkata)

around the globe at VLF band. The network detects the lightning location along with the energy in every strike [98] by measuring the sferic in the VLF band due to a lightning flash from 3 or more stations. On the other hand, LIS onboard International Space Station measures the lightning at 777 nm with a help of CCD camera within the latitude range of +/-48^0. It has a resolution of 4 km at nadir and 8 km at limb in a 500 km swath. Unlike ground network, any point on the Earth is observed by LIS only for about 90 seconds in a single measurement.

MODIS level 2 cloud products have been used for the cloud properties. MODIS is a 36 band (in IR, near IR and visible range) imaging instrument on board Aqua and Terra satellites which regularly provided information about global ~~neutral~~ atmospheric dynamics. Cloud droplet size and cloud top temperature parameters estimated from visible and IR radiance are used in the present study. The cloud effective radius is available with 1 km resolution whereas the cloud top temperature is obtained with a resolution of 5km.

Wind speed data is collected from the Automatic weather station situated at Kolkata airport within an aerial distance of 6 km. Qualitative indication of large scale cloud system is obtained from 10.6 μm brightness temperature from INSAT-3DR, one of the most recently launched meteorological satellite by ISRO which provides weather imaging in six frequency bands. The local cloud coverage and distribution of maximum reflectivity of the events are examined with a Doppler weather radar operated by IMD Kolkata. The radar is located at an areal distance of ~20 km from the disdrometer location. This S-band weather radar is capable of scanning at azimuthal, elevational or volume scanning mode at a maximum speed of 6 rpm and a resolution of 0.25 degree. The present study has used the ‘Max Z’ product of this radar in volume scanning mode. It indicates the maximum reflectivity value in vertical, north-south and east-west direction and it is indicative of the cloud liquid water content.

5.2.2. Data and Methodology of Analysis

Rain DSDs of 48 events measured during the period of November, 2017 to July, 2018 are selected for this study. Amongst these days, 23 events had lightning. The events are described in table I along with type, average wind speed, duration, maximum rain rate and rain accumulation information. Number of lightning flashes, as detected by WWLLN network [113], are also mentioned in the Table 5.1.

Cloud properties such as cloud top temperature and effective droplet radius as well rain microphysical parameters such as drop size distribution (DSD), radar reflectivity and rain attenuation are then analyzed under these two types of rain conditions, i.e. with or without lightning. The cloud properties are studied for 5^0x5^0area surrounding the study location. As the satellite is not geostationary, only a few pass over the study regions are obtained for each selected events. To get a statistically stable observation, a 5^0 x 5^0 grid is taken surrounding Kolkata and all pixels are studied. Hence, a one to one correspondence between rain microphysical parameters with cloud properties are not possible, however, it provide characteristics features of the overall cloud system under different conditions.

To quantify the effect on rain microphysics, lognormal model has been used to model the DSD [114-115] and given by [116]

$$N(D) = \left(\frac{N_T}{\sigma D\sqrt{2\pi}}\right) \exp\left[-\frac{0.5(lnD-\mu)^2}{2\sigma^2}\right] \qquad (1)$$

Where *N(D)* is the number density of rain drops (in $m^{-3}mm^{-1}$), $N_T$is the total number of rain drops, *D* is the rain drop diameter (in mm), μ and σ are the mean and standard deviation of *ln (D).* The lognormal parameters of the model are estimated using method of moments [117] and further modeled in terms of rain rate as:

$$N_T = aR^b \qquad (2)$$

$$\mu = c + dln(R) \qquad (3)$$

$$\sigma^2 = e + f\ln(R) \qquad (4)$$

Since, rain DSD has a strong dependence on the rain rate, the events are further subdivided in four rain rate classes i.e. I) low (1mm/h-5mm/h), II) medium (5mm/h-10mm/h), III) high (10mm/h-40mm/h), and IV) very high (40mm/h-200mm/h). The empirical co-efficient *a, b, c, d, e, f* are obtained by linear regression method. The rain integral parameters are obtained from the DSD [118]. Rain attenuation is estimated using Mie scattering theory assuming spherical shape and 303K medium temperature

Table 5.1 Details of the events studied

	Date	Event type	UTC	Maximum rain intensity (mm/h)	Rain accumulation (mm)	Wind speed	Number of lightning strikes
1	April 7, 2018	Lightning	10:10-14:50	90.67	20.03	15.6	543
2	April 9, 2018	Lightning	16:47-18:12	9.095	3.59	7.4	51
3	April 11, 2018	Lightning	15:18-16:37	1.4	0.42	14.23	9
4	April 21, 2018	Lightning	13:00-13:37	87.75	11.80	5.6	49
5	April 22,	Lightning	09:03-09:23	1.27	0.05		32

	2018					20.3	
6	April 23, 2018	Lightning	13:59-14:19	6.53	0.72	8.2	22
7	April 26, 2018	Lightning	14:29-17:11	80.87	25.33	22.3	663
8	May 13, 2018	Lightning	07:44-10:37	73.56	57.34	11.6	307
9	May 18, 2018	Lightning	09:40-09:59	39.16	5.8	13.2	18
10	May 22, 2018	Lightning	10:50-13:00	76.17	34.11	12.1	171
11	June 1, 2018	Lightning	10:35-17:30	77.35	28.53	7.9	113

12	June 8, 2018	Lightning	12:08-13:17	124.2	16.26	7.2	91
13	June 9, 2018	Lightning	07:51-08:47	47.29	8.80	11.1	4
14	June 10, 2018	Lightning	07:14-07:50	58.2	7.29	7.25	61
15	June 11, 2018	Lightning	10:04-13:28	63.2	9.7	4.63	734
16	Aug 3,2018	Lightning	10:08-13:45	59.77	21.11	8.16	151
17	Aug 6, 2018	Lightning	12:20-13:10	3.34	1.29	9.44	29
18	Aug 22, 2018	Lightning	11:50-13:43	81.97	30.53	8.3	161
19	Aug 25, 2018	Lightning	05:39-06:26	50.10	8.9	9.8	32
20	Aug 27,	Lightning	00:30-01:46	16.83	3.34	14.7	8

	2018						
21	Sep 13, 2018	Lightning	21:30-22:45	60.83	7.99	8.7	56
22	Sep 15, 2018	Lightning	07:50-08:57	23.20	2.40	9.3	211
23	Sep 26, 2018	Lightning	07:00-07:43	49.8	3.40	6.7	35
24	Nov 15, 2017	No lightning	01:30-17:30	23.88	24.28	3.1	0
25	Nov 16, 2017	No lightning	20:00-23:00	58.09	22.97	5.9	0
26	March 15-16, 2018	No lightning	21:30(March 15)-00:50(March 16)	6	0.60	11.1	0

27	April 7, 2018	No lightning	18:30-20:30	2.5	1.11	9.27	0
28	May 16, 2018	No lightning	04:45-05:25	46.71	4.83	15.8	0
29	June 17, 2018	No lightning	02:30-05:23	19.26	3.74	13.3	0
30	July 10, 2018	No lightning	06:10-07:00	13.10	3.79	20.1	0
31	July 14, 2018	No lightning	08:00-08:45	12.79	1.33	17.4	0
32	July 21, 2018	No lightning	01:30-15:10	40.55	17.53	22.5	0
33	Aug 1, 2018	Lightning	00:10-03:45	19.46	19.04	5.7	

34	Aug 2, 2018	No lightning	00:10-03:20	5.35	1.27	13.6	0
35	Aug 5, 2018	No lightning	12:21-13:25	6.7	1.18	5.3	0
36	Aug 7, 2018	No lightning	05:50-07:01	45.46	3.56	20.7	0
37	Aug 8, 2018	No lightning	05:30-6:05	31.29	3.06	15.7	0
38	Aug 13, 2018	No lightning	01:48-02:15	31.64	3.91	7.8	0
39	Aug 14, 2018	No lightning	04:30-05:41	25.72	1.39	15.3	0
40	Aug 15, 2018	No lightning	16:10-17:04	26.60	6.09	14.5	0

41	Aug 20, 2018	No lightning	07:30-06:22	20.7	1.89	12.1	0
42	Aug 28, 2018	No lightning	00:36-03:14	35.63	3.68	12.9	0
43	Aug 29, 2018	No lightning	10:36-11:39	39.50	8.54	13.1	0
44	Aug 31, 2018	No lightning	3:46-10:03	10.89	3.45	8.5	0
45	Sep 2, 2018	No lightning	04:00-07:26	67.02	23.50	14.7	0
46	Sep20, 2018	No lightning	16:08-18:29	82.42	17.36	14.4	0
47	Oct 10, 2018	No lightning	08:45-15:25	4.55	1.88	12.8	0

48	Oct 29, 2018	No lightning	12:27-16:05	3.75	3.29	9.6	0

Table 5.2: DSD parameters of the two rain categories

Event Type	DSD parameters		
With lightning	$N_T = 445\ R^{0.45}$	$\mu = 0.086 \ln R - 0.052$	$\sigma^2 = 0.025 \ln R + 0.081$
Without lightning	$N_T = 992.27\ R^{0.38}$	$\mu = 0.098 \ln R - 0.025$	$\sigma^2 = 0.026 \ln R + 0.063$

5.3 Results and discussion

5.3.1 Case Studies

To understand the characteristics difference of cloud and rain patterns between the lightning and non-lightning events, two events with similar rain pattern are discussed next. These two events are having similar rain intensity and comparable horizontal wind velocities.

5.3.1.1 Lightning event on June 1, 2018

The rain event observed on June 1, 2018 lasted for 420 minutes with a maximum rain intensity of 77.35 mm/h. The rain rate, associated DSD and lightning activity have been shown in Fig. 5.2(a). 113 strikes were detected during this rain event. The average wind speed was 7.9 km/h. The spatial distribution of lightning strikes in a 1^0 x 1^0 vicinity around the study location is shown by assimilation of LIS and WWLLN data during the event (supporting figure given in Appendix-C Fig.C.1(a)). The INSAT satellite imaging shows a large areal expansion of the convective system developed indicated by the low brightness temperature at 10.6 μm (supporting figure given in Appendix-CFig.C.1(b)). This is reported to be a favorable condition for cloud-ground lightning [51].

Further, a close-range cloud image is observed by Doppler weather radar during the event. This shows the presence of a thick cloud system over the study location (Fig. 5.2(b)). The cloud properties during the event are shown in Fig. 5.3(a-b). Both effective radius and cloud top temperature surrounding the study location had a dominance of low values. The radar reflectivity for this event is estimated by empirical relation $Z=aR^b$. The power law coefficients 'a' and 'b' are computed by linear regression method as 630.95 and 1.2, respectively (supporting figure given in Appendix-C Fig. C.2).

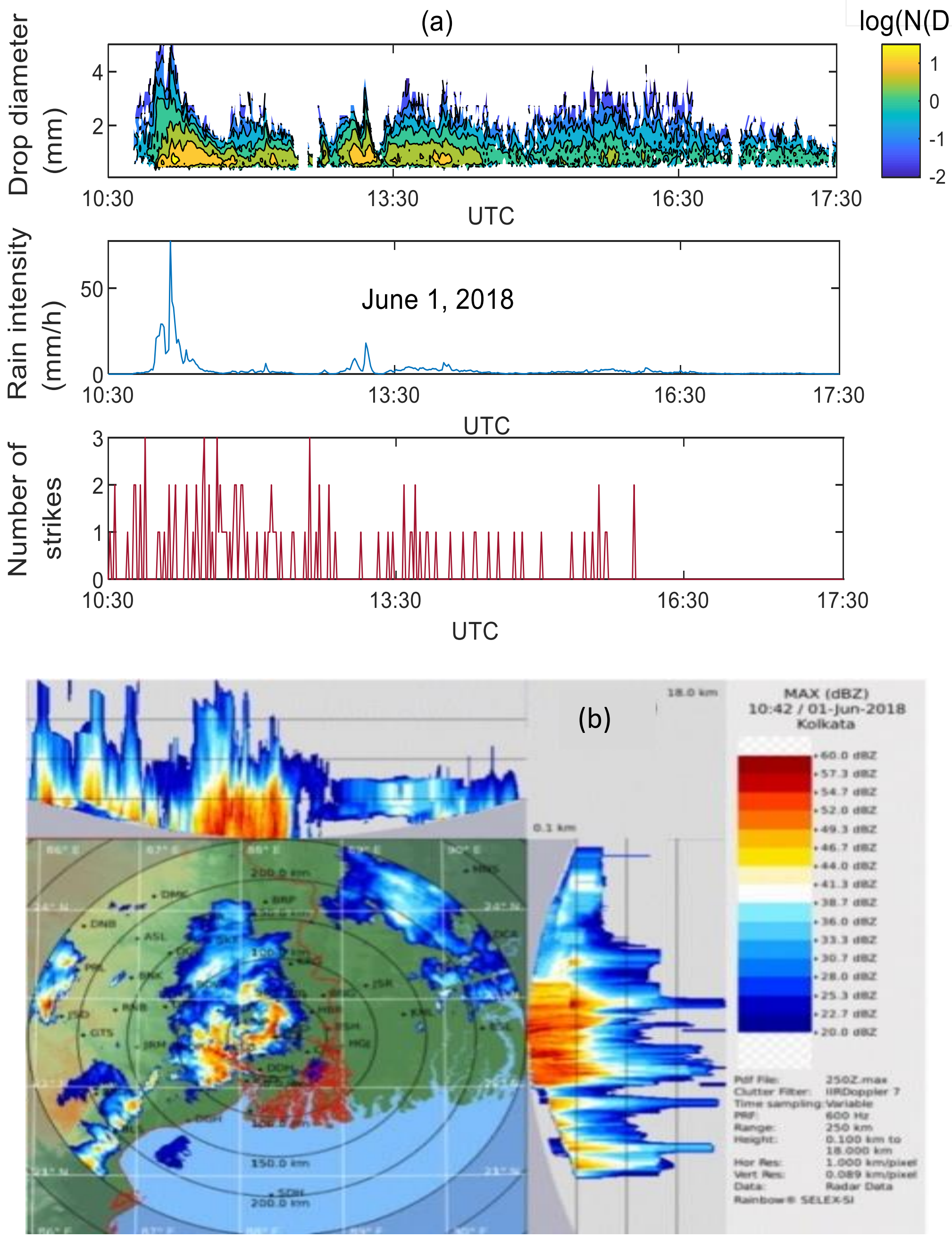

Fig. 5.2 (a) Rain DSD, rain rate and lightning flashes d) Maximum reflectivity obtained from Doppler weather radar volume scan on June 1, 2018

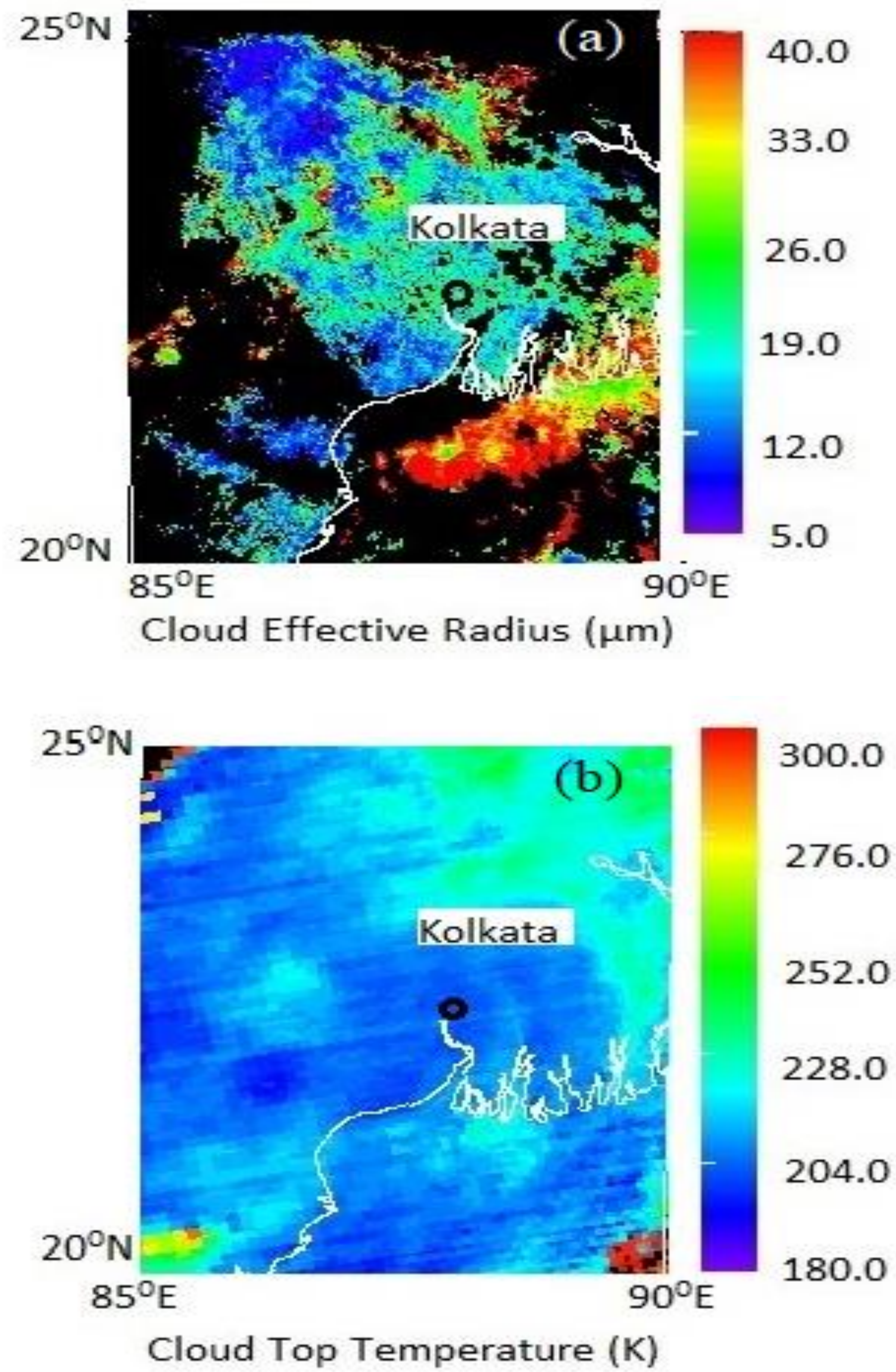

Fig. 5.3: (a) cloud effective radius and (b) cloud top temperature

at 08:00 UT on June 1, 1, 2018

5.3.1.2 Non-lightning event on Nov. 16, 2017

The rain event on Nov 16, 2017 had no lightning (Fig. 5.4(a)). The overall characteristic of this rain event is similar to the previous event. The span of the rain event was about 180 minutes with a maximum rain intensity of 58 mm/h. The average wind speed during the event was 5.9 km/h. No lightning strikes were detected during the event in the vicinity of the study location (supporting figure given in Appendix-CFig.C.3(a)). The areal expansion of the convective system is smaller than the day with lightning (supporting figure given in Appendix-C Fig.C.3(b)).

The close-range ground radar image suggests presence of shallow cloud over the study location (Fig. 5.4(b)). The cloud properties during the event are shown in Fig. 5.5(a-b). Both the effective radius and cloud top temperature values surrounding the study location had a dominance of high values. The coefficient *a* and *b* of Z-R relation for this event was calculated as 125.89 and 1.5, respectively.

5.3.2. Long term statistics

To get a statistically meaningful conclusion about the rain and cloud features during lightning and non-lightning conditions, statistical descriptions of these characteristics are presented next.

A total of 48 rain events have been considered for the statistical study of rain events with/without lightning and depicted in Table 5.1. As already pointed out that rain microphysics has strong dependence on rain rate, the events are divided into four rain rate classes and the analysis are performed separately on each class.

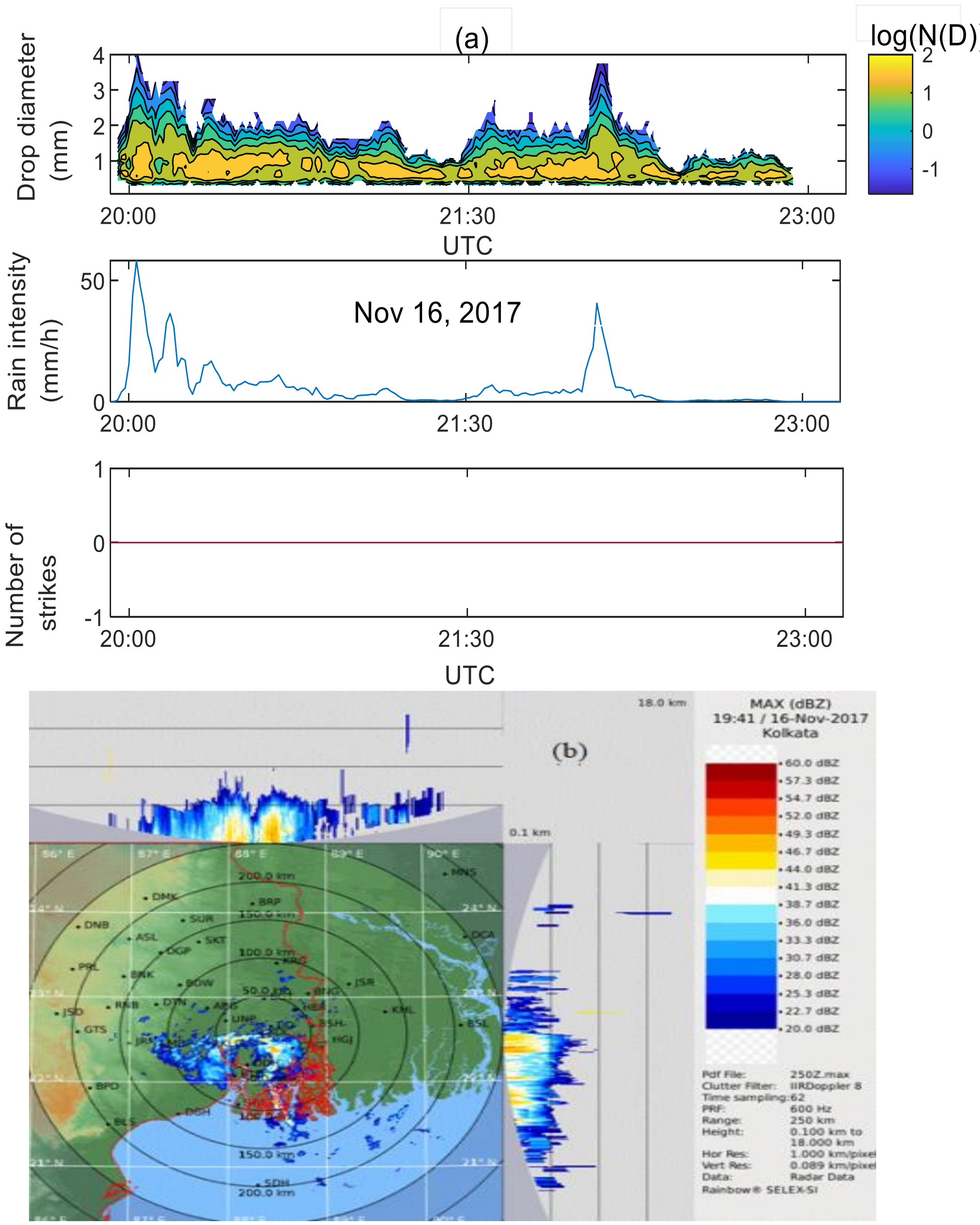

Fig. 5.4 : (a) Rain DSD, rain rate and lightning flashes (b) Maximum reflectivity obtained from Doppler weather radar volume scan on Nov 16, 2017.

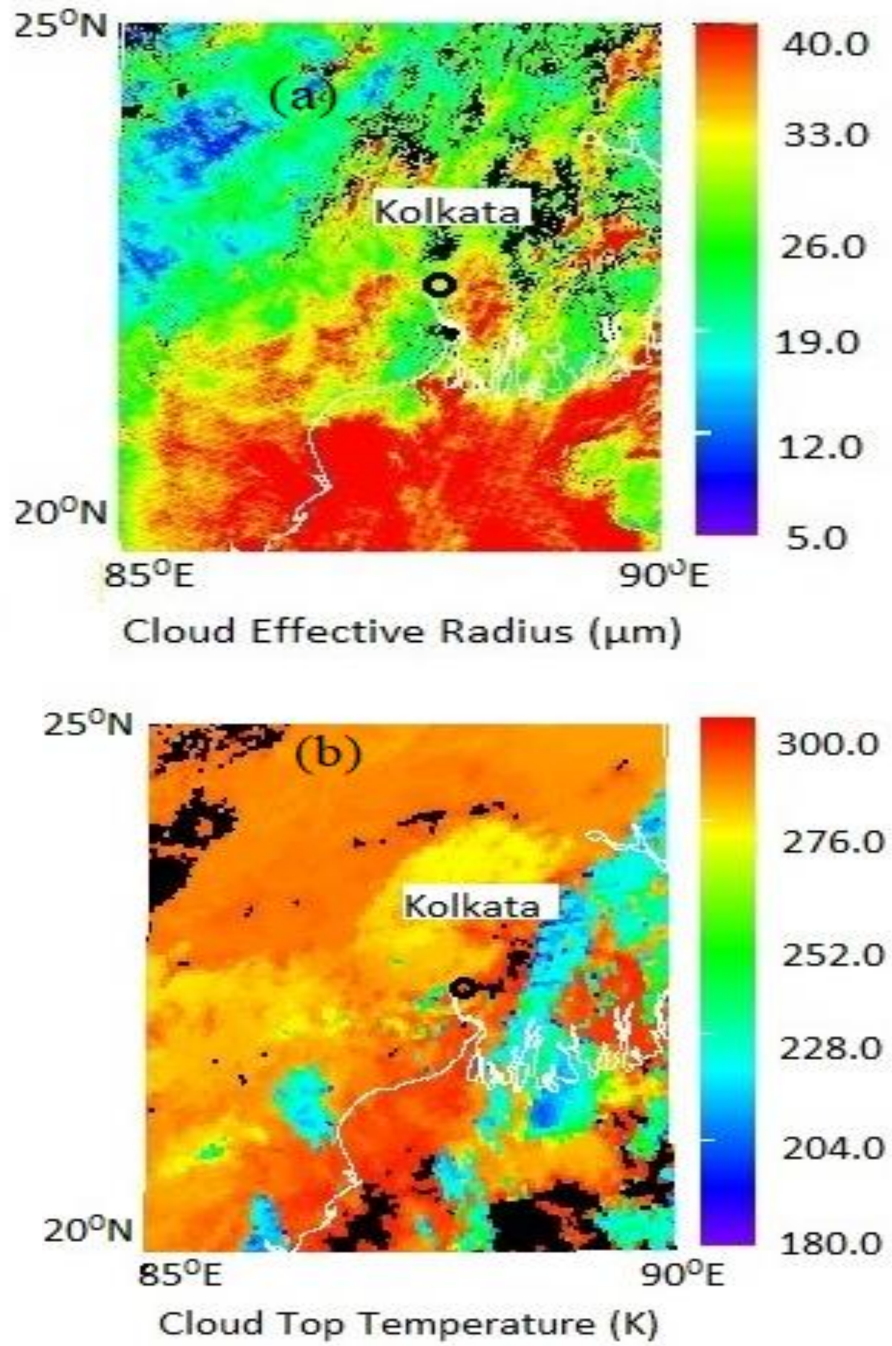

Fig 5.5 (a) cloud effective radius and (b) cloud top temperature on at 16:00 UT on Nov 16, 2017.

5.3.2.1 Rain microphysics

The drop size distribution of these two types of events showed clearly distinct behavior. Fig. 5.6 shows the number concentration of rain drops for these two types of rain. The number concentration is higher for small drops under non-lightning conditions than the lightning conditions in all four rain rate classes. It is to be noted that the instrument has a limitation in counting very small drops. The inverse scenario is observed after a critical drop diameter which shifted towards large drops with increase in rain rate. The critical diameter varies between 1-3 mm drop sizes depending on the rain rate. The result indicates a clear dominance of large drops in rain with lightning. Large rain drops usually indicate coalescence through collision process and the existence of large drops indicate high level of convective activity. The dominance of larger drops in lightning events is further supported by the distribution of mass weighted volume diameter for the two rain categories as indicated Fig. 5.7.

One can note that the peak of the distribution is shifted towards larger drops for lightning events. Detailed comparative analyses of rain DSD parameters computed by lognormal model under these two rain conditions are presented in Table 5.2.

5.3.2.2 Cloud properties

In Fig. 5.8 the distribution of cloud properties, namely cloud effective radius and cloud top temperature, under varied lightning conditions are shown.

The cloud properties have been studied for all the rain events and average values are provided in Appendix-C Table C.1 and C.2. Results clearly indicate the dominance of small cloud particle during lightning (Fig. 5.8(a)).

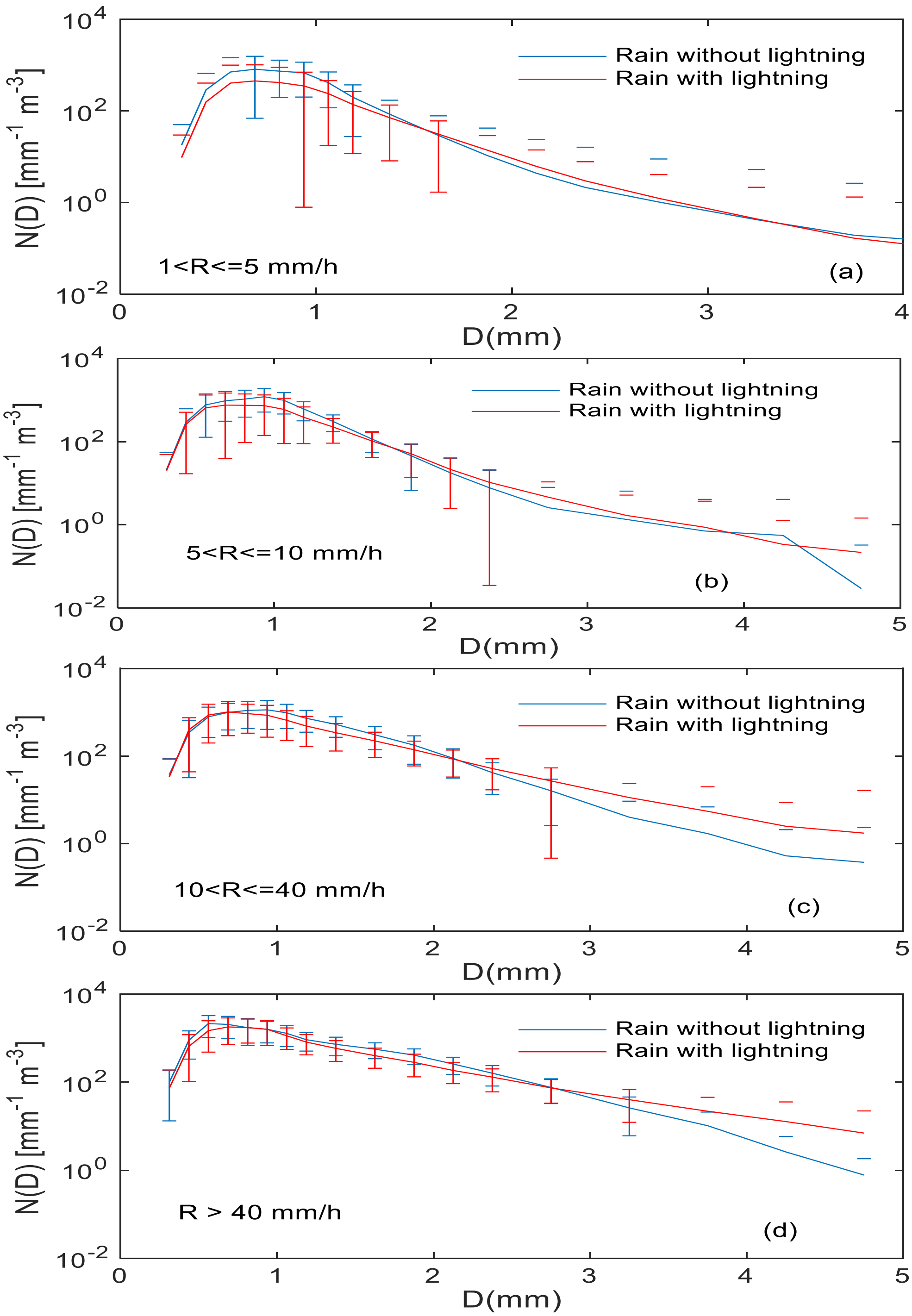

Fig. 5.6 : Average number concentration for rain categories without and with lightning for rain rate (a) 1 -5 mm/h, (b) 5-10 mm/h, (c) 10-40 mm/h, and (d) 40-200 mm/h

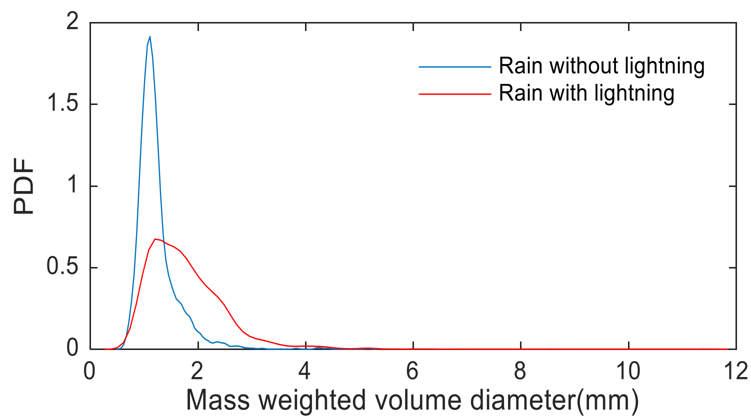

Fig. 5.7 : Mass weighted volume diameter for two types of rain

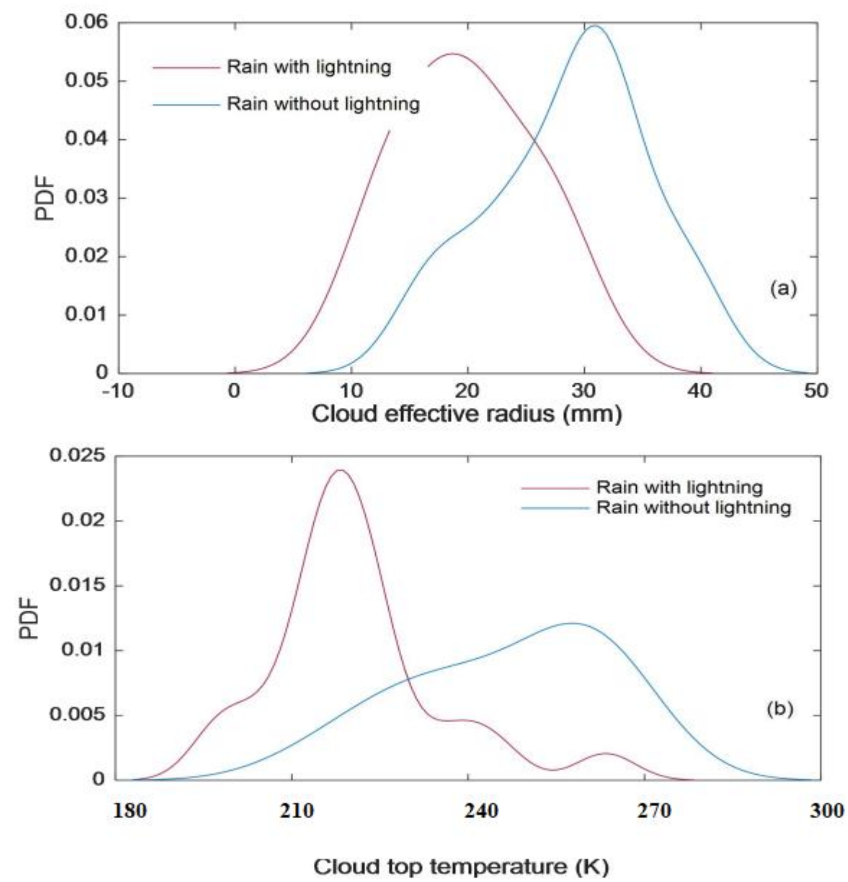

Fig. 5.8: Probability density function of cloud properties: (a) Cloud effective radius (b) Cloud top temperature

The result finds good agreement with the basic growth mechanism of ice particle which often results into breakage of ice into smaller particles which provides the basis of lightning due to its nature of positive charge acquisition. The distribution of cloud top temperature (Fig. 5.8(b)) for rain class with lightning has a peak towards low brightness temperature in comparison with the non-lightning class and in agreement with the previous observations [41-42].

5.3.2.3 Rain integral parameters

A comparative analysis of Z-R relation is done for these two rain categories so that behavioral change of thisrelation can be studied. The power law coefficients (*a* and*b*) for the rain class without lightning are found to be 199.52 and 1.5, respectively. The values were obtained to be398.1 and 1.5 (Fig.5.9) for rain with lightning. This indicates a significant difference in estimated rainfall for same value of reflectivity and will be an important source of errors in QPE for weather radars.

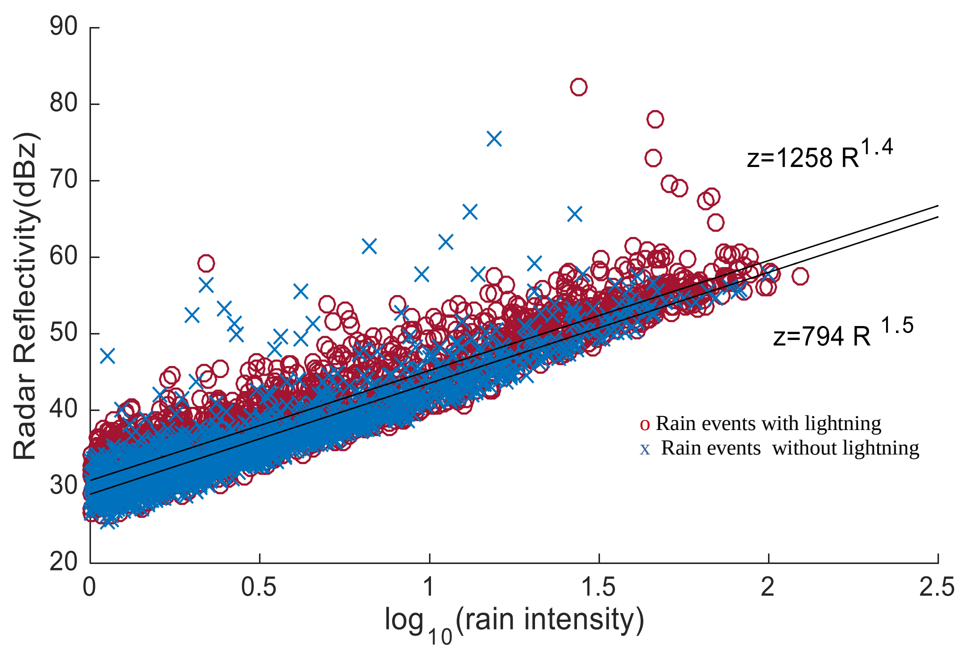

Fig. 5.9: Z-R relation obtained for two rain events with and without lightning

Higher and higher frequenciesare now being used in radars for e.g. precipitation radars are using frequencies upto 36.5 GHz (GPM). However, signals above 10 GHz are very susceptible to rain attenuation. Here, modeling of rain attenuation has been attempted with a special emphasis on GPM frequencies at 13.6 GHz and 35.5 GHz. The specific attenuation (γ) is related to the rain rate by the relation $\gamma = kR^{\alpha}$ and here, it is modeled separately for the two above mentioned rain conditions. The result indicates a higher path attenuation in case of rain with lightning at GPM Ku band frequency whereas, the inverse scenario is noticed for GPM Ka band (Fig. 5.10).

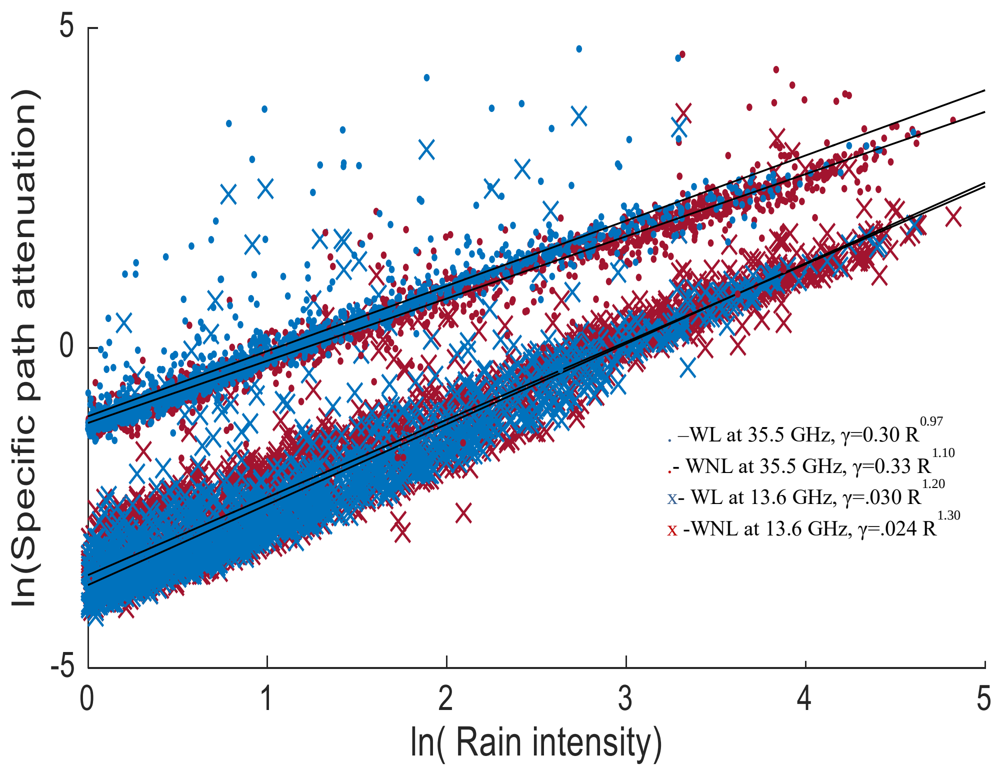

Fig. 5.10: Specific path attenuation for rain with lightning (WL) and without lightning (WNL) at 13.6 GHz and 35.5 GHz

Specifically, K and α valueat the Ka band frequency (35.5 GHz) are 0.300 and 0.970, respectively during rain with lightning whereas, these values are 0.330 and 1.100 during rain with no lightning. On the other hand, the k and αvalues are 0.030 and 1.200 respectively during lightning and 0.024 and 1.300 during non-lightning conditions at Ku band (13.6 GHz).

5.4. Conclusion

The study reports notable differences in both cloud and rain microphysics for rain with/without lightning.The areal expansion of the mesoscale system seemed to be way more larger in case of rain with lightning. The study reports strong association between colder cloud tops with lightning activity.Lightning producing clouds were found to have notable dominance of hydrometeors with smaller cloud effective radius than the non-lightning case.Dominance of large drops were evident in ground rain with lightning which signifies greater degree of convection in the precipitation process. The relationship linking radar reflectivity and rain rate (Z-R) seemed to be modulated significantly during lightning. The study also reports the different susceptibility of the two popular frequencies used in GPM to rain with and without lightning.

Chapter 6

Evidences of super- and sub-terminal drops in different rain categories and climate regimes

This chapter is based on the article "Chatterjee, C.; Porcù, F.; Das, S.; Bracci, A. An Investigation on Super- and Sub-Terminal Drops in Two Different Rain Categories and ClimateRegimes. *RemoteSens.*, **2022**, *14*,2515. https://doi.org/10.3390/rs14112515"

6.1. Introduction

Beside the lightning activities which influence the radar based QPE largely as reported in Chapter 5, another important approximation that introduces significant performance degradation in rain estimation, is the concept of terminal velocities in natural rain. Several studies have presented the evidences of non-terminal drops over different regions around the globe [60, 63]. The DSD characteristics of natural rain have significant spatiotemporal variations due to several reasons, including topography, wind circulation, and climatic conditions [119-120]. This feature is particularly prominent between tropical and temperate locations [14]. Hence, the DSD shape modification and modeling errors inevitably differ in different climatic regions. Furthermore, populations of large drops have been reported to differ enormously over different parts of the globe, with the highest concentration in tropical rain [15]. Therefore, it is interesting to study the occurrence of super-/sub-terminal raindrops in natural rain in contrasting climate regions. Studies on the variation of DSD characteristics and velocity-diameter relationships in different rain categories and climatic regions are hardly available. The very few studies that attempted to study the variation of non-terminal raindrop over different sites were also based on sites in near vicinity. Moreover, the studies mostly were case-based ones.

Break-up has been identified as a major factor controlling the shape of DSD [57]. Numerous laboratory experiments and numerical studies have attempted the understanding of collisional break-up as one of the most important processes in rain formation. Author in [121],reported notable evidence of drop break-up in natural rain. Understanding of drop break-up in natural rain especially over tropics, is extremely poor. It is crucial to investigate the occurrences of drop break-up in natural rain over different latitudes and to understandits role in the percentage of non-terminal drops witnessed.

Turbulence causes the fall speed for a given drop diameter to vary. Besides, the shapecan alter. Several researchers [60,65] have been reporting observationally-based, documenting conditions that sub- or super-terminal fall speeds occur. Even though the entire physics behind it is not known, but sub-terminal velocity after a collision-coalescence event and the super-terminal velocity after breakup have been proposed. [122] reported that mean settling velocity of rain drops modelled as rigid spheres in homogeneous isotropic turbulence (HIT) will decrease depending on degree of turbulence intensity and Reynolds number. [63] predicted enhanced dispersion of the fall speed distribution. A direct numerical simulation (DNS) was used by [123] to study the drop dynamics of 2 and 3 mm sizes in turbulent flow. The study proposed that both the sized drops were seemed to show low fall velocity than the settling speeds by 5 %–7 %.

The current study, for the first time, presents a rigorous investigation of the evidence of non-terminal raindrops on a statistically large rain database over two completely different climatic regimes, one over mid-latitude and another in tropics, namely Bologna (Italy) and Kolkata (India). The present work describes a thorough study on the deviation of actual fall velocities from the empirical relations using a rain dataset measured by PARSIVEL disdrometers. The study presents a comparative analysis of deviation in V-D relationship from GK relation between the two locations along with quantitative analysis of super- and sub-terminal drops. The current work also investigates the role of break-up and coalescence in the percentage of super- and sub-terminal drops in these two locations.

6.2. Materials and methods

6.2.1 Location and experimental setup

The rain DSD information is retrieved by two optical laser-based disdrometers OTT-PARSIVEL2, installed at the Department of Physics and Astronomy "Augusto Righi" of the University of Bologna (Bologna, Italy, 44.49° N, 11.34° E, 65 m a.s.l.), and at the Indian Statistical Institute (Kolkata, India, 22.68° N, 88.38° E, 9 m a.s.l.). The study locations of this work are shown in Fig. 6.1. Bologna has a humid sub-tropical climate with an annual rainfall ranging between 460 and 900 mm. The city is situated at the foot of the Apennine Mountains and maintains a maximum and minimum temperature profile of about 18°C and 8°C. On the other hand, Kolkata, located on the eastern bank of the Hoogly River, has a tropical wet and dry climate with an average temperature of 26°C. The city receives most of its rainfall because of the Bay of Bengal branch of the southwest monsoon from June to September. Annual rainfall is around 1760 mm.

The two disdrometers used in this work are particle size and velocity measuring devices: these disdrometers can measure the raindrops in 32 diameter bins with mid values ranging from 0.062 to 24.5 mm and non-uniform bin sizes of 0.125, 0.5, 1, 2 and 3 mm. The device is capable of measuring raindrop velocities in 32 bins within 0.05 to 20.8 m/s with bin spreads of 0.1, 0.2, 0.4, 0.8, 1.6 and 3.2 m/s. The instrument provides the count of the falling raindrops structured in a matrix of 32x32 diameter and velocity bins [15]. The disdrometer consists of two sensor heads (transmitter and receiver), and a horizontal laser beam is continuously transmitted toward the receiver head. A reduction of laser voltage is produced by raindrops crossing the laser beam.

The duration of the signal decrease is used to compute the drop speed (V), while the amplitude of signal decrease is used to calculate the drop diameter (D).

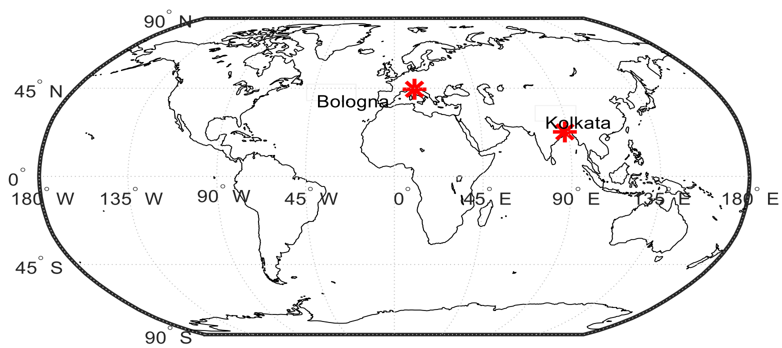

Fig.6.1: Location of the two study areas

Advanced digital signal processing makes it capable of measuring rain intensities from as low as drizzle to as high as tropical thunderstorms. Small drops measured by PARSIVEL disdrometers were known to underestimate the actual count as it misses some small drops, but PARSIVEL2 has improved this significantly from its ancestors [112]. In addition, the surface of PARSIVEL2 sensor heads is equipped with a particular splash protector that breaks up the raindrop impacting sensor heads, thus preventing undesirable passing of raindrop fragments across laser beam. That way, no secondary rainfall spectra are detected by the disdrometer. Furthermore, the sampling time of the measurements is set as 60s to mitigate statistical fluctuations.

6.2.2. Methodology

Bologna dataset consisting 4965 rain minutes within the period of April, 2019 to January, 2021 and 3263 rain minutes during November, 2017 to October, 2018 from Kolkata have been considered here. For both the locations, rain minutes with intensities lesser than 1 mm/h have been removed to minimize noise and non-significant events. The GK relationship has been used for computing the terminal velocities of drops in this analysis. The deviation of the V-D curve is studied from the GK relation However, the first two diameter bins of PARSIVEL are not considered here to minimize erroneous measurements due to the low signal-to-noise ratio [112].

This analysis has been performed focusing, firstly, on the effect of precipitation type on the variation of the V-D relationship. The datasets for both the locations have been separated into the two major precipitation types, i.e., convective/stratiform, see Table 6.1, to study the impact of precipitation type on the super- and sub-terminal drop occurrence. The convective/stratiform separation for Kolkata has been performed, minute by minute, based on the empirical relation between N_0-R as proposed by [122]for tropical rain, whereas the Bologna database has been classified in convective and stratiform rain based on the classification scheme using N_0-λ relationship as proposed by [123]for mid-latitude rain. It is to be noted that this study has taken both deep and shallow convection into the account. The V-D spread and deviation of mean V-D line from GK relationship have been studied for both the locations. The analysis has been carried out for the entire dataset and separately for convective and stratiform rain as well. Further, quantification of super- and sub-terminal drops was attempted. This analysis also was performed for all rain types separately. The drops having a velocity below $0.7V_{terminal}$ were considered sub-terminal drops whereas; drops having a velocity beyond $1.3V_{terminal}$ were termed as super-terminal drops [59]. Here, the distribution of wind speed, measured at a sampling rate of 30 minutes was studied.

The rain datasets were further investigated for the evidence of break-up of drops based on the highest slope (HS) algorithm proposed by [121] in order to assess the relationship between break-up and super-terminal drop occurrence. The HS analysis has been carried out for only rain samples having higher rain intensity (>5mm/h) as proposed in[121]. The HS algorithm analyses the DSD spectrum between 1.0- and 2.6-mm diameters by computing the slope of the linear best fit. The use of the slope of the linear fit was observed to be reliable and robust in identifying the changes in the slope of DSD. This can avoid isolated spikes that exist due to the natural DSD variability. The 1-min disdrometer measurements have been averaged over 2 min to achieve a more stable sampling and to maintain a large-enough dataset. The rain databases have been classified according to the highest slope observed in the drop size distribution.

Next, event-wise analysis has been carried out instead of the rain sample based method used till now. For the following analysis, the entire datasets were grouped into "events": an event is defined as a series of consecutive rain minutes, where rain minutes are defined as minutes with rain exceeding 0.01 mm/h or having more than 10 drops in the DSD. Furthermore, if two events are separated by a dry period shorter than 60 minutes, they are grouped in a single event. A total of 54 events were studied in Bologna whereas 41 events were studied in Kolkata. The fraction of super- and sub-terminal drops were studied in each of these events in both locations.

Thereafter, the events with only average rain intensity higher than 3 mm/h were chosen to investigate the role of break-up and coalescence on the percentage of non-terminal drop in the natural rain of these two study locations. The filtering of events was done in this way because break-up is expected more in events with high rain intensity [124]. This has resulted in 26 events in Kolkata and 14 events in Bologna for this particular analysis.

Here, a baseline approach was attempted. The event databases in each of the two regions have been divided into two classes: 1) events with an average super-terminal fraction of drops (within 0.3-1.6 mm) higher than the average super-terminal percentage of all these events; 2) events having a fraction of super- terminal drops lower than the all event average. Next, the relation between the fraction of break-up minutes i.e., break-up minutes divided by total rain minutes and the fraction of super-terminal drops in a particular event were studied for these events. Finally, to investigate the relationship between sub-terminal drops and increased coalescence, the peak value of mass-averaged drop diameter (D_m), defined as the ratio between the fourth and the third moment of the DSD for each minute, has been studied. The relation between the peak value of D_m in a particular event and the fraction of sub-terminal drops in that event has been studied to investigate whether any direct correspondence exists between the two. The procedure can be summarized as follow

- Data are collected
- The bulk analysis is carried on samples with at least R>1mm/h
- Convective /Stratiform classification performed
- Velocity –diameter relationship in natural rain of the two places studied
- Super- and sub-terminal fraction of drops computed
- Highest slope of DSD is computed for samples with R>5mm/h after averaging DSD in 2 minutes samples
- Events are selected as continuous minutes of rain with at least 10 drops/minute with gaps lesser than 60 minutes
- For the impact of breakup and coalescence we considered events with at least average rain intensity of 3mm/h are selected

- ➢ The non-terminal drops studied as a function of peak mean volume diameter and fraction of break-up minutes.

Table 6.1. Number of DSDs in the C/S classes

	Kolkata	**Bologna**
Convective	1503	2137
Stratiform	1760	2828
Total	3263	4965

6.3. Results

6.3.1. Comparative rain microphysical structure and non-terminal drop occurrence

A comparative analysis is initially performed between the DSDs in the two study locations to determine the basic rain microphysical similarities/dissimilarities. Higher concentration of small raindrops up to 1 mm was noticed in Bologna compared to Kolkata (Fig. 6.2a). Kolkata seemed to show a higher population of medium and large raindrops above 1 mm, with the difference increasing with diameter. Large drops reaching approximately 5 mm in diameter were observed in Kolkata, whereas Bologna showed the largest raindrops around 4mm in diameter. The number concentration was further compared for the two locations separately for the broad categories of rain: convective and stratiform. The DSD for convective rain showed (Fig. 6.2b) almost comparable number concentrations for the small drops (<1 mm) in the two places. Higher population of drops was observed in natural rain of Kolkata for drops greater than 1 mm. Large drops around 5 mm in diameter were noticed in convective rain at Kolkata, whereas Bologna showed large drops approximately around 4.5 mm in diameter. The stratiform rain presented a higher number concentration in Bologna for small and large drops, whereas an abundance of medium-sized drops is noticed in Kolkata (Fig. 6.2(c)). The stratiform rain in Bologna has raindrops up to as large as 3 mm in diameter. On the other hand, the DSD of stratiform rain in Kolkata did not show any drops larger than 2.5 mm in diameter.

Next, the spread of raindrop velocity-diameter relation in the two study locations has been studied for the whole datasets and separately for the convective and stratiform rain as well (Fig. 6.3).

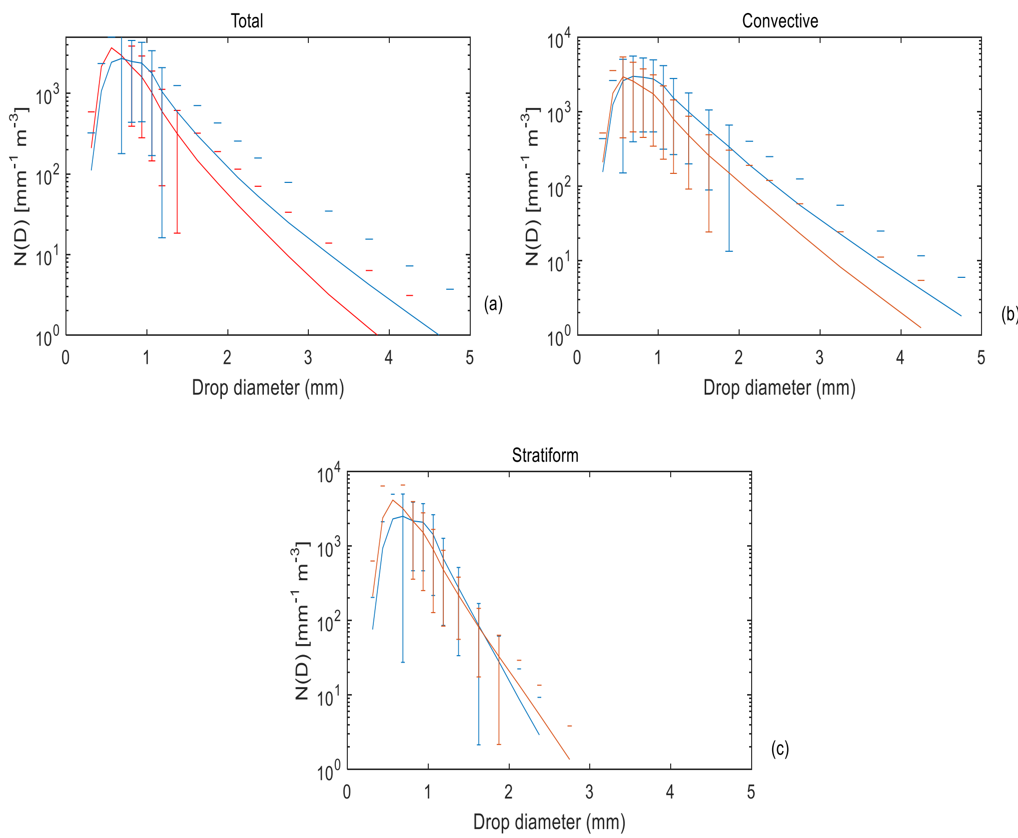

Fig.6.2: Rain drop size distribution in Kolkata and Bologna for (a) whole dataset, (b) convective rain, (c) stratiform rain

The average velocity-diameter (V-D) spread in natural rain in the two places was studied for up to a significant level of drop concentration along with the mean velocity-diameter relation obtained by studying the drop population in different diameter and velocity bins where velocity and diameter are sampled keeping the original PARSIVEL2 classes (Fig. 6.3a-f). Fig. 3a showed the V-D spread for the whole rain datasets in Kolkata and Bologna. In both the places, the mean V-D curve went beyond the GK line for very small drops, which signifies the presence of velocities higher than the terminal velocity. Subsequently, for drops greater than 1 mm, the mean V-D curve deviates toward values lower than GK line, which increases with increasing diameter. This lowering indicates velocity values lower than the expected

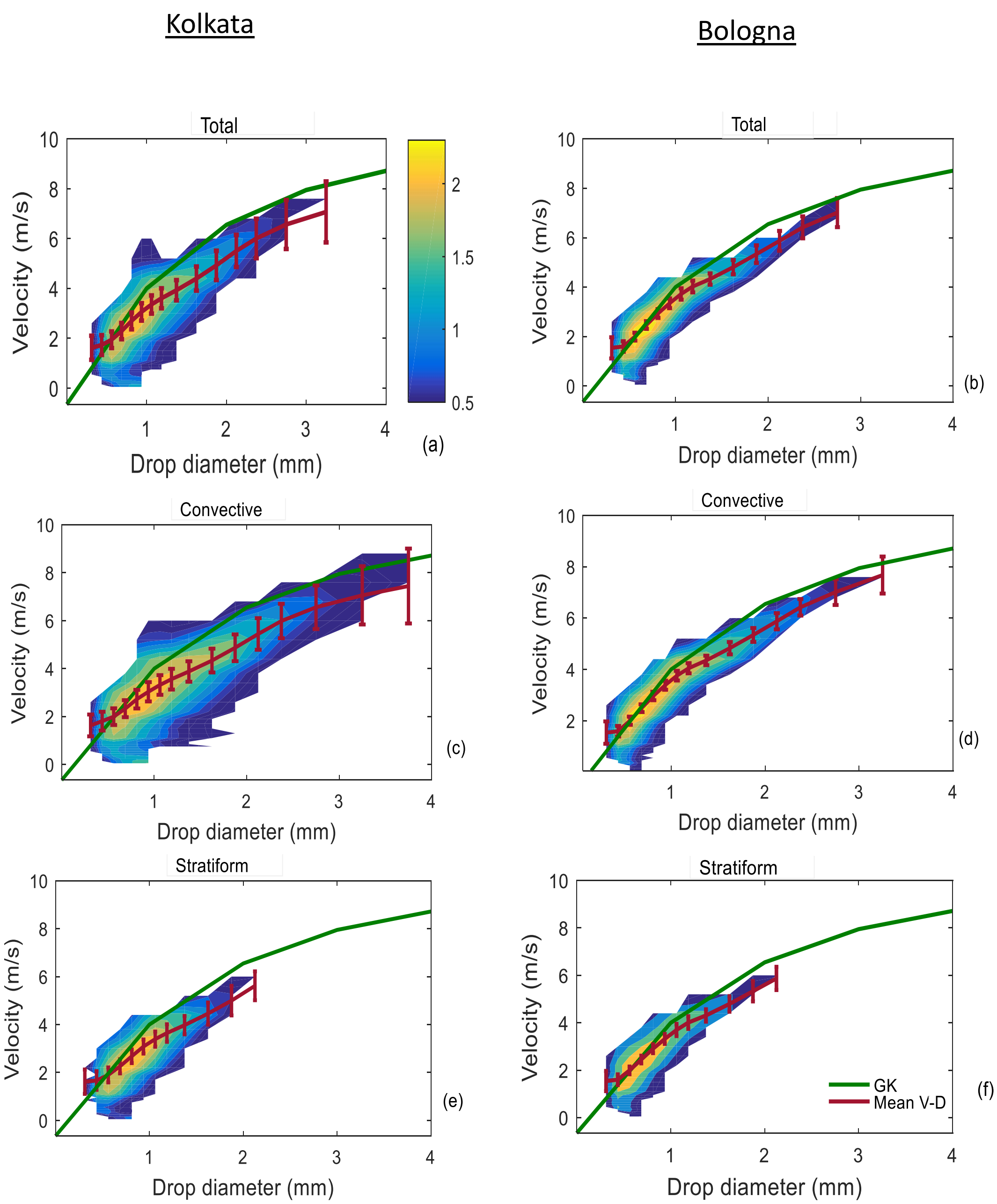

Fig. 6.3: Spread of velocity-diameter spectra for the whole dataset in (a) Kolkata and (b) Bologna; for convective rain in (c) Kolkata and (d) Bologna and for stratiform rain in (e) Kolkata and (f) Bologna. The colors represent the number of drops on the $\log_{10}$ scale. The green line is the GK line, and the red line is the mean of the V-D relationship observed for the dataset with the standard deviation shown as error bars.

ones for a particular raindrop diameter. A wider spread of the V-D spectra has been noticed in Kolkata. A similar analysis was repeated for convective and stratiform categories of rain to investigate the influence of convection on the V-D relationship. The V-D spectra for convective rain (Fig. 6.3(b)) were wider than the mean rain spectra for the entire dataset, both in tropical (Kolkata) and mid-latitude locations (Bologna).

However, the spread was wider in Kolkata as in the case of the whole rain dataset. The stratiform rain, on the other hand, showed slightly less deviation of the mean V-D curve from GK line in comparison with the convective rain for both locations. In both cases, the deviation was more prominent in Kolkata (Fig. 6.3c-f). This analysis points toward the presence of a significant amount of non-terminal raindrops in both locations. Therefore, a quantitative analysis of super- and sub-terminal drops in the rain spectrum was performed to have a deeper view of the matter. Fig. 6.4 showed the fraction of super- and sub-terminal drops in the different diameter bins in both the study locations. The presence of super-terminal drops was witnessed for small drops (up to around 1 mm in diameter) in both the cities. A slightly higher super-terminal drop fraction was noticed in Kolkata (Fig. 6.4a).

On the other hand, the sub-terminal drops were significant for drops larger than ~0.8 mm in both the locations (Fig. 6.4b), which became lowest around 2.5 mm of diameter and again started increasing. Pretty similar signatures were noticed in the sub-terminal drops for both the locations, but the percentage of sub-terminal drops was higher in Kolkata in comparison with that in Bologna.

The DSD samples were studied further to quantify super- and sub-terminal drops separately in convective and stratiform rain. The super-terminal drop fraction in convective rain was slightly higher in Kolkata (Fig. 6.5a). The stratiform rain also showed a similar signature. However, the difference was smaller in this case (Fig. 6.5b). Besides, the percentage of super-terminal drops was slightly higher in convective rain in both locations, probably due to drop break-up, which is dominant in highly convective rain events [121] Sub-terminal drops are reportedly significant for drops larger than 3 mm [60].

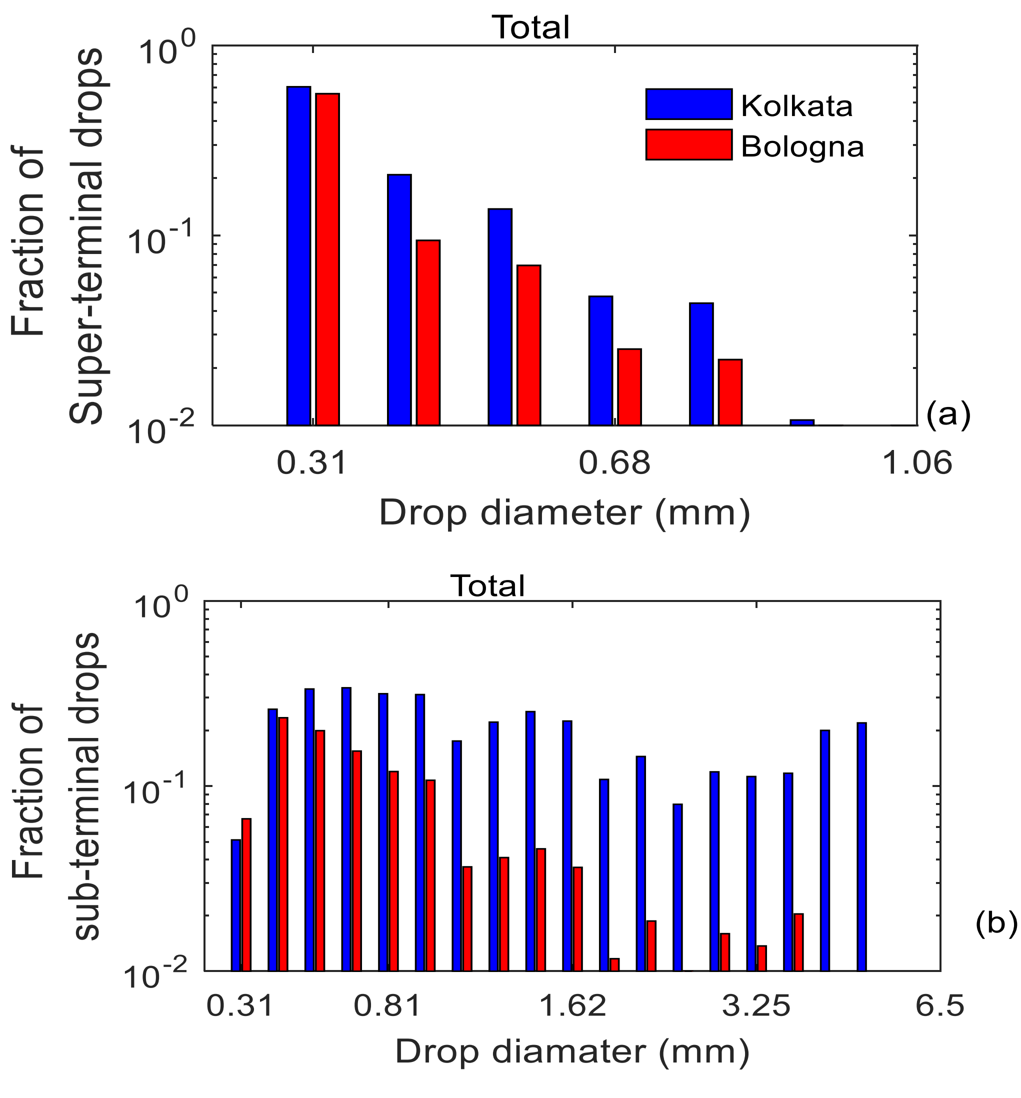

Fig. 6.4: Fraction of (a) super- and (b) sub-terminal drops in the natural rain of Kolkata and Bologna. The fraction of sub- and super-terminal drops represents the ratio between these drops and the total number of drops.

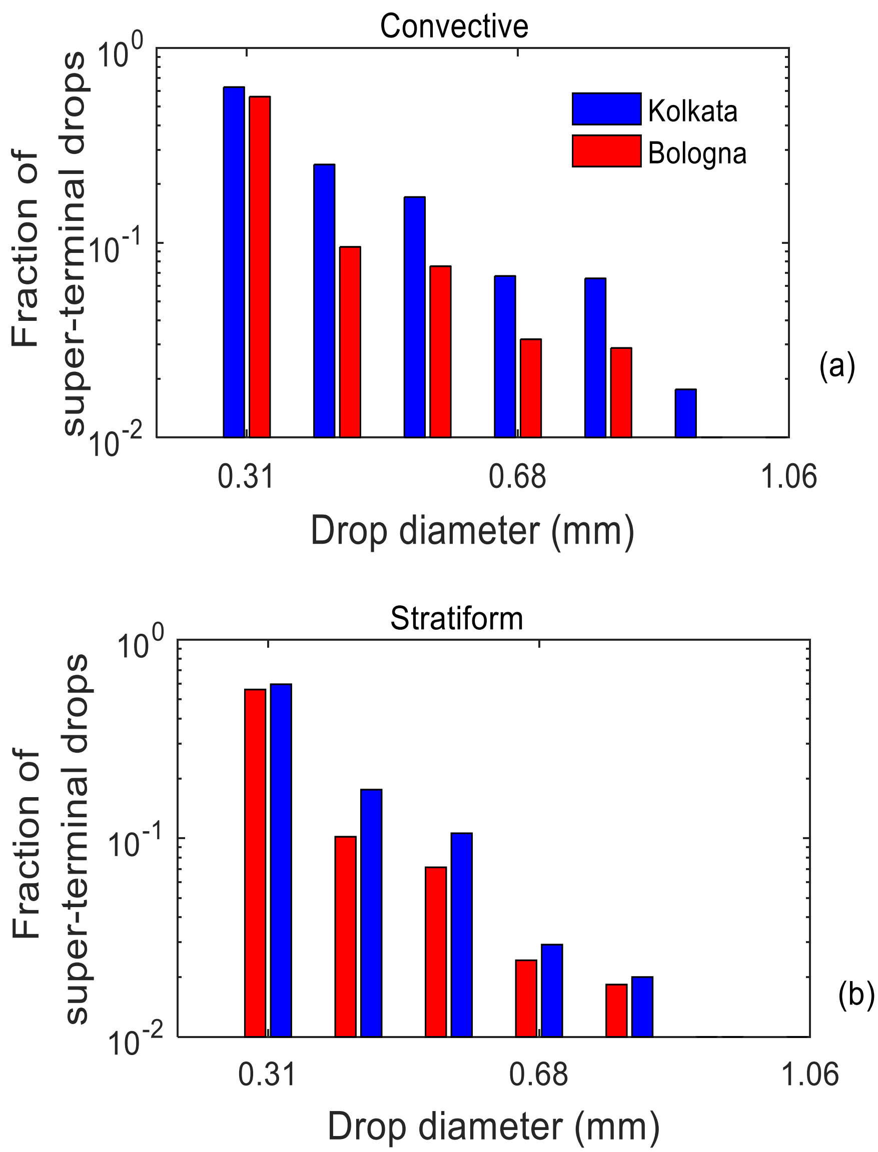

Fig. 6.5: Fraction of super-terminal drops for (a) convective and (b) stratiform rain in Kolkata and Bologna. The fraction of super-terminal drops represents the ratio of these drops and the total number of drops.

Fig. 6.6 (a-b) shows the fraction of sub-terminal drops in convective and stratiform rain in the two study locations considered. In both types of rain, Kolkata showed a higher percentage of sub-terminal drops, more evident for larger drops. The fraction of sub-terminal drops decreased with drop diameter till 3 mm and then started increasing in convective rain for both places (Fig. 6.6a). On the other hand, the stratiform rain showed drops till 3 mm in diameter, and the fraction of drops decreased with the increasing diameter (Fig. 6.6b). However, the decrease of sub-terminal fraction with diameters (till 3mm) was much steeper in stratiform rain.

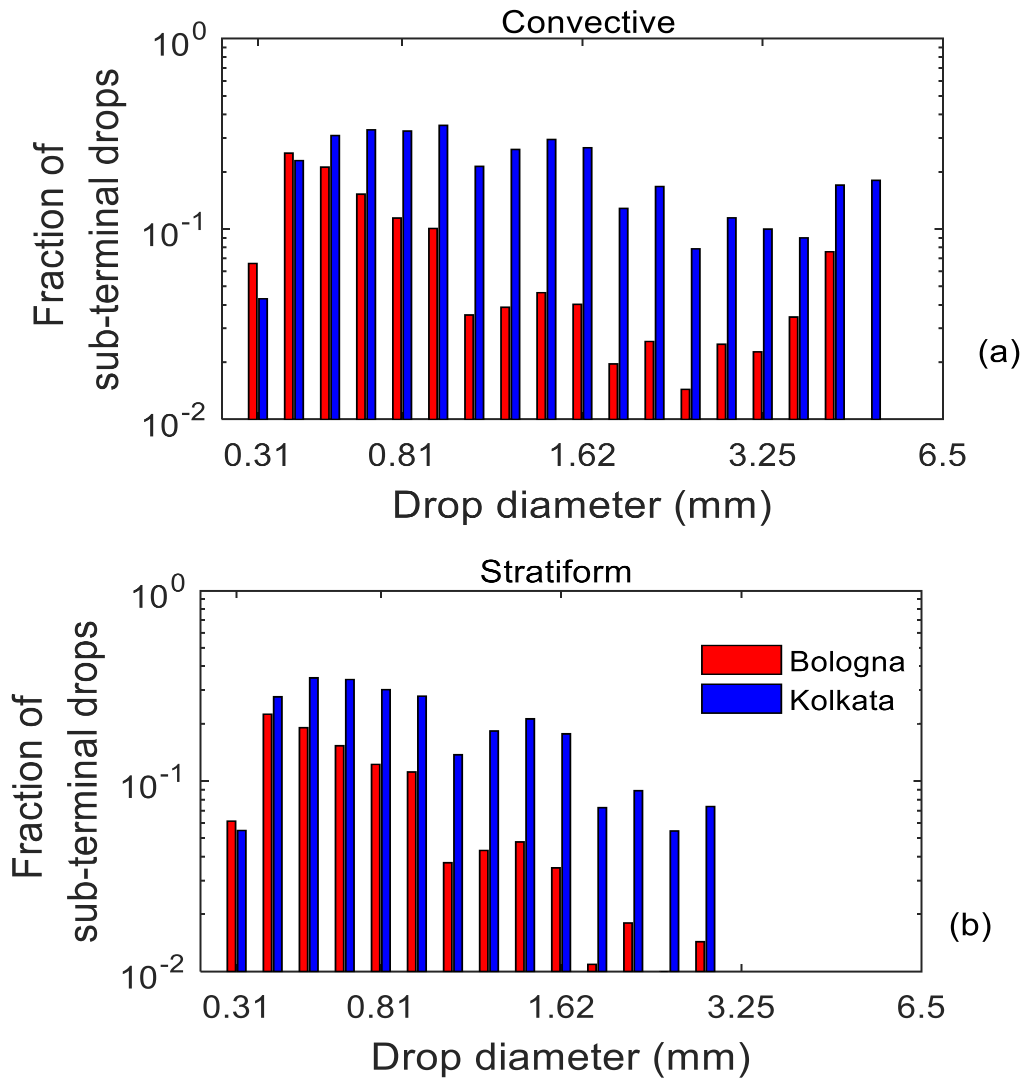

Fig. 6.6: Fraction of sub-terminal drops for (a) convective and (b) stratiform rain in Kolkata and Bologna. The fraction of sub-terminal drops represents the ratio of these drops and the total number of drops.

The above analysis suggests significantly high super- and sub-terminal drop fractions in the natural rain of Kolkata in both the rain types. However, the behavior of non-terminal drops was similar in the two places.

6.3.2. Investigation of physical processes involved in presence of non-terminal raindrops

The probable mechanism that can significantly influence the raindrop velocity is the break-up of drops [58]. Therefore, an investigation has been carried out next to check for the signature of drop break-up in rain DSD. Since the break-up is more likely to occur in intense rain [48], rain samples with an intensity lower than 5mm/h are not considered in this particular analysis.

The highest slope (HS) of DSD is studied within a drop diameter range of 1-2.6 mm to assess the signature of the break-up, based on the algorithm proposed by [125]. The slope of the linear best fit is computed and considered as the highest slope of that instant.

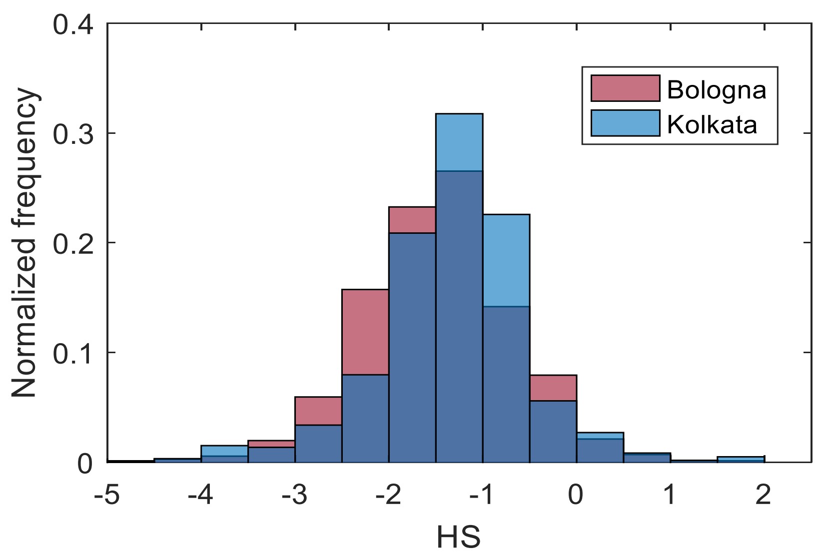

Fig. 6.7: Distribution of HS values in natural rain of Bologna and Kolkata

Here, it is to be noted that the HS algorithm was implemented after a 2 minutes averaging of the DSD samples in order to minimize undesired instabilities. The distribution of HS values in the two places looked comparable except for a little wider spread in Bologna (Fig. 6.7). The HS, in most of the instances, showed a value within the range of -2 to 0 for both the places. So, this interval is subdivided into four uniform classes, and two other classes were defined outside this range (Table 6.2). The drop break-up is expected to exist for HS>-0.5 [121].

It is interesting to note that almost 7 % and 10 % of the rain samples in Bologna and Kolkata correspond to 5th and 6th HS classes, i.e., showed evidence of drop break-up (Table 6.2). Therefore, the break-up in natural rain in these two places cannot be neglected.

Wind turbulence is reported to be a major influencer in the modulation of raindrop velocities and also in the capability of the disdrometers to perform reliable measurements [48].

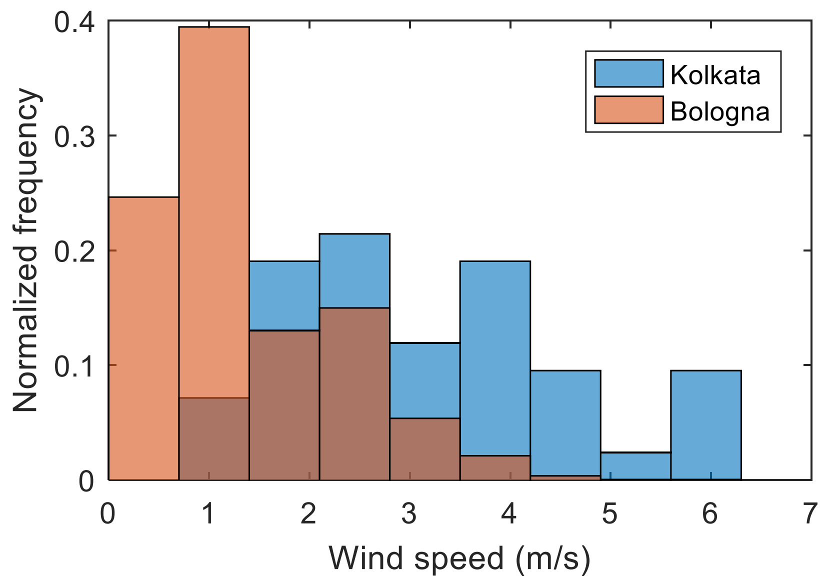

Fig. 6.8: Distribution of wind speed during the rain events

An increase in wind speed during rain episodes has been reported to cause an enhancement in the number of collisional-break-up events, producing larger proportions of super-terminal drops, whereas turbulence can lead to sub-terminal drops [65]. Therefore, it was of valid interest to look at the wind speed during the events considered.

Here, wind speed data measured at an interval of 30 minutes has been obtained from the automatic weather station at the Kolkata airport within an aerial distance of 6 km, whereas, in Bologna, the wind measurements were procured with a cup anemometer placed close to the disdrometer, with 30 minutes sampling rate.

The wind speed distribution (Fig. 6.8) showed the dominance of windy events in Kolkata, which can be a possible catalyst behind the higher non-terminal drops in natural rain of the location.

Table 6.2: Number of DSD samples (2 minutes) in different HS classes. Cells in grey represent classes where break-up exists.

	Kolkata	Bologna
HS<-2	88	176
-2<HS<-1.5	124	164
-1.5<HS<-1	201	187
-1<HS<-0.5	120	100
-0.5<HS<0	39	56
HS>0	26	22

6.3.3. Identification of causes behind non-terminal drops in individual events

The results showing the evidence of non-terminal velocities and the presence of drop break-up in the natural rain of the two places interested us in further event-wise analysis. Therefore, the fraction of non-terminal drops in individual events was studied next for all the events. Few events in Kolkata showed signs of super-terminal drops up to a diameter of 1.2 mm, whereas some events witnessed super-terminal velocity only in tiny drops less than 0.9 mm (Fig. 6.9a). On the other hand, super-terminal drops were witnessed in Bologna for small (< 0.6 mm) drops during most of the events. However, even though the different events studied showed a significantly varied fraction of super-terminal drops (Fig. 6.9b), it is evident that the presence of super-terminal drops was not an event-specific phenomenon.

The event-wise analysis agrees with the previous findings of a higher super-terminal raindrop fraction in Kolkata. Fig. 6.10(a) and (b) showed the fraction of sub-terminal drops witnessed in each of the event respectively in Kolkata and Bologna.

~~The~~ diversity among rain events was well evidenced in sub-terminal spectra, which is more prominent in events at Bologna (Fig. 6.10b).

Most of the events in Bologna showed approximately around 20% of sub-terminal drops within a diameter of around 2 mm, few of them continued till pretty longer in the diameter spectrum and witnessed a much higher percentage of sub-terminal drops.

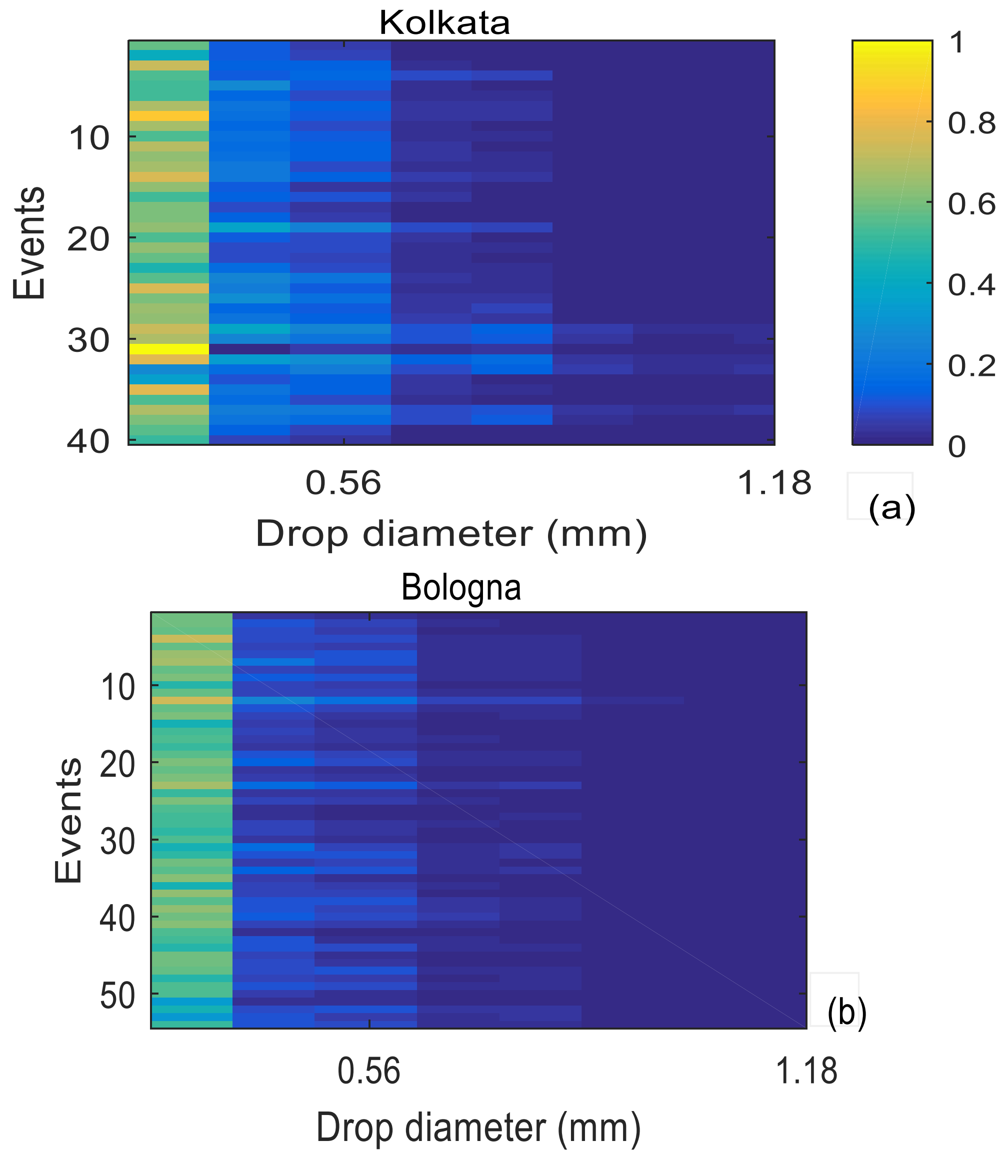

Fig. 6.9: Fraction of super- terminal drops in the rain events in (a) Kolkata and (b) Bologna. The color bar represents the fraction of drops.

In Kolkata, a higher percentage of sub-terminal drops were observed in almost all the events which varied between 20-40 % .The presence of sub-terminal drops were pretty consistent in all events till a drop diameter of 2 mm after which it varied for the different events. However, the percentage of sub-terminal drops were lower within a drop diameter of 2-3 mm after which it again started increasing. The variation among the different events was a little less in Kolkata than that in Bologna (Fig. 6.10a).

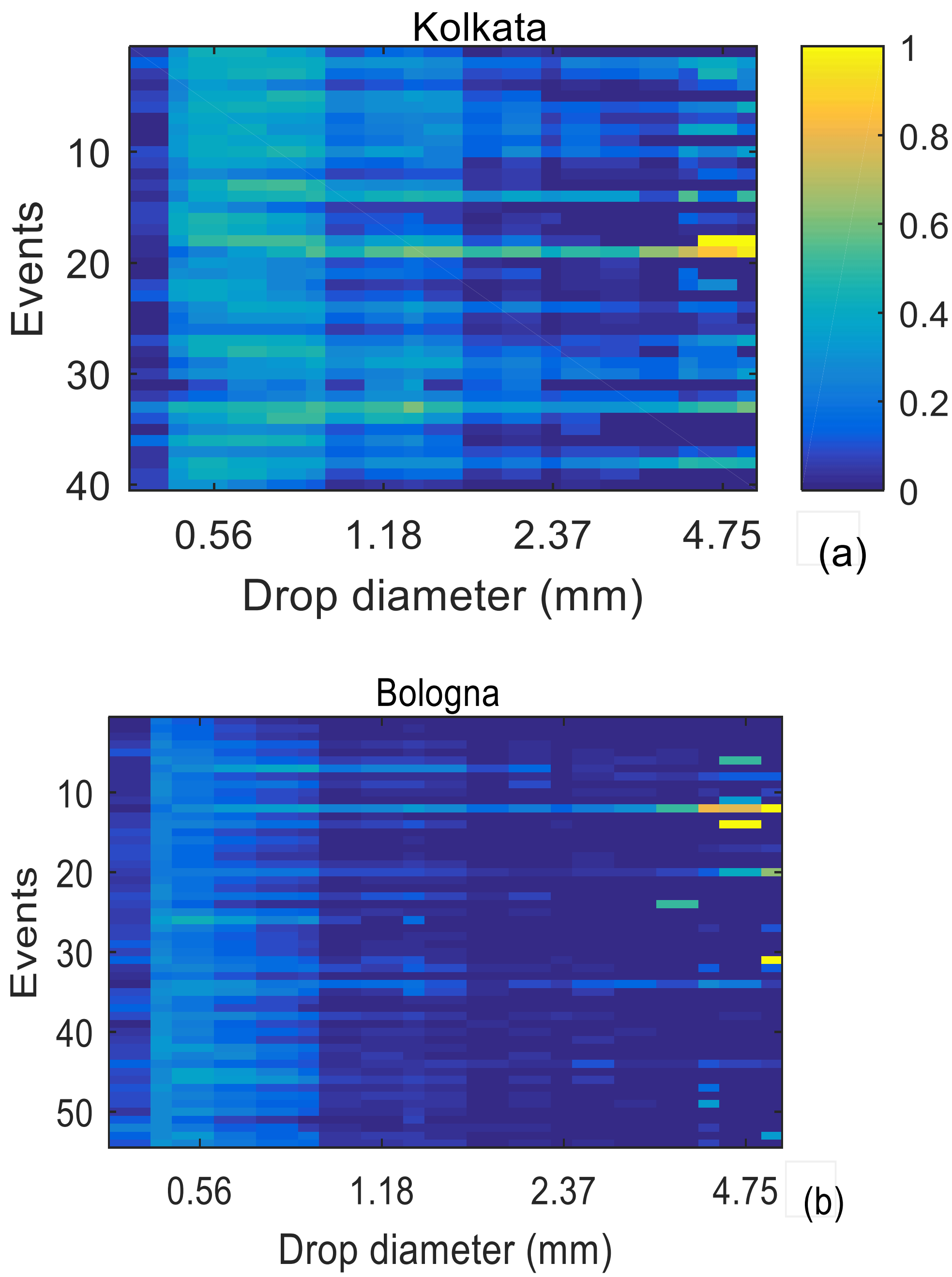

Fig. 6.10: Fraction of sub-terminal drops in the rain events in (a) Kolkata and (b) Bologna. The color bar represents the fraction of drops.

This study has attempted a baseline approach to look at the contribution of break-up in the presence of super-terminal drops in the rain events. It is to be noted that this study has been carried out for only rain events having average rain intensity greater than 3mm/h since the process of break-up and coalescence are dominant in the higher rain intensities [124].

In both the locations, the events were classified into two categories: 1) events with an average super-terminal fraction of drops (within 0.3-1.6 mm) higher than the average super-terminal percentage of the entire dataset; 2) events having a fraction of super- terminal drops lower than the average (Table 6.3). When $-0.5<HS<0$, this class can be considered as a transition where break-up is negligible to equilibrium DSD. When $HS >0$, the break-up starts becoming dominant [121]. Here, for analysing the role of break-up in super-terminal fraction of drops we have considered minutes with $HS> 0.25$ where break-up will be significant.

A clear dominance of break-up occurrences has been noticed in Bologna in the first class (Fig. 6.11b), whereas the signature was not very identifiable in Kolkata. The fraction of break-up minutes was notably high in Bologna.

A similar approach was repeated in the case of sub-terminal drops to verify if the process of coalescence had any visible role in it. The peak mean volume diameter (D_m) seemed to have dominance of higher values in the rain class, having a higher sub-terminal fraction in both the places (Fig. 6.12a-b).Although this study is not sufficient to infer the coalescence as the sole reason behind the process, this abundance of medium and large drops in the rain spectra points toward the occurrence of coalescence in the natural rain of the two locations.

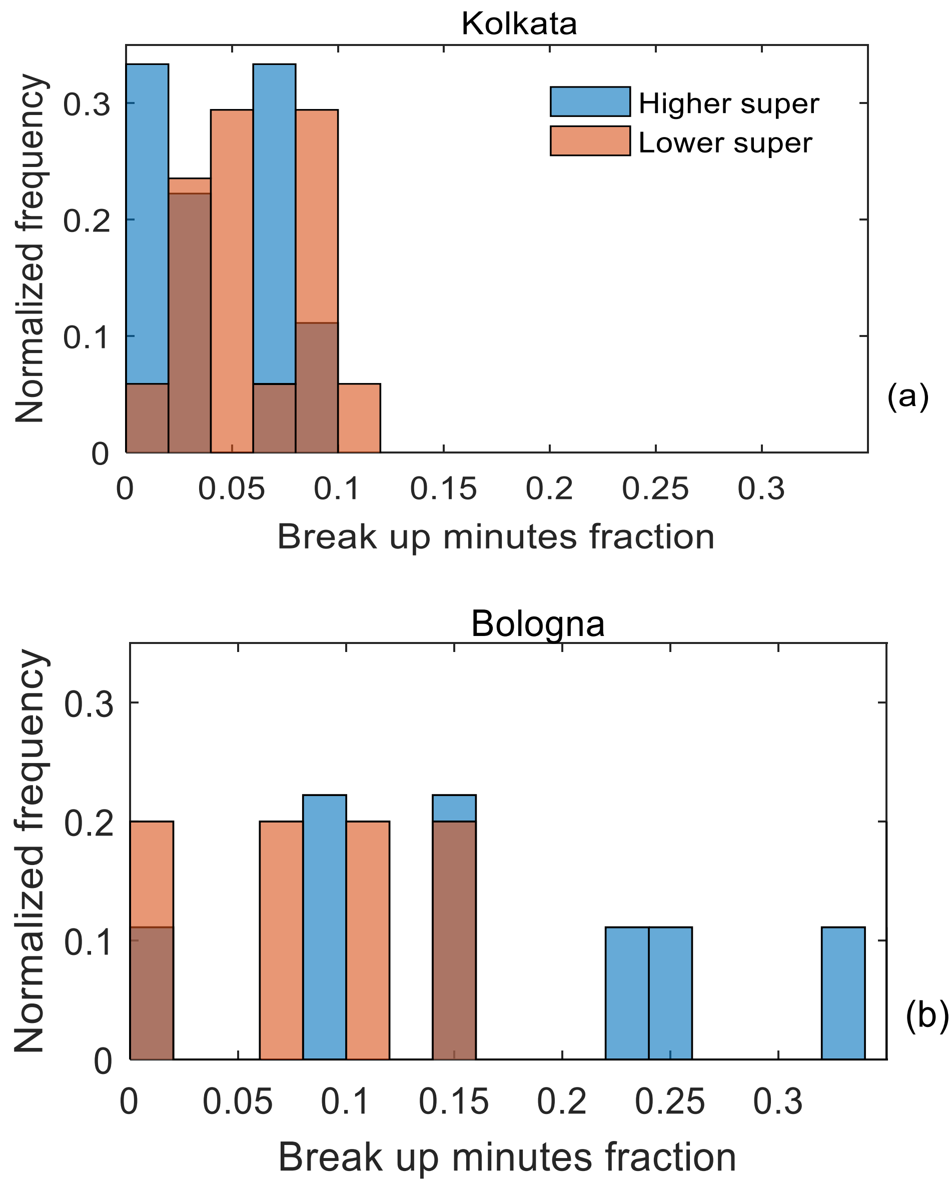

Fig. 6.11: Distribution of fraction of break-up minutes in events with lower (than average) and higher (than average) percentage of super-terminal drops in (a) Kolkata and (b) Bologna. The break-up minutes fraction represents the ratio of the number of break-up minutes with the total rain minutes

Therefore, the event-wise correspondence between non-terminal drops and evidence of significant drops break (HS>0.25) and coalescence have been further investigated.

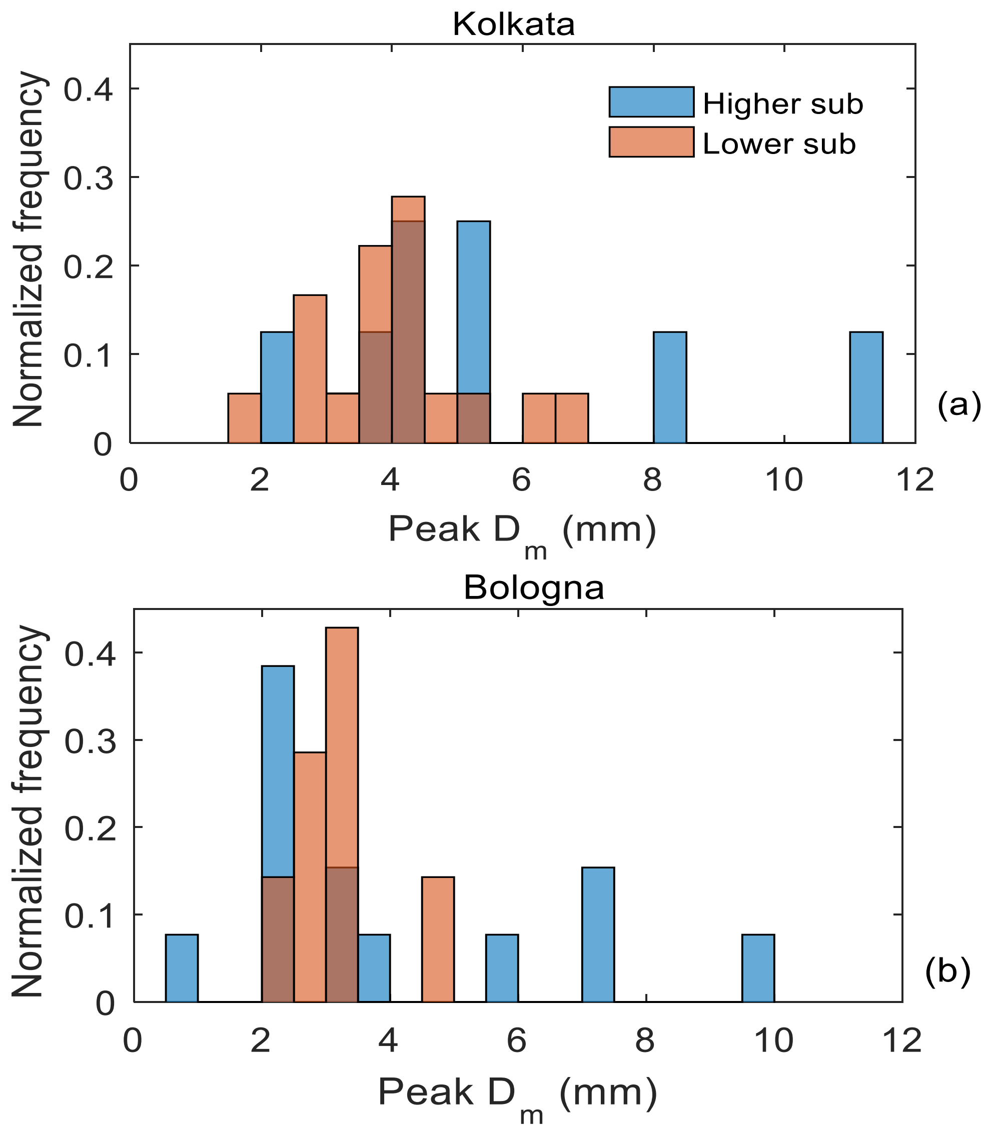

Fig. 6.12: Distribution of peak D_m in events with lower (than average) and higher (than average) percentage of sub-terminal drops in (a) Kolkata and (b) Bologna.

Fig. 6.13 reported for both sites and for each event, the fraction of non-terminal drops as function of break-up minutes fraction and peak D_m. Our previous findings were further supported with a good association between break-up minutes fraction (ratio of the number of break-up minutes and total rain minutes) in Bologna, whereas it did not look that imperative in Kolkata (Fig. 6.13a). Furthermore, significant correspondence was noticed between the peak D_m and sub-terminal drops in both places (Fig. 6.13b) which indicated the major role of coalescence process in the presence of sub-terminal drop fraction in natural rain of these locations.

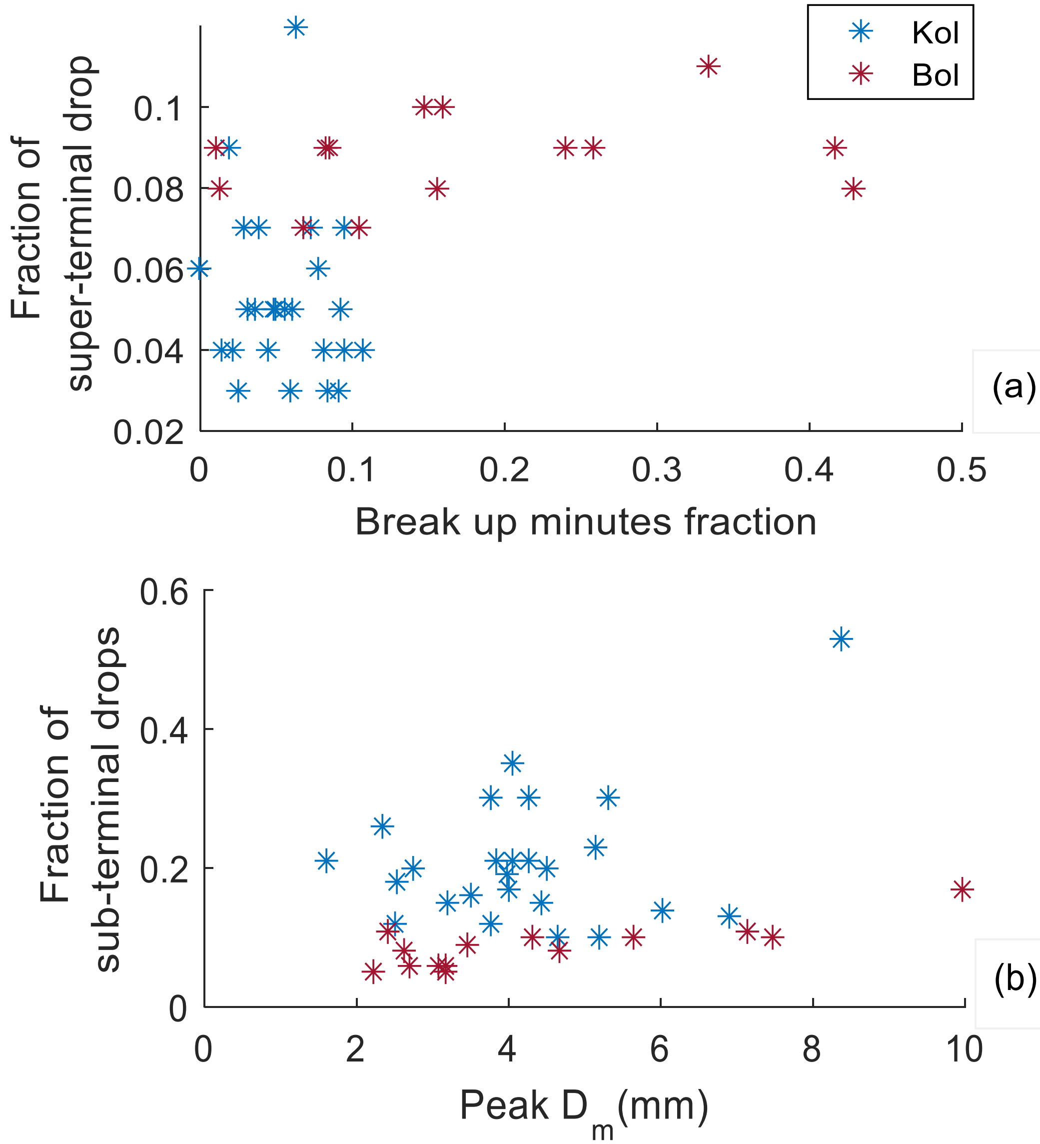

Fig. 6.13: Relation between (a) break-up minutes fraction and fraction of super- terminal drops and (b) peak D_m and fraction of sub-terminal drops in Kolkata and Bologna. The break-up minutes fraction represents the ratio of the number of break-up minutes with the total rain minutes

Table 6.3: Statistics of non-terminal drops in Bologna and Kolkata**.

		Average non-terminal fraction	No. of events higher Non-terminal fraction	No. of events lower Non-terminal fraction
Bologna	Super	0.09	9	5
	Sub	0.08	7	7
Kolkata	Super	0.05	9	17
	Sub	0.21	8	18

**The events with higher non-terminal fraction represent events with higher than average non-terminal drops

6.4. Conclusions

The current work discusses the necessity of reconsidering the terminal velocity notion in velocity-diameter relationships of natural rain. The study reports a thorough analysis on evidences of non-terminal velocities in a tropical and a mid-latitude location. The effects of influential parameters like convection and wind speed are also analyzed in association with the deviation of velocity-diameter relation from standard approximation. The study reveals an abundance of large and medium-sized drops in the convective rain of Kolkata, whereas Bologna seemed to have a clear dominance of small raindrops. On the other hand, the stratiform rain in Bologna presented larger drops (~3mm) than in Kolkata (~2.6mm). Significant lowering of the mean V-D curve has been noticed from the GK line in both Bologna and Kolkata, which increased towards larger raindrops starting from 1mm in diameter. The study has ascertained the presence of significant amount of super- and sub-terminal drops in natural rain of both tropical and mid-latitude regions in all types of rain (convective and strartiform). The percentages of both super- and sub-terminal drops were higher in Kolkata. However, the difference was more notable for convective rain. Percentage of super- and sub-terminal drops were found to be high within a drop diameter of 1 mm. The number of sub-terminal drop showed an increase with an increase in drop diameter for drops larger than ~2.5 mm. This study also points toward the notable drop break-up occurrence in natural rain in the two sites. 7% and 10% of the natural rain samples respectively in Bologna and Kolkata seemed to be subjected to drop break-up. The event-wise study performed in each of the two locations confirmed that the non-terminal drops are not event-specific. Significant correspondence was observed between drop break-up and percentage of super-terminal drops in natural rain of Bologna. Both the places showed a good correlation between sub-terminal drop fraction and large mean volume diameter which signifies the role of coalescence in the percentage of slower drops. The findings imply that ground-based or satellite-borne radars relying on the GK relationships should therefore be verified by disdrometers for the calibration of precipitation remote sensing algorithms. The outcomes of this study once again point toward the need for retrieved raindrop size and velocity instead of consideration of standard velocity-diameter relationships like Gunn-Kinzer for precise measurements.

Chapter 7

Major outcomes and discussion

7.1 Introduction

Recent climatic changes and increasing weather extremities in India have been the primary motivations behind this thesis. Successful identifications of different rain and lightning climatologies were two vital steps in process of understanding the recent rain and lightning pattern over the country. The said process revealed the need of accurate radar based QPE in modeling and prediction of rain related irregularities and extremities over the country. Characterization of the uncertainties in rainfall parameters due to two less explored factors i.e. lightning and the terminal velocity approximation in natural rainfallwere attempted in this thesis. This chapter discusses the major outcomes reported.

7.2 Regionalization of Indian rain

Rain climatology over a region depends on several parameters like rainfall statistics, topography and rain formation process. Inclusion of different rain features related to rain types and extremity is therefore advantageous in defining rain climatologies which can in turn lead to successful measurements, understanding and prediction of rain distribution over the regions in future. Use of satellite data has made the proposed method suitable to be applied in any other region in the globe.The rain regionalization until so far were principally based on rain gauge data with a single rain feature i.e. rain intensity. Rain climatologies having similar rain intensities may have distinct rain features in terms of rain frequency and different rain categories.

The current study have focused on six different rain features including two broad categories of rain (convective and strartiform) and number of ~~extreme~~ rainy days which finds its application in defining different climatologies in the recent scenario. The major outcomes of this study are firstly the identification of the recent rain climatologies and secondly, the different rain trends witnessed by different Indian regions during last four decades.

The clustering process resulted in nine distinct rain zones (Fig. 3.5). C2 and C5 were previously clustered as a single homogeneous region based on rain intensity [30] but it can be noted that the rain frequency is significantly different for these two region (Fig. 3.1(c)). Hence, considering all the rain features, logically it should be clustered into two separate rain climatologies. Major portions of C7, C3 and C6 were also clustered as a single rain zone due to similar reasons. Most of the regions in C5 and C1 zones clustered as a single rain zone due to similar rain amount [33] but interestingly, consideration of rain types divides them in two separate zones as shown in Fig. 3.5. Central Indian regions are observed to have the same rain climatology (C8) which was previously seemed to be two different zones. Authors in [126], has also identified the C2 region (Western Ghats) having different rain climatology. C4, some portion of C5 and C8 were clustered as a rain zone by the authors. Similarly, some portion of C5, a part of C8 and C1 is clustered as a same rain zone. The present study has shown that these regions have distinction in rain frequency and convective and strartiform rain features in spite of having mostly similar rain intensity (Fig. 3.1(a-c)).

Five of the said regions were found to have decreasing monsoon rain trend during last four decades whereas; two other showed increase in rainfall. Summer monsoon over Indian subcontinent is principally a thermally driven process. High positive correlation is observed between surface temperature and monsoon rainfall over Northwest and central part of India [129]. Significant impact of SST over Arabian Sea and Bay of Bengal on Indian monsoon has been reported by several authors [130-131]. However, The

Indian Ocean SST seemed to have a contrary impacts on different parts of the Indian subcontinent. ENSO seemed to have a negative correlation with the Indian summer monsoon rainfall [132] whereas, the formation of monsoon depression associated with occurrence of heavy rainfall is likely during El Nino years [133]. The European surface temperature was also reported have an impact on Indian monsoon [134]. Even though there are some common atmospheric factors affecting monsoon rainfall over the country, the variability of summer monsoon rainfall over different parts of the country have different set of atmospheric influencers to account for [135].

7.3 A Machine learning approach for prediction of lightning over Indian subcontinent

The recent change of climate and increasing extremities has two prominent component visible over Indian subcontinent i.e. irregular rainfall and severe lightning. This work has attempted prediction of lightning density using the ML,for the first time over the entire Indian region. However, lightning is an extremely dynamic process both in spatial and temporal scale. A single model may not be applicable for a large country with enormous topographic variety.Therefore, the current study, has regionalized Indian region in different lightning zones using lightning density andassociated atmosphericvariables. The clustering information has been used here in order to propose a single model for prediction of lightning density for the entire Indian region.

Seven distinct lightning climatologies were identified by the process. The well separable features space in different clusters confirmed the consistency of the clustering process (Fig. 4.6). It also points towards the existence of different lightning zones over different parts of the country. The lightning activities were predicted over the resulting clusters based on the atmospheric variables using four ML based regression models among which Random forest showed the best performance with an overall (averaged over all the clusters) R^2 score of 0.81 during monsoon and 0.71 during pre-monsoon.

Notably varied association was observed between atmospheric features and lightning density both in spatial and seasonal scale (Fig. 4.12). CAPE were found to have strong influence on lightning over most of the land masses during monsoon but the pre-monsoon lightning were found to be primarily governed by the atmospheric humidity and cloud microphysics. On the contrary, lightning activities over major portion of the oceanic region in Indian subcontinent found to be strongly associated with specific humidity at different atmospheric heights during both the seasons.

The model performed significantly well in four of the resulting clusters whereas; it performed moderately in two others. However, the use of satellite data limits the data period to around a decade which is not a sufficiently long period but this approach can be beneficial because of the greater areal coverage received from satellite data. Use of long term lightning measurement can make the model more robust which will be a future area of study to be attempted. Even though the study has been carried out over India, the use of satellite data make it suitable for implementation in any geographic region. In the present form of the study is not an inclusive real time forecast model but this approach can be extended to the output of the NWP models.

7.4 Impact of lightning on precipitation microphysics

This thesis shows the assimilation of satellite data with ground measurements can serve as an excellent pathway in studying the rainfall pattern and its vulnerability to climate change uncertainties. However, satellite based QPE is challenging due to its dependence on rain microphysical structure and empirical relations connecting it to radar based rain estimates. Therefore, the uncertainties in rainfall parameters due to some less explored factors have been investigated next.

The study reports the fundamental differences between precipitation systems during rain with and without lightning from a tropical location. Small cloud droplet size and colder cloud tops were found to be more favorable for lightning. The higher instability in convective cloud results into more collision and breakage of ice particles into smaller particles which moves upwards acquiring positive charge. Thick clouds found to be more favorable for lightning because of a colder cloud top at a greater altitude.

Significant alternations have been observed in ground rain as well during lightning. Both microphysical and integral parameters of rain seemed to have distinguishable behaviorunder lightning condition from non- lightning rain events. The rain DSD showed dominance of larger drops during lightning, indicating greater degree of convection which finds good agreement with the increased instability of the precipitation system during lightning [6]. Moreover, both radar reflectivity and rain attenuation were found to varysignificantly under these two types of rain conditions. The radar reflectivity is greater in case of rain events with lightning likely because of dominance of larger rain drop. Significantly high a(398.1) value in Z-R relation was obtained for lightning events in comparison to non-lightning database (199.52). The modulation of empirical relation between Z-R can be crucial in radar based QPE. Path attenuationscaused by these two categories of rain were found to have opposite influenceson two GPM frequencies. The K_a band frequency seemed to be attenuated more in rain with lightning in comparison to non-lightning case whereas, the K_u band frequency shows opposite behaviour.The empirical coefficients of the relation linkingthe specific rain attenuation and rain intensity were found to vary largely for rain with/without lightning.

7.5 Evidences of super- and sub-terminal drops in different rain categories and climate regimes

The radar based QPE is modulated largely by another approximation in radar estimation of rainfall i.e. the notion of terminal velocities in natural rain process.Comparative studies reporting the microphysical differences between tropical and mid-latitude rain are limited.The current study, for the first time has carried out a thorough analysis on a statistically large dataset belonging to two different climate regimes (a tropical and a mid-latitude location) to investigate the existence of non-terminal drops in natural rainfall.

This study reports significant percentage of non-terminal drops in natural rain of both tropical and mid-latitude location. The V-D curve of rain drops showed visible deviation from GK line in both places (Fig. 6.2). The spread of V-D curve was much higher in convective rain than stratiform rain. It is an established fact that natural rain is accompanied by complex air motions which can deviate the shape, size and velocity of raindrops. Authors of [136-137] also reported the deviation of V-D spread from the GK relationship. Here, a wider spread and deviation of the V-D curve has been observed in convective rain, which finds good agreement with our general understanding of convection. This is because clouds are usually extremely turbulent systems [138] and rainfall is associated with different scales of upward and downward air.The deviation was larger in Kolkata in all rain types. To be specific, the quantification of non-terminal drops showed higher percentages of both super- and sub-terminal drops in Kolkata. Evidence of significant amount of super- and sub-terminal drops was reported over the Indian region by [139] as well. Percentage of sub-terminal drops were found to be high within a drop diameter of 1 mm which continued to decease till ~2.5 mm and then started to increase again. [63, 60] also reported high percentage of sub-terminal drops for rain drop diameter larger than 3mm. Dominance of larger wind speed in Kolkata is likely to serve as one of the major influencers here which find good agreement with the results reported in [61].

The event-wise analysis with 54 and 41 events respectively from Bologna and Kolkata confirmed the occurrences of non-terminal drops were not an event-specific phenomenon in the natural rain of these two places (Fig 6.9-6.10). It is to be noted that the rain databases consist of rain event from all the seasons. All the events presented significant percentage of both sub- and super-terminal drops below 1 mm diameter. Very similar findings were reported in [122] over Indian region. [61]also reported significant fraction of super-terminal drops for drops smaller than 1 mm in temperate region.

There exist a couple of physical processes which dictate the shape of DSD in natural rain. Collisional break-up and coalescence are the two major mechanisms involved in the said process [57-58].Here, respectively 7% and 10% of the natural rain samples in Bologna and Kolkata seemed to be subjected to drop break-up. Notable correspondence was observed between drop break-up occurrences in an event and the percentage of super-terminal drops in Bologna (Fig. 6.13(a)). The results fall in line with the previous reports [60]. On the other hand, both the places showed good agreement between sub-terminal drop fraction and the presence of a large mean volume diameter which signifies the occurrence of coalescence (Fig. 6.13(b)). The current study can be useful in understanding the characteristic differences between the natural rain of the two regions. Moreover, the comparative evidence of non-terminal velocities between tropical and mid-latitude regions and the role of the break-up and coalescence in the same can facilitate the quality improvement of radar based rain meteorology over tropics and mid-latitude.

Chapter 8

Conclusion and future scope

8.1 Conclusion

The socio-economic status of India relies principally on the agricultural resources which is directly linked with thepredictability of amount, frequency and timeliness of rainfall. Besides, the increasing weather extremity in India calls for an improved modeling and prediction of thunderstorm events. Assimilating satellite retrieved rain measurements with ground based observations can serve as an excellent pathway to achieve a successful rainfall analysis over large geographic area of interest like India which seems crucial especially in view of recent climatic changes. This thesis has attempted the same for regionalization of Indian rain climatologies in order to map the susceptibility of different Indian regions to climate change which is emerging out to be an extremely crucial question in view of recent Indian scenario. Moreover, the increasing rain extremity both in terms of rainfall amount and lightning strikes in some places over the country and chances of drought over some others, have created a very urgent need of better projection of Indian rain in coming years. This study has reported statistically significant decreasing monsoon trend in five rain climatologies whereas; two of them have shown significant increasing trend. Further, this work hasidentified the different lightning climatologies over Indian subcontinent based on lightning density and the atmospheric influencers. A single ML based model has been developed to predict lightning over entire Indian region with the help of this regionalization information. Besides, the study reports varied association between lightning activities and atmospheric features over different lightning regions which again have noteworthy seasonal variation. The approach presented here, can be useful in having a better insight into the regionalization of rain and lightning over a large geographic area which can facilitate the understanding and prediction ofsuch activities in near future which is extremely vital in recent climate change scenario.

The thesis also points towards the requirement of corrections in radar based QPE by reliable ground measurements to make it robust against different types of uncertainties. The performance of a radar relying on standard relationships to estimate rain integral parameters from measured reflectivity can be largely modulated under different rain conditions. The microphysical structures of both cloud system and ground rain arefound to change notably under rain conditions with significant lightning. Statistical analyses on anlarge dataset belonging to two categories of rainfall i.e. with/without lightning were presented in the current work for the first time to have an in-depth visualization of the matter. The strong association between lightning and precipitation microphysics can also serve as an excellent a pathway for successful prediction of convective activity in mesoscale systems. The reported modulation of equations linking rain microphysical parameters with radar retrieved rain estimates during lightning can help in improving radar based QPE.

This thesis once again points towards the need of ground based correction in radars converting the rain drop velocity to its size through standard relationships based on terminal velocities.The concept of terminal velocity takes into account the stagnant air condition which is greatly disturbed by the wind turbulence in natural rain process. Thiswork reports noteworthy percentage of non-terminal drops in both tropical and mid-latitude location. The natural rain in tropics was found to have more percentage of both super- and sub- terminal drops which were more evident in convective rain. The role of drop growth mechanism and wind turbulence were investigated in the fall velocity of rain drops in the two said places. 7 % and 10 % of the natural rain samples of Kolkata and Bologna were found to be subjected to drop break-up, respectively. Break-up and super-terminal drops were found to correspond well in Bologna whereas; the association was poor in Kolkata. On the other hands, wind turbulence was found to be likely a major regulator in case of the tropical location (Kolkata).

8.2 Future scope

Rainfall is a complex process which is governed by several atmospheric variables. The set of parameters and their degree of influence on the rainfall pattern is likely to vary over different rain climatologies. Proper prediction of rainfall pattern in near future is directly linked with identifying the set of such parameters. The causal analysis of the recent monsoon trend in the reported rain climatologies comes within the future scope of this thesis. The lightning prediction model developed here is based on a decade long dataset. Therefore, creating a more stable prediction model with a longer dataset is an important future goal to be attempted.GPM mission happens to be the only global source of rain measurements on-board. The thesis reports notable uncertainties in the precipitation structure because of lightning and non-terminal velocities. Successful application of the reported variation in radar data with a specific focus on GPM satellite will be a beneficial future endeavor to be attended. Besides, incorporating measurements from a few more climatic regions on these uncertainties can probably be an excellent way to improve the understanding of the processes in a more robust manner.

Appendix-A

Supplementary material for chapter 3

A.1 Mann Kendall Test

The MK trend test [140] determines whether to reject the null hypothesis (H_0) and accept the alternative hypothesis (H_α). The initial assumption of the MK test is that there is no monotonic trend which is represented by H=0 and that the data must be well convincing against the all possible doubts before this hypothesis is rejected. A typical value of alpha is chosen as 0.05 for the present study. If the probability value (p-value) of a test is lesser than α, the null hypothesis is rejected; otherwise, the test fails to reject the null hypothesis. The test shows an H value of 1 if it successfully rejects the null hypothesis.

However, the H value is not sufficient to describe the nature of the trend present and hence the Mann-Kendall statistics (Z_{MK}) is also estimated. A positive value of Z_{MK} concludes an increasing trend of data over the observation period whereas, a negative value indicates a decreasing signature.

Test statistics S is computed as

$$S = \sum_{i=1}^{n-1} \sum_{j=i+1}^{n} sgn(x_j - x_i) \quad (1)$$

Where, n is the number of data samples and x is the data samples.

S is the difference between number of positive differences and number of negative differences between consecutive data points.

The Mann Kendall statistics Z_{MK} is then computed as

$$Z_{MK} = \frac{S-1}{\sqrt{Var(S)}}, \quad S > 0 \qquad (2)$$

$$= 0\,, S = 0 \qquad (3)$$

$$= \frac{S+1}{\sqrt{Var(S)}}, \qquad S < 0 \qquad (4)$$

A positive (negative) value of Z_{MK} concludes in favour of an upward (downward) trend of data over the observation period.

A.2 Pseudo code for K-Medoids

Input: the number of sub-groups K and the route database D

Output: K sub-groups {Oi| i=1, …, K}

Begin

Randomly choose K data points from D as medoids $m_1, m_2, \ldots, m_K$;

Repeat

Assign remaining non-medoid data points to its closest medoid;

Compute total distance of O_i, T_i, between mi and non-medoid r_j, $j=1, \ldots, |O_i|, i=1, \ldots, K$;

For each medoid m_i do

Select the non-medoid r_j for which T_i is minimal;

Compute $T_i(r_j \rightarrow m_i)$;

If $T_i(r_j \rightarrow m_i)$ is smaller than the current T_i;

```
            Swap m_i and r_j;
        End if
    End for
Until no m_i changes;
End
```

Appendix-B

Supplementary material for chapter 4

B.1 K-Means

Suppose X is a set of N samples. K-means algorithm divides X into K ($K < N$) Clusters C. Each cluster is described by the mean of the samples in the cluster which are also called as centroids (μ_j). K-means tries to choose centroids that minimizes within cluster sum of square:

$$\sum_{i=0}^{N} (\|x_i - \mu_j\|^2)$$

B.2. Ridge regression:

Ridge regression solves some of the issues in ordinary least square method like over fitting and collinearity by imposing a regularization term which penalize the coefficients (θ). Regularization parameter α controls the penalty or the shrinkage. This algorithm tries to solve the following equation:

$$\|X\theta - y\|_2^2 + \alpha\|\theta\|_2^2$$

B.3 Lasso regression:

Lasso is the least square regression with the regularization term added. $\alpha$is a constant that controls the penalty and $\|\theta\|_1$ is the l_1 -norm of the coefficient vector. Lasso minimizes the following function:

$$\frac{1}{2n_{samples}}\|X\theta - y\|_2^2 + \alpha\|\theta\|_1$$

.

B.4 Decision tree regression:

Decision Tree regression is a non-parametric method for regression problems where target variable is predicted by learning decision rules which are inferred from the data. There are various types of decision tree algorithms like ID3, C4.5, CART. In this work, CART model was implemented. This algorithm grows a binary tree using simple binary decisions based on features and threshold values which has the largest information gain at each node.

B.5 Random forest regression:

Random forest regression is an ensemble-based model where many decision trees are trained on bootstrapped sample (sampling with replacement) and randomly selected subset of features. The prediction is the average of the outputs of all decision trees. Individual decision tree ends up with a higher variance. These two sources of randomness help to create diverse decision trees. The final prediction is not dependent on a single tree and averaging the output, makes the variance lower. Thus, random forest regression achieves a lower variance.

Appendix-C

Supplementary material for chapter 5

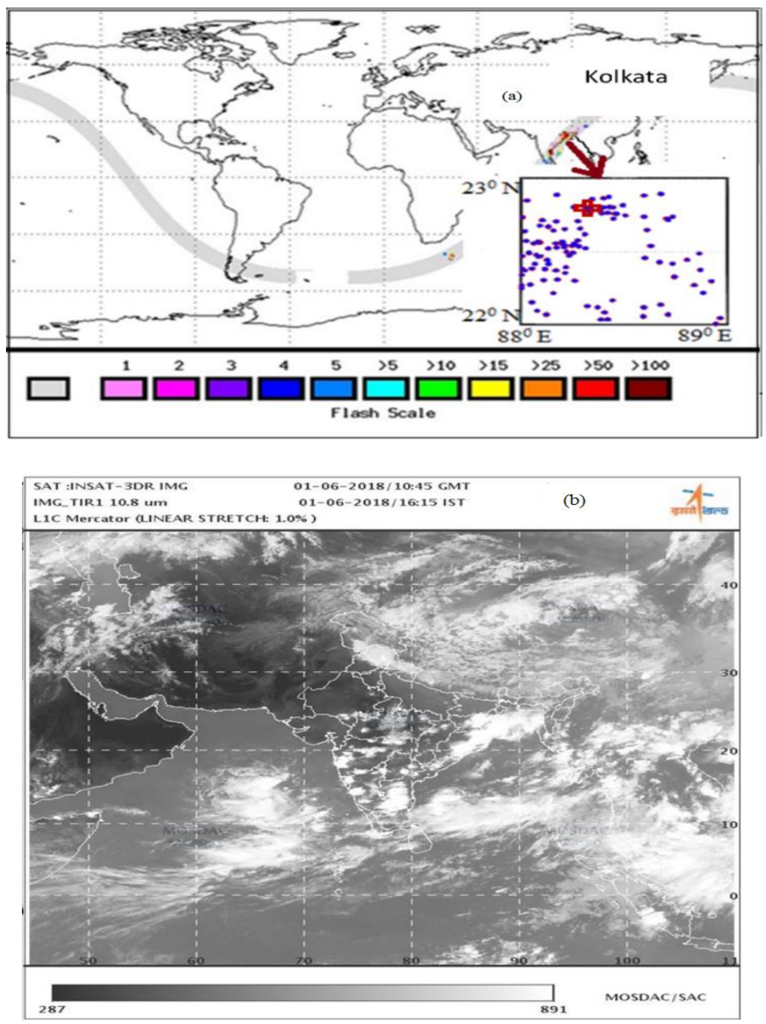

Fig C.1 (a) Lightning during the event as observed by LIS. WWLLN detected lightning flash locations surrounding Kolkata during the rain event is shown in inset figure, (b) Thermal infrared count (mW.cm-2.sr-1.micron-1)of cloud by INSAT-3DR at 10.8 micro meter on June 1, 2018.

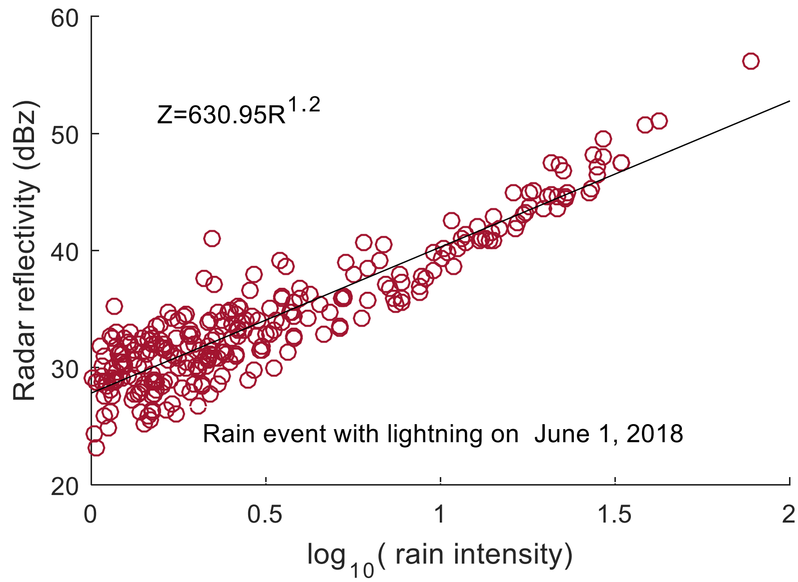

Fig. C.2: Z-R relation for a rain event with lightning

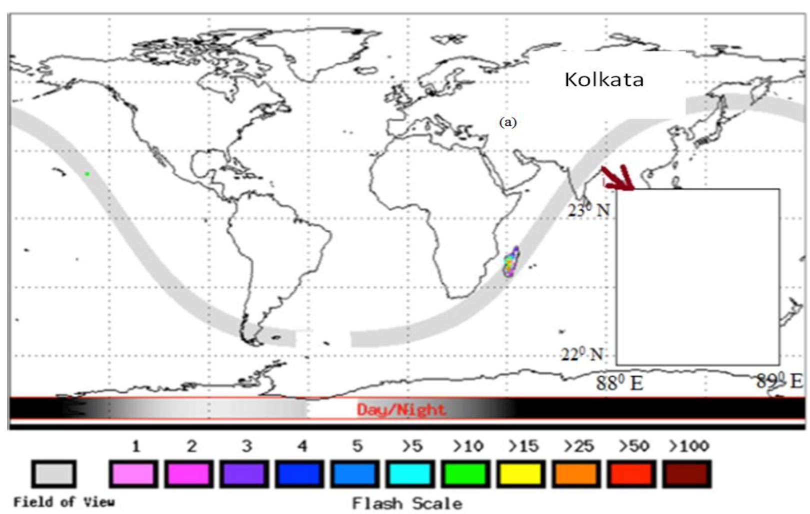

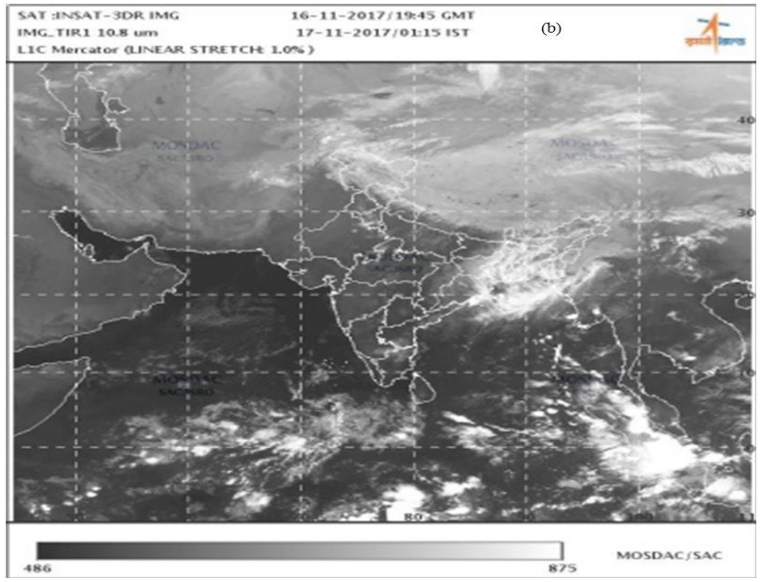

Fig C.3 (a) Lightning during the event as observed by LIS. WWLLN detected lightning flash locations surrounding Kolkata during the rain event is shown in inset figure, (b) Thermal infrared count (mW.cm-2.sr-1.micron-1) of cloud provided by INSAT-3DR at 10.8 μm on Nov 16, 2017.

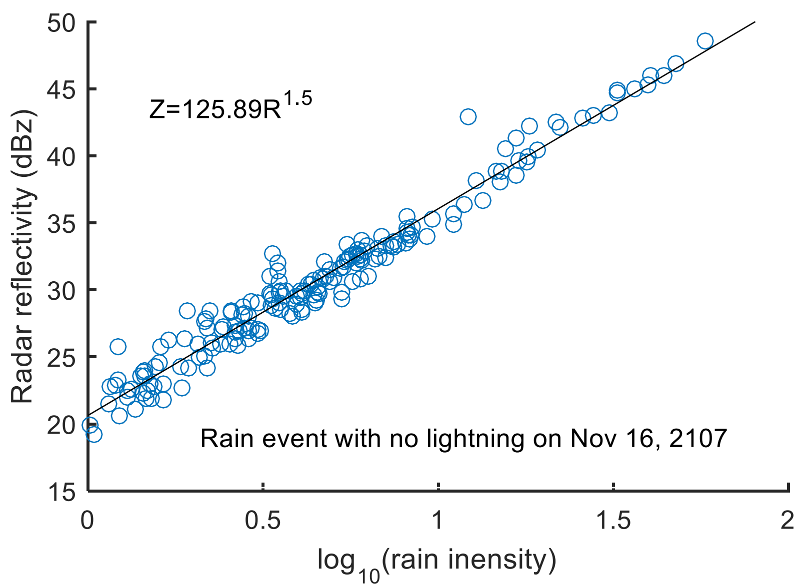

Fig. C.4: Z-R relation for a rain event without lightning

Table C.1: Average cloud properties during rain with lightning

	Date	Cloud Effective Radius	Cloud Top Temperature
1	April 7, 2018	15.37	211
2	April 9, 2018	10.1	180
3	April 11, 2018	-	258
4	April 21, 2018	16.7	223
5	April 22, 2018	20.2	250
6	April 23, 2018	-	219
7	April 26, 2018	19.4	289
8	May 13, 2018	-	207
9	May 18, 2018	18.5	191
10	May 22, 2018	13.8	206
11	June 1, 2018	22.7	217
12	June 8, 2018	27.8	212
13	June 9, 2018	22.2	241
14	June 10, 2018	15.4	180
15	June 11, 2018	27.2	212
16	August 3, 2018	19.5	225
17	August 6, 2018	-	218
18	August 22, 2018	12.1	222
19	August 25, 2018	26.3	210
20	August 27, 2018	-	225
21	September 13, 2018	30.2	206

22	September 15, 2018	25.7	211
23	September 26, 2018	12.8	198
	Mean	19.80	217.86

Table C.2: Average cloud properties during rain with no lightning

	Date	Cloud Effective Radius	Cloud Top Temperature
1	Nov 15, 2017	39.8	246
2	Nov 16, 2017	37.7	225
3	March 15-16, 2018	-	215
4	April 7, 2018	33.4	287
5	May 16, 2018	30.8	283
6	June 17, 2018	23.7	239
7	July 10, 2018	17.3	226
8	July 14, 2018	25.2	272
9	July 21, 2018	29.7	277
10	August 1, 2018	31.3	296
11	August 2, 2018	39	244
12	August 5, 2018	-	-
13	August 7, 2018	33.7	295
14	August 8, 2018	18.4	276
15	August 13, 2018	21.5	203
16	August 14, 2018	-	-

17	August 15, 2018		-
18	August 20, 2018	15.7	230
19	August 28, 2018	24.2	288
20	August 29, 2018	33	297
21	August 31, 2018	29.8	276
22	September 2, 2018	-	252
23	September 20, 2018	31.6	256
24	October 10, 2018	26.4	277
25	October 29, 2018	30.3	288
	Mean	28.69	261.12

‘-‘ indicates the unavailability of data

References

[1] Sinha P., Mohanty U.C., Kar S.C. et al. (2014) Role of the Himalayan Orography in Simulation of the Indian Summer Monsoon using RegCM3. Pure Appl. Geophys. 171, 1385–1407, https://doi.org/10.1007/s00024-013-0675-9

[2] Sanjay J. et al. (2020). Temperature Changes in India. In: Krishnan R., Sanjay J., Gnanaseelan C., Mujumdar M., Kulkarni A., Chakraborty S. (eds) Assessment of Climate Change over the Indian Region. Springer, Singapore (DOI:10.1007/978-981-15-4327-2_2)

[3] Wang G, Wang D, Trenberth KE, Erfanian AYM, Bosilovich MG, Parr DT (2017) The peak structure and future changes of the relationships between extreme precipitation and temperature, Nature Climate Change 7(4), 268–274(DOI:10.1038/nclimate3239)

[4] Thomasa J, Prasannakumarb V (2016), Temporal analysis of rainfall (1871–2012) and drought characteristics over a tropical monsoon-dominated State (Kerala) of India,Journal of Hydrology, 534,266-280

[5] Lacombe G, McCartney M (2014), Uncovering consistencies in Indian rainfall trends observed over the last half century, Climatic Change 123, 287—299

[6] Chatterjee C, Das S. (2022) Change in extreme rainfall over

Indian subcontinent, Proc. of URSI AT-AP RASC, Gran
canaria, Spain, 2022 (In press).

[7] Price C. (2009) Thunderstorm, lightning and climate change, In:Betz et al. (eds.)Lightning: Principles, Instruments and Applications,Springer Science+Business Media B.V. , pp 521

[8] Shamasastry, R., 1915. Kautilya'sArthashastra,(1915 Shamasastry translation).

[9] Huffman G. J., Bolvin D. T., Nelkin E. J., Wolff D. B., Adler R. F., Gu G., Hong Y., Bowman K. P., Stocker E. F(2007) The TRMM Multisatellite Precipitation Analysis (TMPA): Quasi-Global, Multiyear, Combined-Sensor Precipitation Estimates at Fine Scales, Journal of Hydrometeorology, 8(1), 38-55

[10] Arthur Y. H., Ramesh K. K., Steven N., Ardeshir A. A., Christian D. K., Masahiro K., Riko O., Kenji N., Toshio I (2014) The Global Precipitation Measurement (GPM) Mission. Bull. Amer. Meteor. Soc., 95, 701–722.

[11] Chandrasekar V., Bringi V. N. (1987). Simulation of Radar Reflectivity and Surface Measurements of Rainfall, Journal of Atmospheric and Oceanic Technology, 4(3), 464-478

[12] Jameson A. R., Kostinski A.B.(2001) What is a raindrop size distribution? Bull. Amer. Meteor. Soc., 82, 1169–1177.

[13] Bringi V.N., Chandrasekar V., Hubbert J., Gorgucci E., Randeu W., Schoenhuber M. (2003). Raindrop Size Distribution in Different Climatic Regimes from Disdrometer and Dual-Polarized Radar Analysis. Journal of the Atmospheric Sciences - J ATMOS SCI. 60, 354-365(DOI: 10.1175/1520-0469(2003)060<0354:RSDIDC>2.0.CO;2)

[14] Smith P. L., Liu Z., Joss J. (1993)A study of sampling-variability effects in raindrop size observations. J. Appl. Meteor., 32, 1259–1269.

[15]Jaffrain J., Berne A. (2012) Quantification of the small-scale spatial structure of the raindrop size distribution from a network of disdrometers.

Journal of Applied Meteorology and Climatology, 51, 941–953(DOI: 10.1175/JAMC-D-11-0136.1)

[16] Gatlin P. N., Thurai M., Bringi V. N., Petersen W., Wolff D., Tokay A., Carey L., Wingo M. (2015) Searching for Large Raindrops: A Global Summary of Two-Dimensional Video Disdrometer Observations, Journal of Applied Meteorology and Climatology, 54(5), 1069-1089.

[17] Das S., Talukdar S., Bhattacharya A., Adhikari A., Maitra A. (2011). Vertical profile of Z-R relationship and its seasonal variation at a tropical location (2011) IEEE Applied Electromagnetics Conference, AEMC 2011(DOI: 10.1109/AEMC.2011.6256915).

[18]Maki M., Keenan T., Sasaki Y., Nakamura K. (2001), Characteristics of the Raindrop Size Distribution in Tropical Continental Squall Lines Observed in Darwin, Australia. Journal of Applied Meteorology, 40, 1393-1412(DOI: 10.1175/1520-0450(2001)040<1393:COTRSD>2.0.CO;2)

[19] Friedrich K., Kalina E. A., Aikins J., Steiner M., Gochis D., Kucera P. A., Ikeda K., Sun, J.(2016), Raindrop Size Distribution and Rain Characteristics during the 2013 Great Colorado Flood, Journal of Hydrometeorology, 17(1), 53-72.

[20] Das S., Chatterjee C. (2018), Rain characterization based on maritime and continental origin at a tropical location, Journal of Atmospheric and Solar-Terrestrial Physics, doi:10.1016/j.jastp.2018.02.011.10.1016/j.jastp.2018.02.011.

[21] Das S, Maitra A. (2016), Vertical profile of rain: Ka band radar observations at tropical locations. Journal of Hydrology, 534, 31-41.

[22] Cluckie I.D., Griffith R.J., Lane A., Tilford K.A.(2000), Radar hydrometeorology using a vertically pointing radar. Hydrol. Earth Syst. Sci. ,4, 565–580.

[23] Thurai M., Iguchi T., Kozu T., Eastment J.D., Wilson C.L., Ong J.T. (2003), Radar Observations in Singapore and their implications for the TRMM precipitation radar retrieval algorithms. *Radio Sci.* ,38.

[24] Peters G., Fischer B., Münster H., Clemens M., WagneR A. (2005), Profiles of raindrop size distributions as retrieved by microrain radars. *J. Appl. Meteorol.* ,44, 1930–1949.

[25] Biswas S.K., Chandrasekar V. (2018), Cross-Validation of Observations between the GPM Dual-Frequency Precipitation Radar and Ground Based Dual-Polarization Radars. *Remote Sensing*, 10(11), 1773 (DOI: 10.3390/rs10111773)

[26] Tokay A., Bashor P. G., Habib E., Kasparis T. (2008), Raindrop Size Distribution Measurements in Tropical Cyclones, Monthly Weather Review, 136(5), 1669-1685.

[27] Chang W., Wang T. C., Lin P. (2009), Characteristics of the Raindrop Size Distribution and Drop Shape Relation in Typhoon Systems in the Western Pacific from the 2D Video Disdrometer and NCU C-Band Polarimetric Radar, Journal of Atmospheric and Oceanic Technology, 26(10), 1973-1993

[28] Chen C.Y., Lee W.C.(2012) Damages to school infrastructure and development to disaster prevention education strategy after Typhoon Morakot in Taiwan. *Disaster Prev Manag.* ,21, 541–55

[29]Bringi V. N., Huang G., Chandrasekar V., Gorgucci E. (2002). A Methodology for Estimating the Parameters of a Gamma Raindrop Size Distribution Model from Polarimetric Radar Data: Application to a Squall-Line Event from the TRMM/Brazil Campaign, Journal of Atmospheric and Oceanic Technology, 19(5), 633-645

[30] Saikranthi K, Rao T.N., Rajeevan M. (2013) Identification and Validation of Homogeneous Rainfall Zones in India Using Correlation Analysis. Journal of Hydrometeorology, 14, 304-317.

[31] Kulkarni A. (2012) Weakening of Indian summer monsoon rainfall in warming environment. Theoretical and Appl. Climatol, 109, 447–459.

[32] Kakade S., Kulkarni A. (2017) Seasonal prediction of summer monsoon rainfall over cluster regions of India. J. Earth Syst. Sci., 126, 34

[33] Ahuja S, Dhanya C (2012) Regionalization of Rainfall Using RCDA Cluster Ensemble Algorithm in India. Journal of Software Engineering and Applications, 5, 568-573.

[34] Tinmaker I.R., Chate D.M. (2013), Lightning activity over India: a study of east–west contrast, International Journal of Remote Sensing, 34(16), 5641–5650 (DOI: 10.1080/01431161.2013.794987)

[35] Chaudhari H.S., Sawaisarje G.K., Ranalkar M.R. et al. (2010), Thunderstorms over a tropical Indian station, Minicoy: Role of vertical wind shear. J Earth Syst Sci, 119, 603–615 (DOI: 10.1007/s12040-010-0044-3)

[36] Mukhopadhyay P. Sanjay, J. (2003), Objective forecast of thundery/non thundery days using conventional indices over three northeast Indian stations, Mausam, 54, 867-880. (DOI:10.54302/mausam.v54i4.1587)

[37]Saha U, Kamra A, Galanaki E, Maitra A, Singh R.P., Singh A, Chakraborty S, Singh R (2017), On the association of lightning activity and projected change in climate over the Indian sub-continent, Atmospheric Research, 183,173-190. (DOI:10.1016/j.atmosres.2016.09.001)

[39] Mohan G, Vani K, Hazra A, Mallick C, Chaudhari H, Pokhrel S, Pawar S, Konwar M, Saha S, Das S, Deshpande S, Ghude S, Barth M, Rao S, Nanjundiah R, Rajeevan M. (2021), Evaluating different lightning parameterization schemes to simulate lightning flash counts over Maharashtra, India, Atmospheric Research. 255. 105532. (DOI:10.1016/j.atmosres.2021.105532)

[40]Price C, Rind D (1992), A simple lightning parameterization for calculating global lightning distributions, J. Geophys. Res, (DOI:10.1029/92JD00719)

[40] Vani K.G., Mohan G. M., Hazra A., Pawar S. D., Pokhrel S., Chaudhari H. S., Konwar M., Saha S. K., Mallick C., Das S. K., Deshpande S., Ghude S.

D., Domkawale M., Rao S. A., Nanjundiah R. S., Rajeevan M. (2022), Evaluation and Usefulness of Lightning Forecasts Made with Lightning Parameterization Schemes Coupled with the WRF Model, Weather and Forecasting, 37(5), 709-726.

[41] Makela A.(2004), Comparison between Lightning Data and Cloud Top Temperatures in Finland, EUMETSAT Conference proc., Finland.

[42] Molinie G., Jacobson A. R. (2004) Cloud-to-ground lightning and cloud top brightness temperature over the contiguous United States, Journal of Geophysical Research, 109, D13106, 1–16.

[43] Betz H., Price C., Di Paola F. (2013), Using a cloud electrification model to study relationships between Atmospheric lightning activity and cloud microphysical structure, Natural Hazards and Earth System Sci., 13, 1085–1104.

[44] Solomon R, Adamo C, Baker M. (2002), A lightning initiation mechanism: application to a thunderstorm electrification model. Comptes Rendus Physique.1,3(10), 1325-33.

[45] Buiat M., Porcu F., Dietrich S. (2017), Observing relationships between lightning and cloud profiles by means of a satellite-borne cloud radar, Atmos. Meas. Tech., 10, 221–230.

[46] Emersic A., Heinselman P.L., Macgorman D.R., Bruning E. C.(2011), Lightning Activity in a Hail-Producing Storm Observed with Phased-Array Radar, Monthly Weather Review, 139, 1809-1825.

[47] Saylor J.R., Ulbrich C.W., Ballentine J.W., Lapp J.L.(2005), The correlation between lightning and DSD parameters, IEEE Transactions on Geoscience and Remote Sensing, 43, 8, 1806-1815.

[48] Friedrich K., Kalina E., Masters F., Lopez C. (2013) Drop-Size Distributions in Thunderstorms Measured by Optical Disdrometers during VORTEX2. Monthly Weather Review, 2013, 141. 1182-1203(DOI:10.1175/MWR-D-12-00116.1)

[49] Sun E, Che H, XuX,Wang Z, Lu C, Gui K, Zhao H, Zheng Y, Wang Y, Wang H, Sun T(2019). Variation in MERRA-2 aerosol optical depth over the Yangtze River Delta from 1980 to 2016.Theor. Appl. Climatol. 136, 363–375 (DOI: 10.1007/s00704-018-2490-9, 2019a)

[50] Soula S., Chauzy S. (2000), Some aspects of the correlation between lightning and rain activities in thunderstorms, Atmospheric Research, 56 ,355–373

[51] Gungle A., Krider E.P.(2006) Cloud-to-ground lightning and surface rainfall in warm-season Florida thunderstorms, Journal of Geophysical Research, 111, 1–15

[52] Zhou Y., Qie X., Soula S.(2002), A study of the relationship between cloud-to-ground lightning and precipitation in the convective weather system in China, Annales Geophysicae, 20, 107–113

[53] Joss J., Waldvogel A.(1967), Ein Spektrograph fur Niederschlagstrophen mit automatischer Auswertung. Pure Appl. Geophys., 68, 240-246.

[54] Sheppard B.(1990), Effect of Irregularities in the Diameter Classification of Raindrops by the Joss-Waldvogel Disdrometer, Journal of Atmospheric and Oceanic Technology, 7, 180-183.

[55] Gunn R., Kinzer G.D. (1949), The Terminal Velocity Of Fall For Water Droplets In Stagnant Air, Journal of Meteorology, 6, 243-248

[56] Foote G.B., DuToit P.S. (1969), Terminal velocity of raindrops aloft. J. Appl. Meteor., 8, 249–253

[57] Beard K.V.(1967), Terminal velocity and shape of cloud and precipitation drops aloft. J. Atmos. Sci., 33 , 851–864

[58] Pruppacher H.R., Klett J.D.(1978), Microphysics of Clouds and Precipitation. D. Reidel, 1978, 714

[59] Montero-Martínez G., Kostinski A.B., Shaw R.A., García-Garcí F. (2009), Do all raindrops fall at terminal speed? Geophys. Res. Lett., 36 , L11818 (DOI:10.1029/2008GL037111)

[60] Thurai M., Bringi V.N., Peterson W.A., Gatlin P.N. (2013), Drop shapes and fall speeds in rain: Two contrasting examples, J. Appl. Meteorol. Climatol., 52, 2567–2581.

[61] Thurai M., Bringi V., Gatlin P., Wingo M. (2021), Raindrop fall velocity in turbulent flow: an observational study, Advances in Science and Research, 18, 33—39.

[62] Low T.B., List R.(1982), Collision, coalescence, and breakup of raindrops. Part I: Experimentally established coalescence efficiencies and fragment size distributions in breakup. J. Atmos. Sci., 39 , 1591–1606.

[63] Bringi V., Thurai M., Baumgardner D.(2018), Raindrop fall velocities from an optical array probe and 2-D video disdrometer, Atmos. Meas. Tech., 11, 1377–1384(DOI:10.5194/amt-11-1377-2018)

[64] Wilken F, Baur M, Sommer M, Deumlich D, Bens O, Fiener P. (2018) Uncertainties in rainfall kinetic energy-intensity relations for soil erosion modelling. Catena, 1,171:234-44.

[65] Larsen M.L., Kostinski A.B., Jameson A.R. (2014), Further evidence for super- terminal drops, Geophys. Res. Lett., 41, 6914–6918, (DOI:10.1002/2014GL061397)

[66]Montero-Martínez G., García-García F. (2016) On the behaviour of raindrop fall speed due to wind. Quarterly Journal of the Royal Meteorological Society, 142(DOI:10.1002/qj.2794)

[67] Ierace, B., Larsen M., O'Dell K., Kostinski A.B. (2020), Exploring the Possible Physical Origins of Raindrops falling at Non-Terminal Fallspeeds , 2020, A187-0006

[68] Sarkar T., Maitra A. (2017),Characteristics of High Velocity Small Drops in Tropical Convective Rain, proc. of URSI GASS, Montreal, August 2017.

[69] Kaufman L., Rousseeuw P. J. (1987), Clustering by means of medoids. In I. D. Y & editor (ed.), North Holland, Elsevier , 405–416 .

[70] Kumar V, Jain S, Singh Y (2010), Analysis of long-term rainfall trends in India. Hydrological Sciences, 55, 484-496.

[71] Varikoden H., Kumar K.K., Babu C.A. (2013), Long term trends of seasonal and monthly rainfall in different intensity ranges over Indian subcontinent, Mausam, 64, 481-488.

[72] Zhai P, Zhang X, Wan H, Pan X (2004), Trends in Total Precipitation and Frequency of Daily Precipitation Extremes over China, Journal of Climate, 18, 1096-1107

[73] Bhatla R, Singh M, Mall RK, Tripathi A, Raju PVS (2015), Variability of summer monsoon rainfall over Indo-Gangetic plains in relation to El-Nino/La-Nina, Natural Hazards, 78, 837–853.

[74] Krishan G, Chandniha S.K., Lohani A.K. (2015), Rainfall Trend Analysis of Punjab, India using Statistical Non-Parametric Test, Current World Environment, 10,792-800.

[75] Randhawa S.S., Randhawa S., Rai I. (2015), Seasonal Monthly and Annual Rainfall Trends in Himachal Pradesh during 1901-2002, State Centre On Climate Change (Himachal Pradesh) (http://www.hpccc.gov.in).

[76] Singh N ,Sontakke N.A., Singh H., Pandey A.K..(2005). Recent trend in spatiotemporal variation of rainfall over India - An investigation into basin-scale rainfall fluctuations.273-282.

[77] Jayawardene H, Sonnadara D, Jayewardene DR (2005), Trends of Rainfall in Sri Lanka over the Last Century, Sri Lankan Journal of Physics, 6, 7-17.

[78] Beattie, James. (2016). The mechanism of spray electrification: the waterfall effect. Atmospheric Chemistry and Physics Discussions.1-9. 10.5194/acp-2015-892.

[79] Takahashi, T. (1978). Riming electrification as a charge generation mechanism in thunderstorms. Journal of Atmospheric Sciences, 35(8), 1536-1548.

[80] Emersic C., Saunders C. P. R. (2010). Further laboratory investigations into the relative diffusional growth rate theory of thunderstorm electrification. Atmospheric Research, 98(2-4), 327-340.

[81] Ziegler C. L., MacGorman D., J. E. Dye, Ray P. (1991), A model evaluation of non-inductive graupel-ice charging in the early electrification of a mountain thunderstorm, J. Geophys. Res., 96(D7), 12,833– 12,85

[82]Mansell E. R., MacGorman D. R., Ziegler C. L., &Straka, J. M. (2005). Charge structure and lightning sensitivity in a simulated multicell thunderstorm. *Journal of Geophysical Research: Atmospheres*, *110*(D12).

[83] Yu L., Wu S., Ma, Z. (2019). Evaluation of moist static energy in a simulated tropical cyclone.Atmosphere, 10(6), 319.

[84] Chen Z., Qie X. (2017). The Relationship between Lightning Activity and Surface Equivalent Potential Temperature in Two Squall Line Events.In *AGU Fall Meeting Abstracts* (Vol. 2017, pp. AE13A-2226).

[85] Heymsfield A. J., Schmitt C., Bansemer A., Twohy C. H. (2010). Improved representation of ice particle masses based on observations in natural clouds. *Journal of the Atmospheric Sciences*, *67*(10), 3303-3318.

[86] Grewe, V., Brunner, D., Dameris, M., Grenfell, J. L., Hein, R., Shindell, D., &Staehelin, J. (2001). Origin and variability of upper tropospheric nitrogen oxides and ozone at northern mid-latitudes. *Atmospheric Environment*, *35*(20), 3421-3433.

[87] Williams, E. R., Weber, M. E., & Orville, R. E. (1989). The relationship between lightning type and convective state of thunderclouds. *Journal of Geophysical Research: Atmospheres*, *94*(D11), 13213-13220.

[88] Romps, D. M., Seeley, J. T., Vollaro, D., & Molinari, J. (2014). Projected increase in lightning strikes in the United States due to global warming. *Science*, *346*(6211), 851-854.

[89] Williams E., Stanfill S. (2002), The Physical Origin of the Land-Ocean Contrast in Lightning Activity, ComptesRendus-Physique, 3, 1277-1292 (DOI: 10.1016/S1631-0705(02)01407-X)

[90] McCaul, E. W., Goodman, S. J., LaCasse, K. M., & Cecil, D. J. (2009). Forecasting lightning threat using cloud-resolving model simulations. *Weather and Forecasting*, *24*(3), 709-729.

[91] Manzato A.(2013), Hail in Northeast Italy: a neural network ensemble forecast using sounding-derived indices, Weather Forecast, 28, 3–28

[92] Herman G., Schumacher, R. (2018), Dendrology" in numerical weather prediction: what random forests and logistic regression tell us about forecasting extreme precipitation, Mon. Weather Rev, 146,1785–1812(DOI:10.1038/s41612-019-0098-0)

[93] Mostajabi A., Finney D., Rubinstein M., Rachidi F. (2019), Nowcasting lightning occurrence from commonly available meteorological parameters using machine learning techniques, Climate and Atmospheric Science, 2, 41(DOI: 10.1038/s41612-019-0098-0)

[94]Murugavel P., Pawar S., Gopalakrishnan V.(2014), Climatology of Lightning over Indian Region and Its Relationship with Convective Available Potential Energy, Int. J. Climatol, 34.

[95] Collier A., Bürgesser R., Ávila E. (2013), Suitable regions for assessing long term trends in lightning activity, Journal of Atmospheric and Solar-Terrestrial Physics, 92,100-104.

[96] Cecil D. (2006), LIS/OTD 2.5 Degree Low Resolution Monthly Climatology Time Series (LRMTS) [2003-2013], Dataset available online

from the NASA Global Hydrology Resource Center DAAC, Huntsville, Alabama, U.S.A. (DOI: http://dx.doi.org/10.5067/LIS/LIS-OTD/DATA309)

[97] Hersbach H., Bell B., Berrisford P., Biavati G., Horányi A., Muñoz S., Nicolas J., Peubey J., Radu C., Rozum R., Schepers I., Simmons D., Soci A., Dee C., Thépaut D.(2019), ERA5 monthly averaged data on pressure levels from 1979 to present. Copernicus Climate Change Service (C3S) Climate Data Store (CDS). (Accessed on 17-Apr-2021) (DOI:10.24381/cds.6860a573)

[98] Webb et al., (2017), The Cloud Feedback Model Intercomparison Project (CFMIP) contribution to CMIP6, Geoscientific Model Development,10 (1), 359 – 384(DOI: 10.5067/MODIS/MCD06COSP_M3_MODIS.061)

[99] Hartigan J.A., Wong, M.A.(1979), Algorithm AS 136: A k-means clustering algorithm, Journal of the royal statistical society, series c (applied statistics), 28(1), 100-108

[100] Pedregosa F., Varoquaux G., Gramfort A., Michel V., Thirion B., Grisel O., Blondel M., Prettenhofer P., Weiss R., Dubourg V., Vanderplas J., Passos D., Brucher M., Perrot M., Duchesnay E. (2011), Scikit-learn: Machine Learning in Python, Journal of Machine Learning Research, 12, 2825–2830

[101] Hoerl A., Kennard R. (1970), Ridge Regression: Biased Estimation for Nonorthogonal Problems, Technometrics,12, 55-67(DOI: 10.1080/00401706.1970.10488634)

[102] Santosa F., Symes W. (1986), Linear Inversion of Band-Limited Reflection Seismograms, SIAM Journal on Scientific and Statistical Computing, 7 (4), 1307-1330 (DOI:10.1137/0907087)

[103] Gladwin C.H.(1989), Ethnographic decision tree modeling, sage, 19.

[104]Breiman L.(2001),Random Forests. Machine Learning, 45, 5–32 (DOI:10.1023/A:1010933404324)

[105]Unnikrishnan C.K., Pawar S., Gopalakrishnan. V. (2021), Satellite-observed lightning hotspots in India and lightning variability over tropical

South India, Advances in Space Research, 68,(DOI: 10.1016/j.asr.2021.04.009)

[106] Williams E.R. (1995), Meteorological aspects of thunderstorms. In: Volland H (ed) CRC handbook on atmospheric electrodynamics 1, CRC Press, Boca Raton, 27–60

[107]Dewan A., Hossain M., Rahman M., Yamane Y., Holle R. (2017), Recent lightning-related fatalities and injuries in Bangladesh, Weather Clim. Soc., 9 , 575-589 (DOI: 10.1175/WCAS-D-16-0128.1)

[108] Li J., Wu X., Yang J., Jiang R., Yuan T., Lu J, Sun M. (2020), Lightning activity and its association with surface thermodynamics over the Tibetan Plateau, Atmospheric Research, 245, 105118.

[109] Cheng w., Kim D., Holzworth R. (2021), CAPE threshold for lightningover the tropical ocean, Journal of Geophysical Research: Atmospheres, 126, e2021JD035621 (DOI: 10.1029/2021JD035621)

[110] Qie X., Toumi R., Yuan T.(2003), Lightning activities on the Tibetan Plateau as observed by the lightning imaging sensor, J. Geophys. Res, 108 (D17), 4551 (DOI: 10.1029/2002JD003304)

[111] Ahmad R. Latif M. Adnan S., Abuzar M. (2019), Thunderstorm frequency distribution and associated convective mechanisms over Pakistan, Theoretical and Applied Climatology, 137, (DOI: 10.1007/s00704-018-2619-x)

[112] Tokay A., Wolff D.B., Petersen W.A. (2014), Evaluation of the New Version of the Laser-Optical Disdrometer, OTT PARSIVEL2, Journal of Atmospheric and Oceanic Technology, 2014, 31(6), 1276-1288

[113] Lay E., Holzworth R., Rodger C., Thomas J., Pinto J., Dowden R. (2004), WWLLN global lightning detection system: Regional validation study in Brazil Lay, Geophysical Research Letters, 31, 3.

[114] Das S., Maitra A., Shukla A.(2010), Rain Attenuation Modeling in the 10-100 GHz Frequency Using Drop Size Distributions For Different Climatic Zones In Tropical India, Progress In Electromagnetics Research, 25, 211-224.

[115] Vidyarthi A., Jassal B.S., Ieee R.G.M., Shukla A.K., Formatting A. D.(2011),Comparison between Empirical Lognormal and Gamma Rain Drop-Size Distribution Models for Indian Region, Proceedings of the Asia-Pacific Microwave Conference, 1686–1689.

[116] Timothy K., Ong J., Choo E. (2002), Raindrop Size Distribution Using Method of Moments for Terrestrial and Satellite Communication Applications in Singapore, IEEE Transactions On Antennas And Propagation, 50, 10.

[117] Kozu T., Nakamura K. (1991), Rainfall Parameter Estimation from Dual-Radar Measurements Combining Reflectivity Profile and Path-integrated Attenuation, Journal of Atmospheric and Oceanic Technology, 8. 259–270

[118] Ippolito L.J. (1986), Radio wave propagation in satellite communication, New York, Van Nostrand Reinhold company.

[119] Bolek A., Testik F. Y.(2021), Rainfall Microphysics Influenced by Strong Wind during a Tornadic Storm, Journal of Hydrometeorology, 23(5), 733-746

[120] Chatterjee C., Das S.(2020), On The Association Between Lightning and Precipitation Microphysics, Journal of Atmospheric and Solar-Terrestrial Physics, 207, 105350

[121] D'Adderio L.P., Porcù F., Tokay A.(2015), Identification and Analysis of Collisional Breakup in Natural Rain, Journal of the Atmospheric Sciences, 72(9), 3404-3416

[122] Stout J. E., Arya S. P., Genikhovich E. L. (1995). The effect of nonlinear drag on the motion and settling velocity of heavy particles. Journal of Atmospheric Sciences, 52(22), 3836-3848.

[123] Ren W., Reutzsch J., Weigand B. (2020). Direct numerical simulation of water droplets in turbulent flow.Fluids, 5(3), 158.

[124] Tokay A., Short D.A. (1996), Evidence from tropical raindrop spectra of the origin of rain from stratiform versus convective clouds. J. Appl. Meteor., 35 , 355–371

[125] Caracciolo C., Prodi F., Battaglia A., Porcù, F. (2006), Analysis of the moments and parameters of a gamma DSD to infer precipitation properties: a convective stratiform discrimination algorithm, Atm. Res., 80(2–3), 165–186

[126] Li X., Tao W., Khain A.P. , Simpson J., Johnson D.E. (2009), Sensitivity of a cloud-resolving model to bulk and explicit bin microphysical schemes. Part II: Cloud microphysics and storm dynamics interactions. J. Atmos. Sci., 66, 22–40(DOI:10.1175/2008JAS2647.1)

[127]Adirosi E., Roberto N., Montopoli M., Gorgucci E., Baldini L. (2018), Influence of Disdrometer Type on Weather Radar Algorithms from Measured DSD: Application to Italian Climatology, Atmosphere, 9, 360(DOI: 10.3390/atmos9090360)

[128]Mannan A, Chaudhary S, Dhanya CT, Swamy AK (2018), Regionalization of rainfall characteristics in India incorporating climatic variables and using self-organizing maps. ISH J. Hydraul. Eng, 24,147–156

[129] Parthasarathy B, Kumar KR, Sontakke NA (1990), Surface and Upper Air Temperatures over India in Relation to Monsoon Rainfall, Theoretical and Appl. Climatol, 42:93- 110

[130] Shukla J. (1975), Effect of Arabian Sea surface temperature anomaly on Indian summer monsoon: a numerical experiment with the GFDL model. Journal of Atmospheric Sciences, 32(3), 503–511

[131] Kothawale D.R., Munot A.A., Borgaonkar H.P. (2008), Temperature variability over the Indian Ocean and its relationship with Indian summer monsoon rainfall, Theoretical and Applied Climatology, 92, 31–45

[132] Wang X., Li C., Zhou W.(2006), Interdecadal variation of the relationship between Indian rainfall and SSTA modes in the Indian Ocean. International Journal of Climatology 26(5), 595–606

[133] Singh O., Masood T., Khan A., Rahman S. (2000), Impact of Southern Oscillation on the Frequency of Monsoon Depressions in the Bay of Bengal. Natural Hazards, 25, 101–115

[134] Hahn D.G., Shukla J. (1976), An apparent relationship between Eurasian snow cover and Indian monsoon rainfall. Journal of the Atmospheric Sciences, 33, 2461–2462

[135] Vecchi G., Harisson D. (2004), Interannual Indian Rainfall Variability and Indian Ocean Sea Surface Temperature Anomalie, American Geo. Union, 147, 247-260

[136] Niu S., Jia X., Sang J., Liu X., Lu C., Liu Y.(2010) Distributions of Raindrop Sizes and Fall Velocities in a Semiarid Plateau Climate: Convective versus Stratiform Rains, Journal of Applied Meteorology and Climatology, 49(4), 632-645

[137] Lo¨ffler-Mang M., Joss J. (2000), An optical disdrometer for measuring size and velocity of hydrometeors, J. Atmos. Oceanic Technol., 17, 130–139

[138] Voida A., Judith S., Gary M.(2013), Turbulence in the clouds: challenges of cloud-based information work, Proceedings of the SIGCHI conference on human factors in computing systems

[139] Das S. K., Simon, S., Kolte Y. K., Krishna U. V. M., Deshpande S. M., Hazra, A.(2020) Investigation of Raindrops Fall Velocity During Different Monsoon Seasons Over the Western Ghats, India. Earth and Space Science, 7, e2019EA000956(DOI: 10.1029/2019EA000956)

[140] Gilbert R.O. (1987) Statistical Methods for Environmental Pollution Monitoring. New York: van Nostrand Reinhold.